2015

COMMERCIALIZATION OF A SMALL, LIGHTWEIGHT, LOW-COST SEISMIC BOREHOLE RECEIVER

Rachel Adams
University of Kentucky, racheladams@uky.edu

STUDENT AGREEMENT:

I represent that my thesis or dissertation and abstract are my original work. Proper attribution has been given to all outside sources. I understand that I am solely responsible for obtaining any needed copyright permissions. I have obtained needed written permission statement(s) from the owner(s) of each third-party copyrighted matter to be included in my work, allowing electronic distribution (if such use is not permitted by the fair use doctrine) which will be submitted to UKnowledge as Additional File.

I hereby grant to The University of Kentucky and its agents the irrevocable, non-exclusive, and royalty-free license to archive and make accessible my work in whole or in part in all forms of media, now or hereafter known. I agree that the document mentioned above may be made available immediately for worldwide access unless an embargo applies.

I retain all other ownership rights to the copyright of my work. I also retain the right to use in future works (such as articles or books) all or part of my work. I understand that I am free to register the copyright to my work.

REVIEW, APPROVAL AND ACCEPTANCE

The document mentioned above has been reviewed and accepted by the student's advisor, on behalf of the advisory committee, and by the Director of Graduate Studies (DGS), on behalf of the program; we verify that this is the final, approved version of the student's thesis including all changes required by the advisory committee. The undersigned agree to abide by the statements above.

Rachel Adams, Student

Dr. Michael E. Kalinski, Major Professor

Dr. Y. T. Wang, Director of Graduate Studies

COMMERCIALIZATION OF A SMALL, LIGHTWEIGHT, LOW-COST SEISMIC BOREHOLE RECEIVER

THESIS

A thesis submitted in partial fulfillment of the requirements
for the degree of Master of Science in Civil Engineering
in the College of Engineering
at the University of Kentucky

By

Rachel Anne Adams

Lexington, Kentucky

Director: Dr. Michael E. Kalinski, Associate Professor of Civil Engineering

Lexington, Kentucky

2015

ABSTRACT OF THESIS

COMMERCIALIZATION OF A SMALL, LIGHTWEIGHT, LOW-COST SEISMIC BOREHOLE RECEIVER

Herein, conceptualization of a recently patented seismic borehole receiver and its components is developed for commercialization. The device is significantly cheaper, lighter, and smaller than existing technologies on the market. Additionally, it has the potential to achieve better seismic readings than its competitors via patented sensor-to-borehole coupling mechanism. It is the hope that the commercialization of this device will not only provide a more affordable alternative to engineers and geophysicists in the existing market, but the significant cost difference may open new seismic measurement opportunities in the developing world. Its compact size and light weight will increase mobility, allowing investigators to conduct surveys where previously deemed infeasible. Many impoverished states in regions of high seismicity lack the seismic data this and other such devices can provide. This data has been crucial to infrastructure advancements and public safety in seismic hazard areas of the developed world, yet the technology used to ascertain it is inaccessible in the developing world due to cost and availability. This thesis will outline the potential impact of the device, review governing seismic wave behavior and the current state of the seismic measurement field, as well as outline the components, development, and future development of the instrument.

KEYWORDS: borehole seismic, earthquake engineering, geophysical equipment, geotechnical engineering, engineering geophysics, MEMS accelerometer

Rachel A. Adams

November 24, 2015

COMMERCIALIZATION OF A SMALL, LIGHTWEIGHT, LOW-COST SEISMIC BOREHOLE RECEIVER

By

Rachel Anne Adams

Dr. Michael E. Kalinski
Director of Thesis

Dr. Y. T. Wang
Director of Graduate Studies

November 24, 2015

ACKNOWLEDGEMENTS

I would first like to thank my advisor, Dr. Michael Kalinski, for his guidance over the past two years. From my undergraduate independent study, to obtaining a valuable internship, to the completion of this thesis, Dr. Kalinski has provided me with many opportunities to learn and grow under his tutelage. The independence that he has allowed me during this time has pushed me to expand my knowledge and understanding of the geotechnical and related fields. I am grateful to Dr. Kalinski for the chance to work on such an innovative and impactful project as this. I am truly inspired by his humanitarian efforts on this and related projects and aspire to pursue such work in my own career.

I would also like to thank the other members of my committee, Dr. Sebastian Bryson and Dr. Ed Woolery, for donating their time and expertise. Both have served as excellent instructors during my graduate program. Dr. Woolery has contributed greatly to my understanding of geophysical studies and instrumentation, as applied in this project. I owe a special thanks to Dr. Bryson, not only for building my geotechnical knowledge, but for aiding in my research and taking such a vested interest in my education.

There are many other professors who have contributed greatly to my success at the University of Kentucky. I would like to thank Dr. James Fox for stimulating my interest in research and helping me gain valuable field experience. I would also like to thank the Director of Graduate Studies, Dr. Y.T. Wang for his time and assistance during this process. I would also like to thank the Director of Undergraduate Studies Dr. Scott Yost for his support and advice during my time at UK.

I am also very grateful to those who directly and indirectly worked on this project. I would like to thank Shelia Williams and Jim Norvell from the Civil Engineering Department at UK. Shelia has been indispensable with part ordering and coordination, while Jim greatly aided in the technical aspects of component testing and prototyping. I would also like to thank fellow graduate student Raghava Bhamidipati for his help in the laboratory.

From the Electrical Engineering Department at UK I need to thank Dr. Bruce Walcott, Richard Anderson, and Tim Lim. Dr. Walcott has supported my academic pursuits throughout my time at UK and introduced me to Richard and Tim who were indispensable in constructing the MEMS accelerometer devices. I am especially grateful to Richard for donating so much of his time in aiding my understanding of the electrical systems in this project.

I would also like to thank Dennis Sack, Phil Sirles, Dave Fidelman, and Larry Olson, all of Olson Instruments for their input on the project and in advance of their continued work.

I owe much gratitude to those responsible for funding both this project and my graduate education. I would like to thank the Kentucky Science and Engineering Foundation for their support of this project and my education. I am also thankful to the many donors of the UK Civil Engineering Department scholarship fund, namely the endowers of the Raymond Fellowship.

There are certainly many others who have contributed to my success. Thank you to my friends and colleagues in the UK and Stantec communities, too numerous to name,

for your continued support. A special thanks to Hayden Barrows whose unwavering cheerful disposition kept me smiling through the stress.

Lastly, thank you to my family. From a young age, my parents instilled a love of learning and a solid work ethic which has seen me through this project and will continue for the many more to come. I am eternally grateful for that and the many other gifts you have given me. To my mom, dad, brother, grandparents, and extended family, without your encouragement and faith, this would not be possible.

TABLE OF CONTENTS

LIST OF TABLES

LIST OF FIGURES

1. Introduction

1.1. Device Background

Seismic data measurement has a wide array of applications throughout the geophysical and engineering fields. This study will focus on near-surface engineering applications. One of the most commonly used measurement devices in this field is the seismic borehole receiver. These devices have been in use since the 1970s, with little change over the past several decades. The new seismic borehole receiver introduced herein, looks to change the market and accessibility of such instruments.

The device was originally developed in 2007 during a tailings dam investigation in Eastern Kentucky. Dr. Michael Kalinski created the device after his old equipment proved unreliable at the required depths. After experiencing success with that preliminary investigation, Dr. Kalinski continued to test and develop the device, eventually filing for a patent in 2009, which was granted in 2011 (Kalinski, 2011). The initial prototype was successfully used to collect data on several research projects.

Seismic investigations performed in the aftermath of the 2010 Haiti Earthquake by Dr. Kalinski in-part inspired the further development of the seismic receiver that is the topic of this thesis. Geophysicists without Borders, the humanitarian arm of the Society of Exploration Geophysicists, sponsored the ground characterization research near the epicenter of the earthquake, in Port-au-Prince (Kalinski et al., 2014). Due to the state of the nation's infrastructure and the nature of the field study, the equipment used was required to be highly portable. Additionally, the equipment had to be inconspicuous enough to avoid theft, and inexpensive enough that it could be donated to local

researchers who would continue the work after the study ended. This experience contributed to the pursuit of improving the previously patented seismic borehole receiver as a cheaper, lighter weight alternative to those devices currently on the market. The device would provide better ease of travel and use on such humanitarian trips, and the lower cost would make it more accessible across existing and new markets.

Shortly after the 2013 trip, Dr. Kalinski applied for and received funding to commercialize the device through the Kentucky Science and Engineering Foundation Kentucky Commercialization Fund Program, which is the topic of this thesis.

1.2. Research Needs

Seismic data has been used and collected for centuries, since a rudimentary seismoscope was developed in ancient China (Stewart, 2009). The device consisted of an urn with small balls suspended along its exterior. If a seismic event occurred, these balls would drop into the open mouths of carved frogs below. It is believed that by examining which balls were displaced, the propagation path of the seismic wave could be determined. Since that time, seismic instruments and acquisition methods have evolved to trace the origin, propagation method, and magnitude of seismic events using analog and digital recording technology. Seismic data are now also commonly used to classify subsurface conditions, locate underground resources, and predict ground response to future seismic disturbances. Arguably the most crucial of these functions to humanity, in terms of safety, is that of predicting ground response. Ground response is essentially how the ground with behave during an earthquake or other seismic stimulation. This information is used to design structures that will be more stable during future seismic events. This is crucial since earthquake fatalities typically occur when structures fail.

In 2008 the National Academy of Engineering released a list of 14 grand challenges for engineers in the next century (NAE, 2008). Among energy, healthcare, and information needs, was the call to "restore and improve urban infrastructure." By restoring structures destroyed in earthquakes, and improving its seismic stability, lives can be saved and future damage to infrastructure minimized. In the United States and throughout many developed nations, owners are now required to perform seismic surveys prior to erecting new structures in areas of seismic concern. The International Building Code has become the unofficial standard in the United States and has been adopted by many locales as the governing regulation. Among other standards, the code requires the spectral response acceleration of the site to be known and incorporated (ICC, 2009). The code certainly establishes the norm and direction of the requirement of site-specific seismic data for structural design and construction. While these seismic surveys have seamlessly been incorporated into construction practices in the developed world, more impoverished regions lack the resources to require or even voluntarily conduct such investigations. It makes it very difficult for these countries to implement building codes to ensure safety of their citizens, when the seismic potential of their land is not understood.

Poorer nations do not experience more frequent or larger earthquakes, but they do typically experience more damage from them. The average Gross Domestic Product (GDP) per capita rank among the world's 228 nations was compared using the most recently available data. Among nations experiencing the *largest* earthquakes from 1990-2012 the rank of the average GDP per capita is 102nd. The rank of the average GDP per capita among nations experiencing the *deadlies*t earthquakes during that same period is

140th (CIA, 2014). Those ranks correspond to nations with average GDP per capita values of $7,300 and $15,600, respectively. The nation of Haiti, the site of the most fatal seismic event in the past 35 years, currently ranks 209th on that list with an average GDP per capita of $1,300. Despite the widespread destruction in the country, the GDP per capita has not changed significantly since the event, likely due to the catastrophic loss of life (ERS, 2015). The devastating 2010 earthquake caused the deaths of 3% of the Haitian population. It registered as a 7.0 on the moment magnitude scale. The most comparable urban earthquake in the United States, which ranks 14th in the world with an average GDP per capita of $52,800, is the 1994 Northridge Earthquake, which occurred in the San Fernando Valley of Los Angeles, California. It registered with a magnitude of 6.7, with more than three times the peak acceleration of the 2010 Haiti Earthquake. The Northridge Earthquake killed only 57 people, less than 0.02% of those killed during the recent Haiti Earthquake (USGS, 2014).

This example shows how big of an influence preparation and infrastructure can have on the outcome of such disasters. At that time, Los Angeles had already implemented strict building codes dealing with earthquake structural stability, which helped prevent catastrophic loss of life and property like what occurred in Haiti. Much of the infrastructure in Haiti prior to the earthquake was not designed with seismic hazards in mind, let alone up to modern standards. This is the case throughout much of the developing world. Engineers are working to develop novel, affordable ways to create and modify infrastructure to be earthquake resistant. However, without characterization and data of the underlying strata, it is difficult to employ these practices. Thus, there is a great

need to increase accessibility to seismic data, specifically in the realm of site characterization for construction and engineering practices.

1.3. Research Objectives

This research looks to bring to market a device that will increase the accessibility to and accuracy of seismic data. Whenever the ease and cost of information acquisition is reduced, it can be anticipated that quantities of information gathered will be increased. It is in this way that the seismic device discussed in this thesis may open the doors to better development of infrastructure, with regards to seismic stability.

This device is significantly cheaper, lighter, and smaller than the existing technologies on the market. Additionally, it has the potential to achieve better seismic readings than its competitors via its patented sensor to borehole coupling mechanism. These features, coupled with the same ease of use as traditional borehole receivers, will drastically lower the barrier to seismic measurement equipment and data.

In order to achieve this, new prototypes of the device will be designed for continual development in the research field, as well as for the commercialization and eventual large-scale production by an instrumentation company (Olson Instruments). Design will focus on identifying components and processes to be used in the final product. The design will reflect the ideas of mobility via consideration of the device weight and size, as well as that of any accompanying equipment necessary for operation. Cost is another main concern, and will be minimized in all components and the production process. Consideration will also be given to how the instrument will be used in the field, including the functionality and modular nature of key components. The

accuracy of the data collected by the receiver is also of the utmost importance. This thesis looks to create a new design that embodies all of these standards and prototypes that can be further advanced and brought to market.

1.4. Thesis Contents

The potential impact of the device has been reviewed. Prior to introducing the development of the device, a review of the state of the seismic measurement field, including governing behavior and understanding of seismic waves, their applications, measurement methods, and existing devices, will be conducted. The device overall design and the background selection, and testing of the components will be introduced. Finally, the final recommendations and future work will be identified.

2. State of Field

In near surface seismic exploration, wavelets are generated from a seismic source and measured at a receiver after they pass through a material. How the waves change from the source to the receiver contains information about the material through which they traveled. This chapter reviews the physical behavior of those waves and the underlying principles and assumptions that allow engineers and geophysicists to use and interpret them. Current practices and comparable existing devices are also explored.

2.1 Basic Principles of Seismic Wave Forms

At the basic level, a wave is the transmission of energy through a material via particle motion and interaction. This particle motion defines the different types of seismic waves, and the particle interaction differs with the properties of various materials. However, all wave forms can be defined and modeled using the same basic formulations and components.

2.1.1. The Wave Equation and its Components

In order to obtain information from a seismic wave, components of wave form must be identified. Wave form and behavior is typically expressed in the realm of oscillating functions. For simplicity, the behavior of a simple harmonic wave will be discussed.

The propagation modes of seismic wave types allow them to be described by sinusoidal functions. These functions usually represent particle position with respect to time and in terms of wave properties like amplitude of displacement, angular frequency,

and the phase angle. For a simple harmonic wave, the function of a wave is typically given in terms of time, t, as:

$$u(t) = Asin(\omega t + \varphi) \tag{2.1}$$

where A is the amplitude of displacement, ω is the angular frequency, and φ is the phase angle. Wave amplitude (A) is often conceptualized as the maximum "height" of a wave form as shown in Figure 1. Amplitude is proportional to the square root of the energy transmitted by the wave. Angular frequency (ω) is the radians a particular portion of the wave form (crest, trough, etc) travels per unit time. When not expressed in angular terms, frequency (f) is simply the cycles of a wave per unit time. Frequency is related to the period (T) of the wave, or the time it takes for one cycle to pass. While period is the temporal measure of a wave cycle, the wave number (K) is the spatial measure. Wave number is the distance traveled during a cycle. The phase angle quantifies how out of phase the wave is from the pure sine wave.

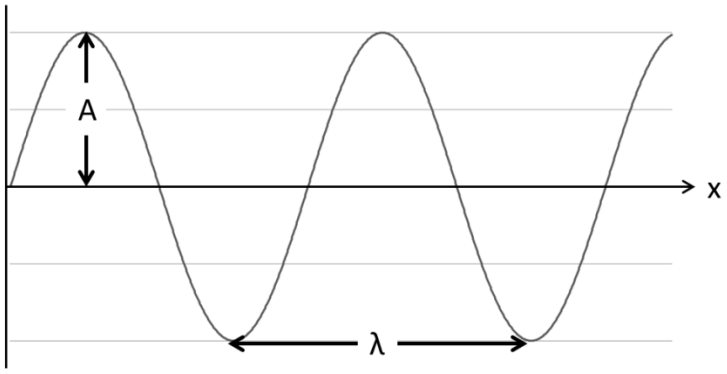

Figure 1: Wave expressed as a seismic function of distance with amplitude and wavelength.

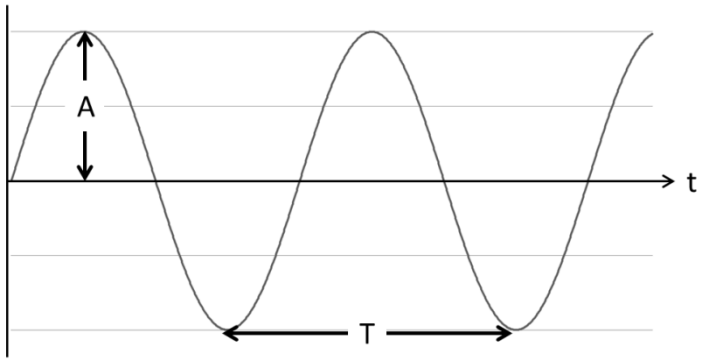

Figure 2: Wave expressed as a seismic function of time with amplitude and period

A simple harmonic wave can also be given as a sum of sine and cosine functions:

$$u(t) = \text{acos}(\omega t) + bsin(\omega t) \tag{2.2}$$

where *a* and *b* are the amplitudes of the individual cosine and sine functions, respectively.

Of the components discussed, frequency is possibly the most crucial to monitor in seismic surveys. The data collected is only as good as the instrument used, and for most applications, the response frequency of a transducer is the controlling factor. The frequency of any given wave varies with the media through which it passes. That frequency of the signal interpreted by the transducer must be within the operating range, or frequency response of the device. The frequency response is dependent on different factors for each transducer type, but it is often related to resonance. Resonance is the exponential increase in wave amplitude as a system's vibrating frequency approaches its natural frequency. A system will vibrate at its natural frequency without any applied external forces. If a transducer is at resonance, the excessive vibrations prevent it from taking accurate readings of the signal.

2.1.2. Elastic Properties of Media

While these functions are used to quantify and study waves, they do not fully encapsulate wave propagation theory. The modern accepted theory can be broken into two major components: elastic theory, represented by Hooke's Law, and the rigid theory, represented by Newton's Second Law of Motion. Together they comprise continuum mechanics. While both rigid and elastic mechanics are critical to the application of the previously discussed wave equations, the elastic portion is of particular importance when trying to characterize the media through which the waves travel.

Several parameters, known as elastic properties, have been defined using the basic tenets of Hooke's Laws. By nature of the definition, the elastic constants are unique to the composition and behavior of a given material. These properties are found during seismic exploration and are used to characterize subsurface conditions by "loading" the materials with wave forms and recording how they behave. It should be noted that these constants assume complete recoverability of all strains, or no permanent deformation. While this is certainly not true of earth materials, it is a good assumption when dealing with relatively small strains, like those encountered in the seismic field.

At the basic level, Hooke's law state's that the ratio of a material's stress to strain under *normal* loading is proportional and defined by the first of the elastic parameter, the modulus of elasticity, E (or Young's Modulus). Similarly, the modulus of rigidity, G (or the shear modulus), is the ratio of a material's stress to strain under *shear* loading. The bulk modulus, K (or modulus of compressibility), is a function of the pressure required to compress the volume of the material. Poisson's ratio (ν) is the proportion of the lateral strain to axial strain under axial loading. Additionally, the velocities at which waves

travel through a medium are considered to be elastic constants. The two velocity constants, dilatational and shear, are defined by the type of wave traveling through the medium.

2.1.3. Types of waves

Seismic waves are classified by how and where they travel. Body waves propagate through material, while surface waves along the material's edge, at an interface or surface. Body waves can be further subdivided by the mode of propagation. Longitudinal waves propagate via dilative behavior (Figure 3). The density of particles along the axis of propagation is varied as the wave moves through the material. Transverse wave propagate via distortion (Figure 4 and Figure 5). When picturing the classic sinusoidal motion, this is the wave one thinks of. The particles shift relative to one another in a direction perpendicular to that of the wave propagation. Of the two body wave types, transverse waves have the slower speed due to the meandering nature of their propagation. Thus, transverse waves are often known as the secondary arrival, or S-waves. They are also referred to as shear waves due to their distortional propagation. Longitudinal waves are then the first (primary) arrival waves, or P-waves. S-waves can be further subdivided into SV- and SH- waves by the direction (vertical or horizontal) of the distortion.

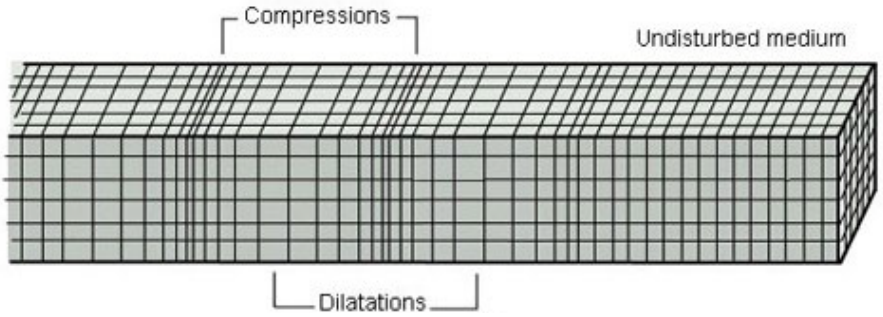

Figure 3: Side view of P-wave propagation (IRIS, 2014).

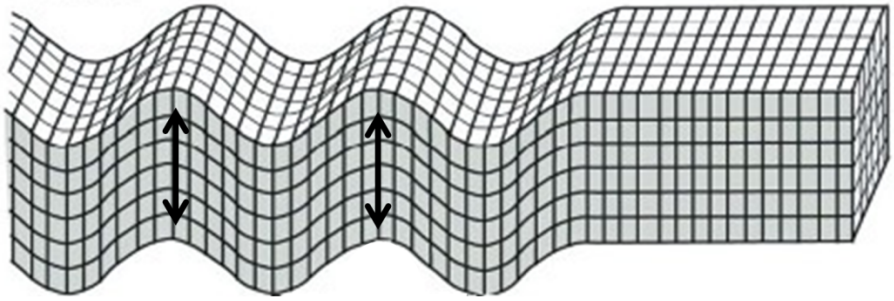

Figure 4: Side view of SV-wave propagation (IRIS, 2014).

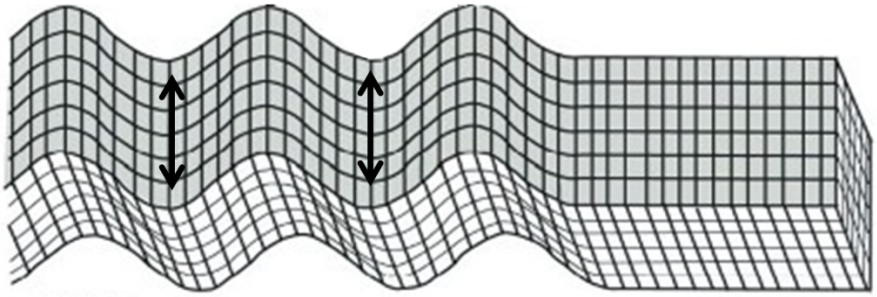

Figure 5: Plan view of SH-wave propagation (IRIS, 2014).

Body waves will be the primary focus of this thesis; however for completion, it should be noted that there are various types of surface waves. They, too, are further classified by their propagation modes. Rayleigh waves propagate via a rolling motion that decreases with depth (Figure 6). This motion is very similar to that of oceanic surface waves. The motion occurs in both the longitudinal and transverse directions, which is

logical since Rayleigh waves are created by the interaction of P- and SV-waves. Love waves are transverse surface waves caused by the interaction of SH-waves with the surface boundary (Figure 7). Love waves are most typically associated with the feelings of shaking during earthquakes.

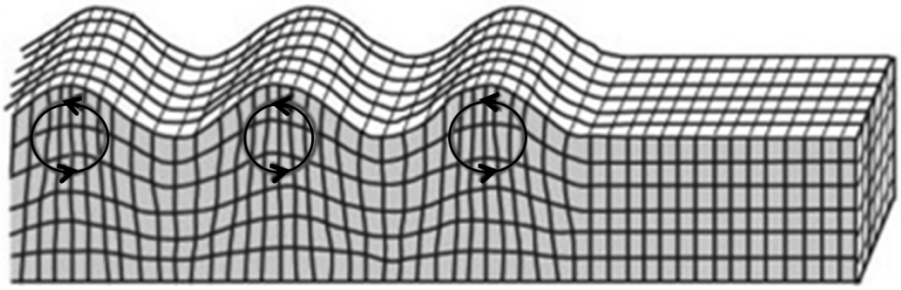

Figure 6: Side view of Rayleigh wave propagation (IRIS, 2014).

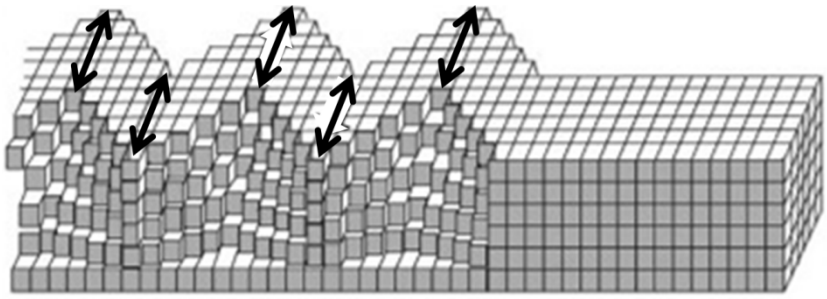

Figure 7**:** Side view of Love wave propagation (IRIS, 2014).

2.1.4. Wave Behavior in Media

Despite differences in propagation modes, general wave behavior is uniform. A wave is the continuous transmission of energy through matter. By this basic definition, wave behavior must follow the law of energy conservation and not simply stop at boundaries. The boundaries concerning waves are impedance boundaries. Impedance is the product of the density of the material the wave is passing through and the velocity of that wave. Since P- and S-wave velocities are considered to be material constants,

impedance boundaries typically occur at material boundaries. For geotechnical engineers and geophysicists attempting to characterize the subsurface, these boundaries are the underlying strata. Understanding *how* waves behave at these boundaries is the basis of modern seismic surveys.

Wave interface behavior can be broken down into reflection and transmission. During transmission, the wave's energy is conveyed through the boundary. During reflection, the wave's energy does not pass through the boundary and is redirected away from it. Transmission and reflection occur together via a process known as energy partitioning, where the energy of the incident wave is divided and continues in multiple directions. Because some of the energy is no longer available due to reflection, the transmitted portion deviates from path of the incident wave during refraction.

The type of incident wave dictates what forms will be reflected and refracted based on the components of particle motion and propagation direction. Dilatational incident waves produce reflected and refracted P- and SV-waves. Incident SV-waves also produce reflected and refracted P- and SV-waves. SH-waves produce only reflected and refracted SH-waves. This is crucial to the application of seismic surveys, as reflection and refraction are the primary enablers of modern seismic surveys. The device developed herein will primarily utilize refracted waves.

The angles of reflection and refraction are governed by Snell's Law which states

$$\frac{\sin(\theta_1)}{\sin(\theta_2)} = n \tag{2.3}$$

where θ_1 and θ_2 are the angles of incidence and reflection/refraction, respectively, from the vertical and n is the relative refraction index of the media on either side of the boundary.

Fermat's Law of Refraction quantifies the relative refraction index by stating

$$\frac{\sin(\theta_1)}{\sin(\theta_2)} = \frac{V_1}{V_2} \tag{2.4}$$

where V_1 and V_2 are the wave velocities on either side of the boundary. This utilizes Fermat's Principle of Least Time, that it is the shortest travel *time*, not the shortest travel *distance* that controls a wave path. This concept combines with critical refraction to form the basis of refraction surveys. Critical refraction occurs when the incident wave is refracted 90° from the vertical, such that the refracted wave travels along the impedance boundary. However, a wave path is a simple representation of a spherical spreading of energy. Huygen's Principle holds that while traveling along the boundary, the wave constantly emits fronts of wavelets, which can then be transmitted back and recorded.

However, even without encountering impedance boundaries, seismic waves will not continue infinitely. There are two main processes which contribute to the attenuation, or dampening, of a wave form. Attenuation is visually represented by the gradual decrease in amplitude over time or distance. Geometric spreading accounts for the multidimensional quality of a wave. As a wave travels, it radiates outward from a central source in an expanding sphere, representing the edge of the wave front. As the surface area of that sphere increases, more particles are encountered. Via the law of conservation of energy, no additional energy is created for the additional particles encountered, thus the energy available per particle is reduced. In the simplified wave path model, this

results in decreased amplitude. The other attenuating process, absorption, relates to conversion of some energy to heat due to particle motion.

Understanding of wave principles, behavior, and function has led to the development of various seismic measurement devices and techniques. These approaches will be discussed.

2.2. Wave measurement

The device developed herein will measure body waves. Often in subsurface exploration surface waves are considered seismic "noise" and are attenuated or removed from the data. This study will focus on the use of body waves to characterize the composition and seismic behavior of underlying strata.

2.2.1. Components of seismic measurement

The two basic components of any exploratory seismic measurement setup are source and receiving devices. A source can be as simple as mallet struck against a metal bar on the surface, or as complex as an electrical sparking system (Werner et al., 2013). The receiver is generally more complicated, as it must receive and configure the waves originating from the source into a useful form. At the basic level, a receiver will output the disturbances it experiences from a seismic wave as changes in voltage. Other equipment is then used to take the voltage output signals and transform them into interpretable pulses. The most common types of receiver transducers, geophones and accelerometers, will be discussed further in Chapter 3.

2.2.2. Types of seismic measurement devices

2.2.2.1. Surface Receivers

The device in development is a receiver for use in drilled boreholes. Inherent with the location of the seismic receiver in the body of the material (i.e. in the subsurface), is its measuring of body waves. However, a borehole receiver is only one receiver type. Surface receivers, as the name implies, lie on top of the media and measure waves as they exit or pass along the edge of the body. These receivers are most commonly used to measure body waves in reflection and refraction surveys. By understanding the basic behavior of waves at material interfaces, as previously discussed, the surveys use arrival times and known distances between instruments to determine layer thicknesses, inclination, and velocities. Surface receivers can also be used in conjunction with subsurface (i.e. in a borehole) sources to capture body waves. This is known as uphole testing. Other receivers utilize surface waves. For example, the Spectral-Analysis-of-Surface-Waves (SASW) method utilizes both a surface source and surface receivers to emit and measure surface waves of varying wavelengths (Stokoe et al., 1994).

2.2.2.2. Borehole receivers

While relatively easier to perform, surface surveys are more limiting than those utilizing a borehole receiver in terms of identifying characteristics of individual layers. In the geotechnical field, when feasible and cost effective, borehole receivers are often preferred to surface receivers because they utilize shear waves instead of P-waves. In reflection and refraction surface surveys, only the first-arrival wave velocities are determined. While P-wave velocities are useful for identifying strata, S-waves contain more information about the engineering properties of the materials. Additionally, the

crosshole seismic method (ASTM D4428), which utilizes a borehole receiver, eliminates some of the encumbering assumptions of surface surveys, like an increasing velocity profile and issues with thin layers and "blind" zones in the velocity profile. Shear wave velocity surveys performed with borehole receivers are gaining in popularity due to the usefulness of their results, and the requirement of shear velocity data in the characterization of building sites. While standard penetration testing (SPT) and cone penetrometer testing (CPT) are approved correlation methods for developing the velocity profiles required by the International Building Code for site classification, shear velocity surveys are generally favored for their direct correlation with the shear stiffness of soil and rock (ICC, 2009). One limitation to using shear wave surveys is that, because water has no strength in shear, they cannot immediately identify groundwater tables. However, from an engineering perspective, the benefits of borehole receivers greatly outweigh the detriments.

Borehole receivers may be used with either surface or subsurface sources. If the source is placed at the surface, the testing configuration is known as downhole testing (ASTM D7400). Downhole testing requires only one borehole, which can reduce drilling costs, but is often deemed less reliable due to attenuation and uncertainty associated with the additional travel distance from the surface to receiver (Crice, 2002). To perform a survey using downhole testing, a receiver is lowered through the borehole, and a shear wave is generated at the ground surface (Figure 8). Wave travel times are measured at different known depth increments as the receiver is lowered from the source. From this information, the wave velocity may be determined. Due to the assumptions of most equations developed for this method, the source should be located only a short lateral

distance from the receiver hole. Then the wave velocity is found as the transducer depth from the surface receiver divided by the wave travel time (Das & Ramana, 2011).

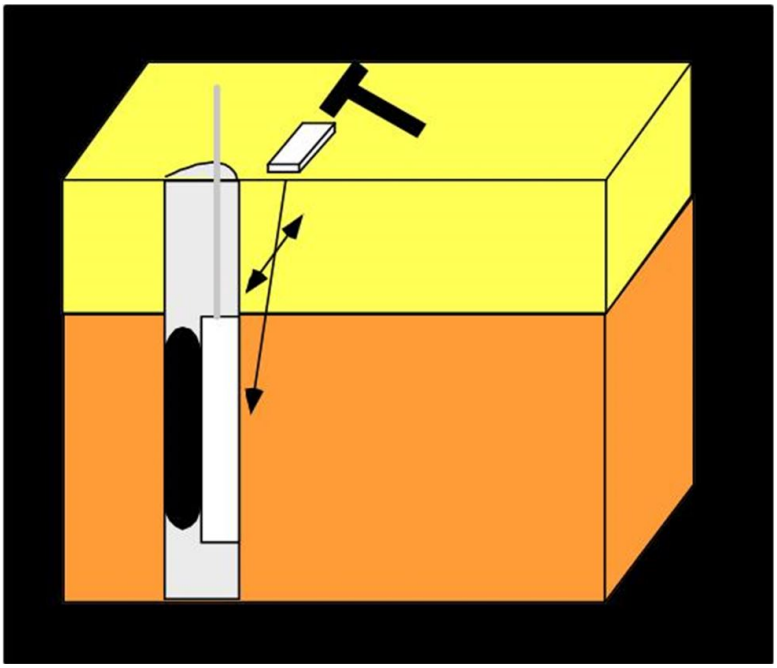

Figure 8: Typical downhole testing configuaration.

Sources may also be placed in boreholes adjacent to that of the receiver. This is known as crosshole testing (ASTM D4428). Crosshole testing can be used with one or multiple receivers and sources, thus requiring a minimum of two boreholes (Figure 9). The holes should be closely spaced to reduce destructive refraction influence (Crice, 2002). To perform a survey using the crosshole method, as a receiver is lowered through one borehole and a downhole source is lowered to the same depth in an adjacent hole. In this manner, only one horizontal stratum is being measured at any time. Wave travel times are measured laterally between the source and receiver. From this information, the wave velocity is found as the distance between source and receiver divided by the wave travel time (Das & Ramana, 2011). By increasing the number of receivers for a source,

the wave arrival times, and thus velocities, can be better estimated by providing more samples and reducing the influence of error. The multiple receiver method may also be used to characterize areas of horizontal anisotropy, as it can provide a three-dimensional representation of the area surrounding the source using differences in wave velocity. Additionally, the number of sources can be increased, or the locations of source and receiver reversed, to better estimate wave velocity.

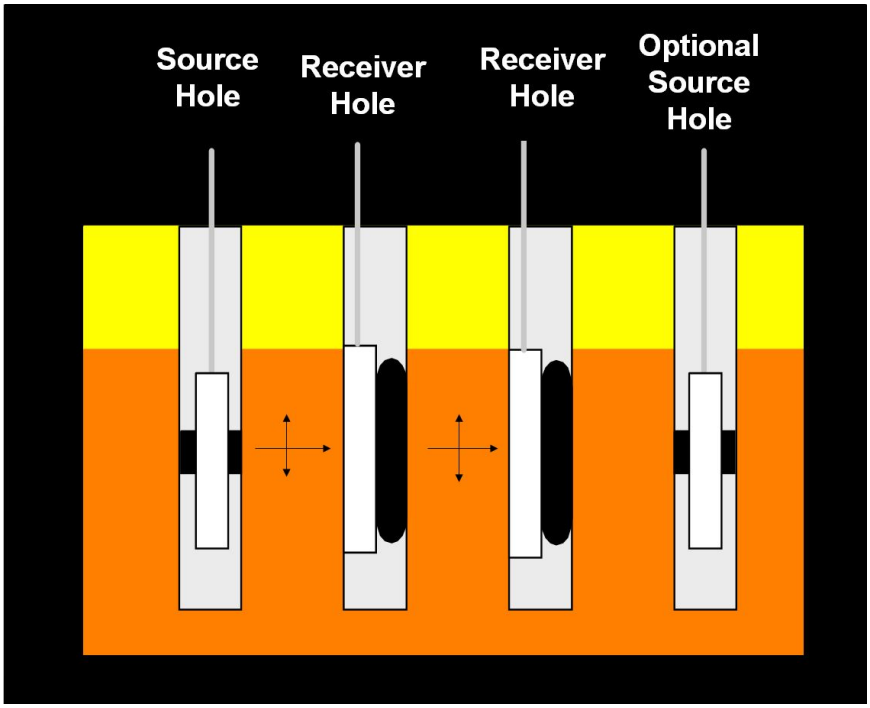

Figure 9: Typical crosshole testing configuaration.

2.2.3. Data Application and Interpretation

As previously mentioned, the great advantage to using borehole receivers is the acquisition of shear wave velocity data. The shear velocity profiles produced from the results are crucial to near-surface design. For example, the International Building Code uses the velocities in its site classification system. The site classes essentially rate the

stability of the strata under potential seismic loads. The class then dictates to which parameters any structure designed for the site should satisfy. (ICC, 2009)

While the discussion of borehole receivers has focused on their sensing of S-waves, receivers in both crosshole and downhole configurations can be used to collect P-wave data. In this way P-wave velocities can be obtained in addition to the S-wave velocities for each material. With these two parameters and a good estimation of the material density, all of the remaining elastic constants (Poisson's ratio and the moduli of elasticity, rigidity, and compressibility) can be found. These constants are crucial to the determination of the design strength and dynamic behavior of subsurface material.

Because borehole surveys can provide reliable shear wave velocity data, the methods and instruments used are very important to geotechnical engineering applications. The data obtained from borehole receivers is of particular use in designing structures to withstand seismic disturbances from earthquakes. Despite the importance of these surveys, the cost associated with commercially available borehole equipment restricts their use in the field. The research described in this thesis was performed to to increase the accessibility by creating a cheaper, smaller, and lighter alternative to the borehole receivers on the market. First, the current state of technology and potential competing devices will be explored.

2.3. Existing Technology

Most borehole receivers currently in use can be broken down into two categories: those constituting a complex system purchased through an instrumentation developer or those created by practitioners themselves. Some instrumentation companies, like the

partner developer of this device Olson Instruments, do market components that would allow individuals to build or modify their own devices. The commercial devices tend to be extremely expensive, whereas the "home-made" devices tend to be cumbersome to build and maintain. At the basic level, all devices consist of one or more transducers to intercept the seismic signal and something to couple the transducer to the wall of the borehole for accurate readings. This coupling is essential to collecting valid data. Without it, the waves will travel through other media (e.g. air) before reaching the receiver, which may skew results. After drilling, borehole walls are often unstable due to the loss of confining pressure. For this reason, rigid casing is installed in many holes (Wightman et al., 2003). Any receiver must be able to not only conform to the wall of cased holes, but also unlined ones. Coupling is a key challenge in the development of good borehole receivers.

2.3.1. Traditional Borehole Receivers

In the typical configuration, the borehole transducer housing is separate from the wall coupling device (Figure 10). An inflatable bladder is most commonly used as the coupling device. The uninflated bladder and receiver are lowered into the borehole simultaneously. The receiver is rotated so that the transducers are facing the source and the bladder is inflated to maintain the positioning. Modified bicycle tire tubes are often used as the bladder. It is inflated using a surface air compressor. These devices are cumbersome and are an added expense to the survey.

While the air bladder provides good pressure to hold the transducer housing against the borehole wall, the rigidity of the instrument may prevent good contact between the media and transducers. Very rarely are exploratory holes drilled exactly

straight. So if there is any concavity in the boring wall at the point of measure, there could be a significant gap between the medium and transducer. The transducer used in these configurations is usually a geophone. Geophones have been the standard in the geotechnical field for decades and will be discussed further in Chapter 3.

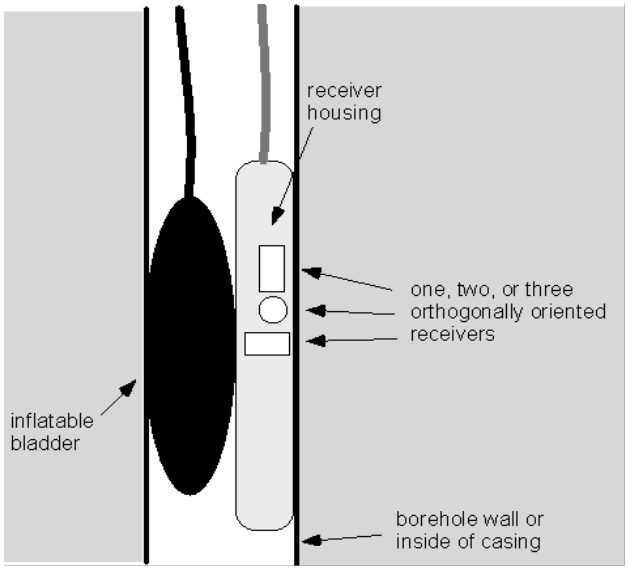

Figure 10: Traditional borehole receiver configuration. (Kalinski, 2012).

Because so many of the devices of this type are "homemade," they tend to not be as streamlined as other devices. Depending on the skill of the builder, they may require complex technical understanding to operate. What they save on cost is lost in the limitations of those who do not possess sufficient knowledge and expertise to construct and use them.

2.3.2. Modern Commercial Devices

Commercially available devices can be used by professionals with only basic training. One of the most apparent differences between the traditional borehole receiver and the modern devices is the coupling mechanism. Instead of utilizing a separate device,

like the inflatable bladder, many instruments house a motorized clamp, often referred to as a "wall lock." The clamp supports the instrument against the opposite wall of the borehole. In the Geostuff BHG models, the clamp is composed of a leaf spring (the second and third instruments from the left in Figure 11). For larger holes they market a mechanical arm (the first instrument from the left in Figure 11) which uses a mechanism similar to that in other downhole receivers, like those produced by Sercel.

Figure 11: Geostuff BHG borehole receiver system

These coupling mechanisms usually require the instrument to be very long in order to achieve the force required to hold them in place. This exacerbates the issue of gaps between the transducers and the media in concave holes. In extended areas of nonlinearity, longer devices cannot get as close to the wall as smaller devices. This length also poses a problem with the ease of use of the instrument. The Geostuff BHG line models are up to 1.1m long, the shortest still a lengthy 0.7m. A similar model, the Sara Instruments SS-BH, weighs more than 15 pounds. Such instruments are difficult to

transport in the field, and very improbable to fly or travel long distances with, creating a barrier to data acquisition. Additionally, the cost of the equipment can be relatively high. For example, the Geostuff BHG models are marketed for around $12,000.

2.3.3. Field Direction

As is the goal of the device developed herein to provide an affordable, yet technologically competent and competitive borehole receiver alternative to those currently on the market, the design will consider and reflect the direction of the field. Like with the trends of other technology-based fields, the geophysical exploration field is moving towards smaller, lighter, and higher performing devices. The continually developing technology not only increases the quality of field data, but also its quantity and accessibility by lowering the cost and mobility barriers.

Since its inception, seismic data acquisition has been limited by the storage and manipulation of massive amounts of data. With the ever increasing capacities and capabilities of devices over the past few decades, the focus has begun to shift to other aspects of the collection process. In near surface applications, much of the discussion has been over transducers. Traditionally, geophones have been used. The field appears to be moving away these mechanically-based devices to all-electrical MEMS accelerometers (Stewart, 2009). The MEMS receivers provide several advantages over the conventional geophone, which will be discussed in upcoming sections.

Consideration will be given to each component with regards to the practicality, usability, and durability for in-field engineering applications. In the aim of staying relevant in an ever-growing field, the device design will utilize the most modern

technology that is feasible and cost-effective. Additionally, the design will endeavor to be light-weight and compact to facilitate easy transportation and use in difficult field environments. It is in this light that the device components will be selected and discussed in the following chapter.

3. The Device Design and Components

As previously stated, borehole receivers consist of two basic systems: one or more transducers to intercept the seismic signal and a mechanism to couple the transducer to the wall of the borehole for accurate readings. This device, like most commercially available instruments, combines the transducer and coupling mechanism into one body. Unlike those instruments, this device utilizes the concept of an inflatable bladder as the coupler, like with most "homemade" apparatuses. Both of those designs involve pushing a rigid frame to which the transducer is fixed against the borehole wall. The patented design of this device inflates a flexible membrane *around* the body. Transducers are affixed to the interior of this membrane, which, due to the elasticity of the material, allows the device to better conform to the non-uniform shape of boreholes. This allows for a better coupling of transducers to the walls of the hole, increasing data accuracy. The preliminary design of the device is shown in Figure 12 below.

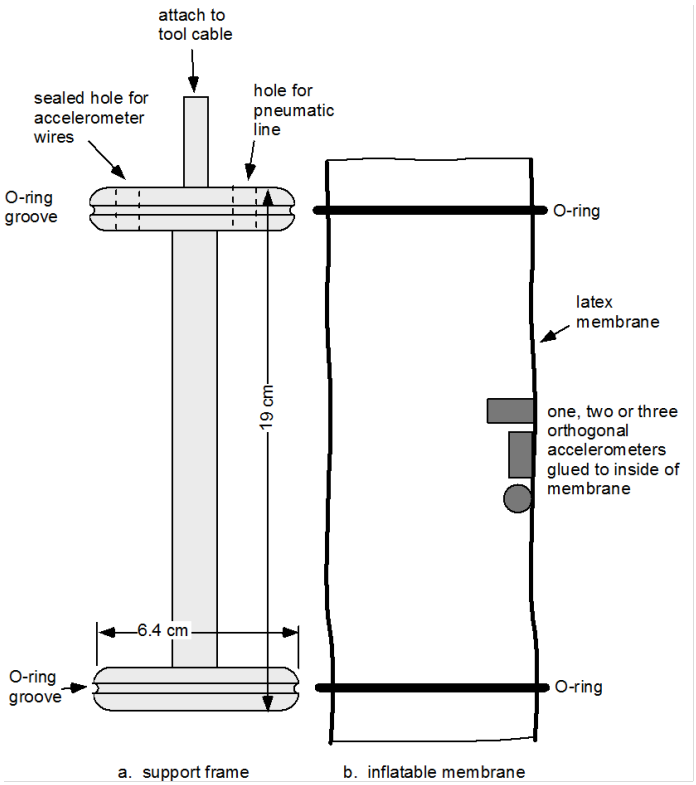

Figure 12: New borehole receiver configuration. (Kalinski, 2012).

The preliminary design, as illustrated Figure 12, was derived from an initial prototype created in 2007 during a tailings dam investigation in Southeastern Kentucky. The device was successfully used to capture shear wave velocities comparable to those found using SASW and CPT methods (Salehian, 2013) for materials in the studied Abner Fork Tailings Impoundment. Potential design improvements from that investigation were proposed for development.

These improvements can be broken down by component. The transducer is arguably the most vital of the device components, as it drives the data accuracy and resolution. It also controls the price of most devices. The component perhaps most crucial to the mobility of the device is the inflation mechanism. In the original design, an air compressor was used at the surface to inflate the device membrane. These

compressors are bulky and add to the load that must be transported for field work. A small, on-board air pump will be investigated as a light-weight alternative. Certainly, the membrane itself is of utmost importance, as it is what makes the device unique and innovative. While the initial prototypes use of a basic latex membrane was sufficient, more resilient material options should be investigated. Additionally, the method of attaching the transducer to the membrane is carefully considered with respect to in-field replaceability. Another potential improvement is the addition of some sort of orientation mechanism to rotate the device in the hole and reference which side the transducers are on. A similar device is also proposed to measure and correct for device inclination, as any deviation from the known orientation may skew measurements. Among other potential improvements are a self-measuring depth recorder and the ability to interface with existing recording equipment.

From these proposals, three components considered crucial to device functionality were selected. These components of the transducer(s), inflation mechanism, and flexible membrane are developed in this chapter to compile the basic device. The additional potential improvements are discussed in Chapter 5.

3.1. Transducer

3.1.1. Background

The two major classes of transducers used in seismic geotechnical applications are geophones and accelerometers. Geophones consist of a mass suspended (typically by a spring) within a coiled wire. When the instrument experiences motion relative to the degree of freedom of the mass, the inertial response of the spring causes it to move

relative to the coiled wire, which generates a voltage. The voltage is the ground response (in the measured axial direction) in terms of velocity. The mechanical system of geophones is very reliable, giving the sensors significant stability and longevity. Additionally, the system enables geophones to operate without any power input. However, the same mechanical system often causes geophones to be relatively heavy and bulky. While geophones range in size, miniature geophones for this application would be on the order of 20 mm in height and diameter with a mass in excess of 20 grams. Seismic-quality geophones typically cost several hundred dollars per sensor. The casing and internal mechanisms of inertial geophones are shown in Figure 13 and Figure 14.

Figure 13: Geophone case

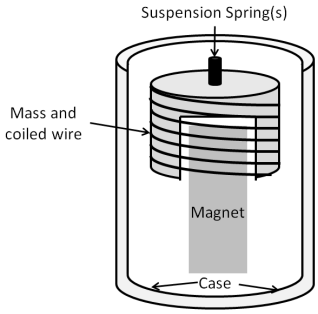

Figure 14: Geophone mechanism

Conceptually, accelerometers also consist of a mass-spring system. These devices use varying methods to record the point at which the acceleration of the damped mass is equal to that of its casing. In other words, the devices record the acceleration of the mass when its acceleration relative to the case (and thus the material it measures) is zero. Thus, accelerometers output signals in terms of the acceleration of the material. One of the most common accelerometer types in geotechnical applications is piezoelectric. Such systems tend to have reduced sensitivity. Popular crystal systems have a low sensitivity that is maintained overtime, which ceramic systems begin with high sensitivity, which degrades

over time (PCB Piezotronics, 2004). These transducers do require an outside power source for operation. The piezoelectric ceramic accelerometers used in the original device prototype required inputs in the range of 18 – 30 V. Wilcoxon T736 accelerometer, for example, are 24 mm long, 12 mm in diameter, 13 grams in mass, and cost around $800 each (Meggitt, 2012). Three of the devices are often used to capture three orthogonal components of motion. The casing and internal mechanisms of a piezoelectric accelerometer are shown in Figure 15 and Figure 16.

Figure 15: Accelerometer case

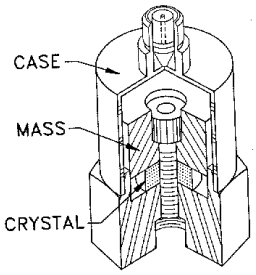

Figure 16: Accelerometer mechanism

Another class of accelerometers utilizes micro electro-mechanical systems. Known as MEMS accelerometers, the transducers operate similarly to geophones and traditional accelerometers. However, rather than using inductance, the MEMS devices use differential capacitance to quantify the acceleration of the suspended mass (Andrejasic, 2008). Because they rely on alternative methods for mass suspension (i.e. cantilever beams), MEMS accelerometers can be made extremely small and light, even allowing for multidirectional measurement contained within one package. With MEMS technology, the three accelerometers used in the initial prototype could be combined into one small, lightweight package, less than one square inch in area. MEMS accelerometers do not degrade like their piezoelectric counterparts. They are even more stable over time

than mechanical geophones due to their simple construction and robust materials (Mougenot & Thorburn, 2004). Most modern MEMS devices are micromachined; such construction precision results in a very sturdy and reliable instrument. Like traditional accelerometers, MEMS transducers do require an outside power source; however, the required input for one triaxial sensor is one-tenth of that required for a uniaxial Wilcoxon accelerometer. While the cost of piezoelectric accelerometers is expressed in terms of hundreds of dollars, the cost of comparable MEMS accelerometers in on the order of tens of dollars. The casing and internal mechanisms of a MEMS accelerometer are shown in Figure 17 and Figure 18.

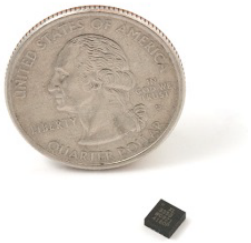

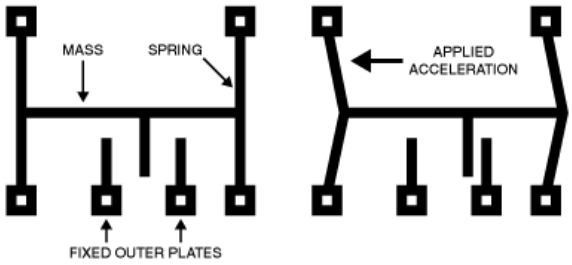

Figure 17: MEMS accelerometer case Figure 18: MEMS accelerometer mechanism

These advantages, coupled with the low cost and high advancement rate of MEMS technology, make these devices appealing for seismic and geotechnical applications. However, such benefits matter only if the performance of MEMS accelerometers is comparable to or exceeds that of geophones and traditional accelerometers.

3.1.2. MEMS Accelerometers in Seismic Applications

MEMS accelerometers have been around for more than thirty years, but they are still relatively new in the seismic field. Researchers began initial studies and tests on MEMS devices around the turn of the century. The debate is still ongoing over the best way to apply the technology, but most researchers agree that MEMS accelerometers provide significant advantages for multicomponent (multidirectional) survey applications. Aside from the weight, size, and cost advantages previously discussed, researchers identified MEMS devices for their performance at low frequencies. The MEMS accelerometers operate at frequencies beneath resonance, while geophones operate above it. For this reason, geophones cannot be used for low frequency signals (typically less than 10Hz). Unlike geophones, the resonance is not the limiting factor for the MEMS accelerometers' operational frequency band. MEMS devices have such high resonant frequencies that noise often overpowers signal before resonance is reached. This is not to say that MEMS accelerometers necessarily have more inherent noise. In fact, some studies have found geophones to have more electronic noise than comparable MEMS accelerometers operating in the same high frequency domain (greater than 50Hz) (Mougenot & Thorburn, 2004). The majority of the electronic noise associated with MEMS systems is due to amplification from using improperly shielded connections and cables.

Thus far, testing and commercial development of MEMS accelerometers for seismic applications has focused on replacing geophone arrays for surface surveys. Early on, studies performed at Sercel, the manufacturing component of the major geophysical services company CGG, identified the potential of MEMS accelerometers to replace

geophones as the industry standard. The two barriers identified were the ability of digital sensors (i.e. MEMS) to be recorded in a multiple receiver array and the manufacturing costs (Mougenot, 2004). The multiple receiver issue is not of concern to the single borehole unit being developed. The concern regarding manufacturing costs is from the viewpoint of a component producer. The device under development will use and modify prefabricated accelerometers. Overall, the study found MEMS devices to have satisfactory response, range, and signal levels for subsurface applications. Sercel has since produced a MEMS-based seismic array system.

Several other researchers have conducted field tests comparing the MEMS transducers to traditional geophones. These studies have primarily focused on low-frequency applications and noise levels of the transducers, though general performance is also observed. One such study by Hons et al. (2008) converted geophone output to acceleration for direct comparison to the output of a MEMS accelerometer. The study conducted surface reflection surveys at two sites using both geophone and MEMS accelerometer arrays. The MEMS device was observed to output lower noise levels at high frequencies and higher noise levels at low frequencies. The study concluded that the two transducer types recorded apparently equivalent reflections. Issues encountered with MEMS noise levels were attributed to improper coupling to the ground media.

Another field study performed in Austria focused on the processing aspect of MEMS and geophone-collected data (Stotter & Angerer, 2011). Stotter and Angerer found that with polarization filtering, the MEMS devices produced "very encouraging results for the higher frequencies." This is significant because while MEMS have historically been investigated for their operation at low frequencies, this device will be

used in broad frequency applications, including higher frequency bedrock. A Canadian study field tested transducers across a 0 to 100 Hz band. The MEMS devices were found to perform well in the range, with instrument noise increasing below 3Hz (Margrave et al., 2012).

Other research has focused on the capabilities of MEMS devices themselves, without comparison to state-of-field technology. Hoffman et al. looked at performance in civil engineering applications, focusing on practicality and usability (2006). One focal area was the calibration of the transducer, with special concern given to sensitivity and frequency range. A calibration technique using a piezoelectric accelerometer is proposed. The MEMS accelerometer was found to perform well within the sensitivity bounds established by the manufacturer. However, it was observed that the noise level became too high at the upper end of the stated frequency bandwidth. The published frequency response of the instrument was 0-1,000 Hz, while the study found the noise too high around 900 Hz. Another potential area identified for additional development concerned the durability of the instrument in harsh civil engineering applications. As previously discussed, the MEMS unit itself is very sound, however the external connections required for power and signal transmissions are very vulnerable. The study recommended packaging the transducer and external connections for durability (Hoffman et al., 2006). The application of these durability study results to the device that is the topic of this thesis will be discussed in Section 5.

The transducer tested by Hoffman is produced by Analog Devices, one of the top producers of MEMS accelerometers for general applications. The ADXL 250 used by Hoffman is no longer produced; however, the company's current line of MEMS

accelerometers makes excellent candidates for seismic applications. Bhattacharya et al. (2012) tested the Analog devices ADXL 335 triple-axis accelerometer against reference traditional accelerometers. The MEMS device was found to perform well across the established frequency range. Ground response tests were performed across dry and saturated soils with satisfactory results. Researchers also performed the calibration and packaging methods recommended by Hoffman et al. (2006). Perhaps most significantly, the study found the signal and noise to be distinguishable up to and even beyond the established frequency response (Bhattacharya et al., 2012).

Outside of Analog Devices, several other companies have developed MEMS accelerometers specifically for seismic applications. These include the DSU428XL accelerometer used in Sercel's MEMS-based seismic array system, the Hewlett Packard (HP) MEMS accelerometer, the MEMS-based MST accelerometer used in Input/Ouput Inc.'s VectorSeis Module, and an entire range of custom MEMS sensors by Colibrys.

The HP seismic MEMS accelerometer was developed for seismic sensing and imaging applications in the oil industry. The device was tested and found to have a good frequency response from 0 Hz to 200 Hz (Homeijer et al., 2011). Preliminary testing by the United States Geologic Survey (USGS) looked at potential ground vibration monitoring applications, comparing the MEMS device against a traditional seismometer (Homeijer et al., 2014). The USGS study recommended improvements in the hardware of the device and the dynamic sensing range for larger amplitude applications, while the noise levels were found to be satisfactory.

The Input/Output Inc. MST and Colibrys accelerometers were also initially designed for seismic exploration in the oil and gas fields. However, the potential for a diversity of applications was immediately recognized. Input/Output Inc. even recommended its device for use in vehicular stability and control in the auto industry (Goldberg et al., 2000). Colibrys studied the potential for MEMS accelerometers' use in rugged field environments, like those often associated with civil engineering applications (Stauffer, 2006).

A more recent study from the group at Sercel introduces a "new generation" of MEMS-based seismic accelerometers (Laine & Mougenot, 2014). In keeping with the general industry trend, the study focuses on lowering the noise levels in devices. Specifically, the study looks to reduce the noise floor at extremely low frequencies (< 5 Hz). The study develops new technology accomplishes this, while also increasing the dynamic range (for use with larger amplitudes). While the developing device is not necessarily concerned with recording such low frequencies, this study does reflect the continual and rapid advancement of MEMS technology. Since the first studies of MEMS-based seismic sensors fifteen years ago, the topic has blossomed from a conceptual goal to a full-fledged industry of commercial instruments. It is the hope that a MEMS accelerometer may be integrated into the device prototypes produced in this project. Even if that is not achieved with technology available today, the development rate of the MEMS field indicates that it can be achieved in the very near future.

3.1.3. Technical Needs

This section will focus on identifying the transducer requirements for this developing device. After the requirements are identified, a transducer will be selected.

While MEMS accelerometers are considered to be the future of seismic sensors and it is greatly desired that they be implemented in this device, data quality cannot be sacrificed. In addition to developing a MEMS-based transducer, thought will also be given to the limitations of current technology. The use of more traditional transducers in this device will be considered. This section will address the technical needs of any transducer for the purpose of this device. In all of the testing and literature on MEMS accelerometers in seismic applications, very little is mentioned on what parameters a good device should have. Those parameters and appropriate values will be identified and established.

Several barriers to seismic application of MEMS accelerometers have been identified in the reviewed studies. Perhaps the largest barrier is the need for external filter capacitors and power regulation. Installation of those devices requires a specific skill set when working with such small connections. Once created, the fragility of the connections is also of concern for the longevity of any instrument (Hoffman et al., 2006). Figure 19 illustrates a typical configuration of a triaxial MEMS accelerometer with locations for external power supply and filter capacitor connections. While the MEMS device itself is entirely self-contained, a capacitor is required for each axis of measurement. Including the power source, this totals four external connections for a typical triaxial accelerometer.

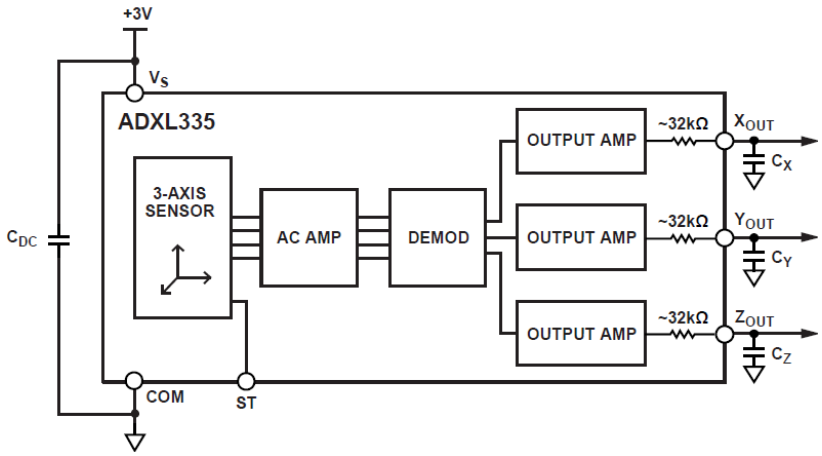

Figure 19: MEMS trixial accelerometer block diagram. (Analog Devices, 2009).

Aside from device construction, data collection quality has also been of concern. For any accelerometer, there are several key parameters that define the device data collection capabilities. These specifications include sensitivity, frequency factors like frequency response and resonant frequency, and noise factors like noise density. All of these pieces contribute equally to the functionality and data collection quality of an accelerometer. They are explored in the following subsections.

3.1.3.1. Sensitivity

Sensitivity is a measure of the transformation of mechanical energy experienced by the internal mass into electrical signal. Expressed as a ratio of the electrical output to the mechanical input of the device, sensitivity essentially defines how apparent the seismic vibrations will be in the output signal. This ratio can vary across the device's frequency range, so specifications typically define it at a particular reference frequency (or voltage for variable MEMS devices).

This sensitivity term is also known as the scale factor, but there are other parameters relating to sensitivity. For multi-component devices, cross-axis sensitivity is

of concern. Cross-axis, or transverse, sensitivity is a function of how well each axial component is measuring its own directional movement, without influence from the motion in the other directions. The specification is expressed as a percentage of the maximum output signal on a given axis that may be due to motion across a different axis. At high percentages, cross-axis contamination becomes a serious noise concern. Values around 5% are considered typical, while values less than 3% are considered low (Endevco, 2009). A value less than 3% is desired for this application.

3.1.3.2. Frequency Response

Another term involving sensitivity is the reference sensitivity. This is more commonly known as the frequency response.

The frequency response is the range of frequencies over which the device will return equivalent signal. Basically, it defines the frequencies over which sensitivity does not significantly change. Most often, frequency response is discussed in terms of the amplitude response of the device. Figure 20depicts typical frequency response curves for the types of transducers discussed. The curves are created by initiating a test signal across many frequencies. The amplitude response (output) of the transducer to the broadband frequency input signal is recorded. The magnitude (amplitude) of the output signal is the frequency response. A “flat-line” or uniform response is expected over the frequency bandwidth. This bandwidth is the range of frequencies that may be accurately measured by the system without skew. On the plot, this bandwidth is represented by the plateau beginning after the resonant frequency for the geophone and by the flat line before the resonant frequency for the accelerometer.

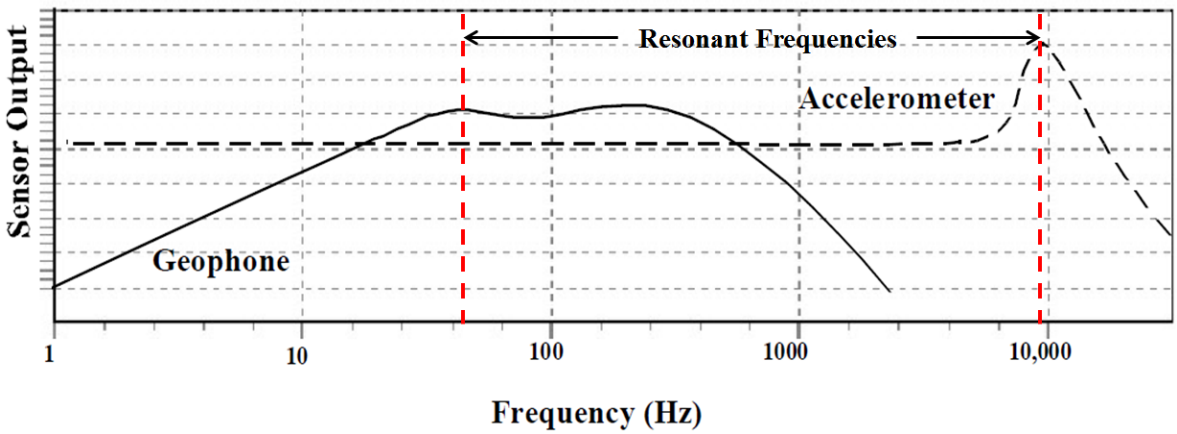

Figure 20: Typical frequency response curves for transducers (Baziw & Verbeek, 2010).

From the understanding of the frequency response curves, it is easy to see that the device's frequency response range is essential to capturing all of the input motions. Selecting an appropriate range for the device application becomes the challenge. While few sources go as far to define such ranges in literature, it is generally understood that a ballpark in the tens to hundreds of Hz is acceptable. In their 2003 Federal Highway Administration report on geophysical methods and applications, Wightman et al. give a range of 25Hz to 300Hz for crosshole seismic waves.

A study investigating the potential to identify thin beds in subsurface surveys found beds as thin as 1 meter in thickness could be identified at the target resolution using a bandwidth of 10-500Hz for hard-rock velocities exceeding 5000 fps (Johnson & Clark, 1992). A surface reflection survey performed as part of the study in South Carolina tested several sources including several hammers and strike plates, as well as a rifle and downhole shotgun device to assess the frequency content of the waves passing through the subsurface. The subsurface included clayey, sandy, and silty soils, as well as limestone bedrock. For P-waves, frequencies were found to range from 60Hz to 350Hz.

For S-waves, frequencies were found to range from 40Hz to 200Hz. It should be noted that the study used 40Hz geophones; therefore, recording of frequencies below that threshold is unlikely (Johnson & Clark, 1992). A separate study looked at the amplitude spectrum of explosive energy sources. The predominant wavelet frequencies produced were around 100Hz, with some approaching 400Hz at 10m from the detonated blasting cap (Knapp & Steeples, 1986). The study also cited wavelet frequencies of other sources: 40Hz to 60Hz for general explosives and 100Hz to 200Hz for rifle shots (Knapp & Steeples, 1986). Another shear wave downhole study found dominant frequencies in the range of 200Hz to 300Hz in frozen clay and ice (Hunter et al., 1998). Based on these studies, a frequency response bandwidth of 30Hz to 400Hz is recommended for this device.

MEMS accelerometers typically do not come with an established frequency response range. Instead, the user will "set" the upper end of the bandwidth by selecting capacitors for each axis of measure. The low-frequency capabilities of MEMS devices are sufficient such that selection based on the low-end of the bandwidth is not of concern for this application. Most manufacturers provide a table or simple formula for capacitor sizing based on the desired bandwidth. This top-end frequency should be within the overall bounds set by the manufacturer in the specifications. Increasing the frequency range, especially above the specified bandwidth, will increase the noise potential in the device. For this reason, care must be taken when selecting the operation frequency range. If it is unnecessarily high, additional noise may be added into the system.

For geophones, the range is more related to the device's resonant frequency. The signal quality of MEMS devices are limited by noise before inputs can reach the device

resonance frequency. Geophones, however, operate beginning immediately above their resonance frequency. This can be observed in the response curves in Figure 20. Rather than selecting for top end of frequency range like with MEMS, when choosing geophones, the range is primarily defined at the bottom end of the range. The resonant frequency of the device must be less than the lowest desired frequency to be measured. Frequency bandwidth should also be checked to verify high frequencies fall within the range.

3.1.3.3. Signal-to-Noise Ratio

For any device, a high signal to noise ratio is desirable. For the purposes of this thesis and device development, signal is defined as the coherent output produced from the reflections, refractions, and other anticipated wave transmissions that are the object of a given study. Noise may also be coherent, the difference being that the outputs classified as noise are not the objects of the study. Signal must out-weigh noise for any successful study, and must do so at a rate such that results are clearly interpretable. This concept can also be expressed in resolution of the output. When signal and noise become jumbled, results are rendered useless. Noise influences have countless sources for any given study. This section will focus on the sources inherent to the transducer, itself.

The noise density specification of a device can give a good idea of the noise baseline. This noise is the random, white noise consistently contributed by the system operations. For MEMS, noise density is expressed as a factor relating the measurable accelerations across the entire bandwidth, as determined by the selected maximum frequency value. It essentially defines the acceleration noise floor, below which signals cannot be distinguished. The acceleration floor is found by multiplying the noise density

by the square root of the maximum value in the frequency bandwidth. Thus, noise increases with increasing bandwidth. For this reason, the selected bandwidth should not exceed what is truly necessary for the device application. Though only field and lab testing will verify this, the noise density for this application should be no greater than 1 $mg/Hz^{0.5}$.

While the noise density gives a general idea of the noise associated with a particular device, there are other factors not included in the parameter that should be considered. As previously mentioned, for devices with multiple axes, transverse sensitivity can be of concern. Low transverse sensitivity values are essential to ensure little to no cross-axis motion contamination. Noise can also be introduced from connections, power sources, and the like. The selected MEMS device should include provisions for decoupling the power source from the accelerometer. Wire connections and the long cables required in downhole and crosshole survey techniques can also introduce noise. Product selection should consider system integration that limits messy connections. Care should also be given to ensure a device cable with sufficient capacitance is selected to pass the survey frequencies without noise. There are also external noise sources. These may include unshielded powerlines or other device systems, such as the on-board pump. A study by Hoffman found external noise to be reduced when the MEMS accelerometer and its connections were encapsulated in a urethane package (Hoffman et al., 2006). This will be further explored with the discussion of the device components. Methods to isolate any vibrations from the inflation pump will be discussed in that component's section.

The topics of external noise and the influence of long cables also apply to geophones. However, with geophones, because the internal system is purely mechanical, the electronic noises associated with MEMS device connections and power supply do not apply. Noise does become a concern when the mechanical motions are converted into signal. Geophones produce an analog signal, which must be converted to digital for survey purposes. This process introduces noise into the system. MEMS devices are available with analog or digital output capabilities. A digital output eliminates noise contributed from the analog conversion.

3.1.3.4. Device Selection

In keeping with the goals of the project, accelerometer selection focused on inexpensive, small, and lightweight models that could be used across the required frequency spectrum. Multiaxial devices were of particular interest due to the reduction of cost, size, and wiring requirements by consolidating the functions of three devices into one. Though MEMS technology itself is not expensive, the commercially available seismic MEMS accelerometers, such as the ones discussed in previous sections, are. A single axis digital MEMS accelerometer from PCB Piezotronics costs around $500. The high prices are likely due to the research and development startup costs the companies have invested in the relatively new field. Costs should come down on those transducers as the technology is refined. Other commercially available MEMS devices, which are produced for general applications, are much more affordable and can be modified to suit the device needs.

Analog Devices is one of the largest producers of MEMS accelerometers for general use. Their ADXL line has been widely studied and used due to its relatively large frequency bandwidth capabilities among other MEMS devices on the market. Additionally, the devices are cheap, readily available, and easily used with other technologies for a multitude of uses. Several mass-market electronics retailers have also developed and modified ADXL devices for even easier integration. These commercial systems and the individual accelerometers have been tested with good results in several civil engineering and seismic applications.

A 2003 study compared several commercial MEMS accelerometers, including the dual-axis ADXL210. The ADXL was found to have the most linear response behavior of the devices tested. The goal of the study was to provide resources for future MEMS accelerometer design and development (Acar & Shkel, 2003). In 2006 a study by Hoffman compared specifications for the single-axis ADXL250 and two "traditional" accelerometers. The ADXL model was again identified for its low cost ($1/20^{th}$ of that of the lowest price competitor) and high performance (having similar frequency response and sensitivity). The study successfully calibrated and packaged the ADXL device. Its frequency response and sensitivity were tested against an industry standard piezocrystal accelerometer. The ADXL250 was found to perform satisfactory during preliminary rod testing and after integration into a geotechnical monitoring system (Hoffman et al., 2006).

Both the ADXL210 and 250 models tested in those studies are now obsolete. This demonstrates the rapid growth and development of the MEMS field. The next generation of ADXL devices is more sensitive, has less noise and error in measurements, and

incorporate more bandwidth over additional axes. The triple-axis ADXL335 is the most seismic-applicable model in this line, and has been thoroughly vetted in recent studies.

As previously referenced, this type of device requires external power regulation and external capacitors to set the upper limit of the frequency range. A capacitor is required for each for each axis of measurement, so with focus shifted to multi-axis devices, more attention has been given to stream-lining the connections of these many devices. Breakout boards with the ADXL335 and required accessories are available. Developed by third-party electronics retailers, these boards provide rigid connections between all components with compact spacing. The boards may include capacitors and power regulation, while maintaining a low price. They provide a solution to many of the problems with working on such small scales and with such delicate connections. Thus, several researchers have opted to use them in their testing and applications of the ADXL335.

One of the first studies to do so looked at testing the board and developing packaging for use in geo-engineering applications. Again, the study compared the ADXL335 to a traditional accelerometer for calibration and performance evaluation. The MEMS device was found to perform well within its set frequency bandwidth across all three axes. The signal to noise ratio was satisfactory from near DC through just below the set bandwidth maximum. The ADXL noise levels were found to be around 0.003 *g*. While these levels were slightly higher than that of the traditional accelerometer, the signals were near identical and easily distinguished for both transducers. The study utilized the ADXL335 package to estimate the ground response of dry and saturated soils.

The devices were successfully embedded in soil stacks to find the shear wave velocity and natural frequency of the soil (Bhattacharya et al., 2012).

The broad application of the ADXL335 includes a 2013 study on its potential for wind turbine monitoring. In this case, rather than using a commercial breakout board, one was essentially created using a printed circuit board and capacitor components. The bandwidth established in this study more likely mimics the conditions that will be used for the borehole receiver device. In the 2012 Bhattacharya et al. study, bandwidth was limited to 50 Hz. The turbine application expands it to near 500 Hz. Accelerometers were attached blades, which were then struck with an impact hammer. The resultant accelerations were found to exceed the noise floor for most tests throughout the bandwidth. However, the noise and acceleration signals became exceedingly close above 100 – 200 Hz (Esu et al., 2013).

The ADXL335 was once more selected for a study looking at economic seismic monitoring. The 2015 study examined its applications for use in seismographs for continual ground vibration monitoring. The ADXL335 was praised for its high sensitivity and produced satisfactory results (Patil et al., 2015).

The ADXL335 triple-axis accelerometer from Analog Devices was selected for development in this device. It is selected on the basis of both commercial and technical considerations. Its low cost, high availability, and easy incorporation makes it a very logical choice from the market standpoint. Its large bandwidth, high sensitivity, and small size make it a sound technical choice with regards to data quality and instrument functionality. At only 1.45 mm thick and 4 mm square, the ADXL335 weighs a fraction of a gram. The accelerometer is shown in Figure 21. The cost of a single unit is $10, with

the price decreasing with larger quantities. The device operates on direct current in the range of 1.8 to 3.6 Volts. External power regulation is required. Manufacturer testing is performed at 3 Volts. Two of the axes have a variable bandwidth of 0.5 Hz to 1600 Hz, with the third at 0.5 to 550 Hz. External capacitors are required to set the upper limit of the frequency range (Analog Devices 2009).

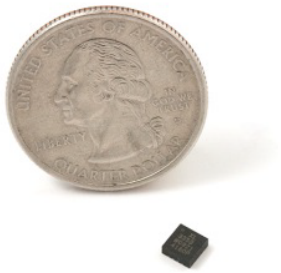

Figure 21: Analog Devices ADXL 335 MEMS accelerometer

Due to the small size of the transducer and difficulty with creating connections at that scale, the accelerometers were purchased pre-installed on breakout boards with power regulation and filter capacitors. The included capacitors limited the bandwidth to 50 Hz, which is too low for hard rock applications. Thus, new capacitors were installed to increase the bandwidth. Per the specifications provided by Analog Devices, a capacitor of 0.01 μF should set the bandwidth to 500 Hz. This should capture the 30 to 400 Hz needed by the borehole receiver, without exceeding the noise constraints of the accelerometer. The bandwidth provided by any given capacitor can be checked using the following simple calculation provided by the manufacturer, where *F* is the bandwidth produced by capacitance, *C*:

$$F_{-3dB} = \frac{1}{2\pi(32k\Omega)C_{(X,Y,Z)}} = \frac{1}{2\pi(32k\Omega)(0.01\mu F)} = 497Hz \approx 500\text{Hz}. \qquad (3.1)$$

Capacitor selection was also limited by the physical constraints of installation on the breakout board. Connections had to be spaced close to the same as the original capacitors, and couldn't exceed the dimensions allotted by the board layout. Capacitors with 0.011μF capacitance were selected. This slightly restricts the available bandwidth to below 500Hz, but still allows for capture of the maximum predicted survey frequencies. The new bandwidth is calculated per the equation below.

$$F_{-3dB} = \frac{1}{2\pi(32k\Omega)C_{(X,Y,Z)}} = \frac{1}{2\pi(32k\Omega)(0.011\mu F)} = 452Hz \approx 450 \text{ Hz}. \quad (3.2)$$

The selected board provides 3.3 V power regulation, which is the same as was used in the turbine study (Esu et al., 2013). The regulator can take inputs as high as 5 V and regulate them down to 3.3 V. While this voltage is slightly above the manufacture-tested 3 V, it is within the recommended 1.8 – 3.6 V. The board also includes another 0.1 μF capacitor to decouple the power source from the accelerometer. This should help reduce some of the noise potential of the device.

The reported noise density for the ADXL335 is 150 μg/Hz$^{0.5}$ for the X and Y axes and 300 μg/Hz$^{0.5}$ for the Z axis. These specifications are within the stated desired maximum of 1 mg/Hz$^{0.5}$. However, the level of the noise floor should be checked to ensure readings can be obtained within the desired acceleration range. The maximum noise floor for the device can be calculated from the established bandwidth for axis Z per the following equation:

$$Noise\ Floor = \text{Noise Density} * \sqrt{F_{-3dB}} = 300\,\frac{\mu g}{\text{Hz}^{0.5}} * \sqrt{452\text{Hz}} = 6.38\text{m}g. \quad (3.3)$$

This value is the root mean square (rms) noise of the device. The manufacturer acknowledges that this noise floor may be exceeded during normal device operation. They indicate the floor may be as high as twice the rms value (12.76 m*g*) 32% of the time, as high as four times the rms value (25.52 m*g*) 4.6% of the time, six times the rms value (38.27 m*g*) 0.27% of the time, and eight times the rms value (51.03 m*g*) 0.006% of the time. This absolute maximum value of 51.03 m*g* represents 1.4% of the device's ±3.6*g* measurement range, while the rms floor, and the practical maximum value of 12.76 m*g* represent only 0.1% and 0.4% of the measurement range, respectively.

The sensitivity of the ADXL 335 is proportional to the power supply because it has a ratiometric output. The specifications cite the sensitivity at 360 mV/*g* for a power supply of 3.6V and at 195 mV/*g* for a power supply of 2V. At the selected voltage for this application (3.3V), the sensitivity is assumed to be 330 mV/*g*. The cross-axis sensitivity is at 1%. This low value is due to the accelerometer's construction as a single, micro-machined device, without separate sensing structures for each axis.

The breakout board, capacitor replacement, and retooling brings the accelerometer material costs up to $20 per unit. The board is 19 mm square, and approximately 3mm thick (including components) at its widest point. The unit weighs 1.3 grams. The board is shown in Figure 22. The unit is still sufficiently lightweight and small to satisfy the goals of the device. Using the board reduces some of the delicacy of connections cited by several authors as a barrier to practical seismic MEMS use (Hoffman et al., 2006; Bhattacharya et al., 2012). All inter-component connections are rigid and protected by the board's structure. The layout of the board is such that it may

also be easily encased into waterproofing packaging or incorporated into the design of the membrane.

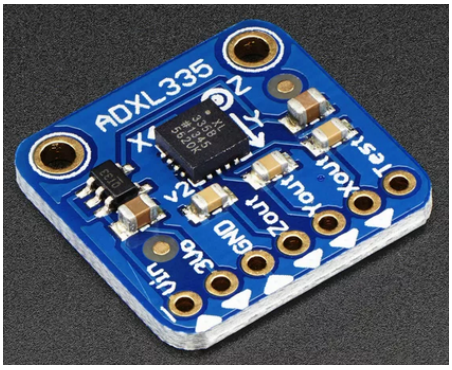

Figure 22: Adafruit breakout board with ADXL 335 accelerometer

While this MEMS accelerometer appears to be a good candidate for this device application, more traditional transducer options are also selected in case of unforeseen obstacles with MEMS use. The Wilcoxon T736 accelerometers used in the original device prototype are sufficient; however, there are smaller, lighter, and cheaper models that will perform just as well as for this application. The PCB 353B16 is a piezoelectric crystal accelerometer with comparable properties to the Wilcoxon model. The 353B16 has a very large frequency response of 1 – 10,000 Hz. At 100 mV/*g,* its sensitivity is less than that of the ADXL335 MEMS transducer. It requires a much larger power supply with a range of 18 – 30V. The noise floor is comparable to the MEMS accelerometer, with a broadband equivalent acceleration levels ranging from 64 to 2800 μ*g* at the high and low ends of the frequency bandwidth, respectively. The accelerometers are 18.5 mm long, 7 mm in diameter, weigh 2 grams, and cost $320 each (PCB, 2002). Three would be required for the device, bringing the total for the instrument to $960. Suitable triple-axis piezoelectric accelerometers are also available, but typically cost around $1,300. Little is

gained in exchange for the cost tradeoff, thus, the more readily available single axis transducers are selected.

With regards to geophones, miniature geophones would be most applicable for this device. As with the piezoelectric accelerometers, three separate geophones will need to be used to capture motion in each orthogonal direction. Thus, size and weight constrictions take some prevalence over cost considerations. While several candidates may exist on the market, the GS-20DM geophone produced by Geospace Technologies has been identified for its dimensions and capabilities. The GS-20DM is 26.4 mm tall with a 22.2 mm diameter. Each unit weighs 43 grams. The 10 Hz (natural frequency) version has a bandwidth in excess of 300 Hz, which should satisfy the majority of device applications. Alternatively, the 14 Hz version has a bandwidth in excess of 400 Hz. Intrinsic sensitivity values for the models are 19.7 and 17.7 V/m/s, respectively, which should be sufficient (Geospace, 2012). The cost per unit for both models is $55, bringing the total for the instrument to $165.The 14 Hz GS-20DM is recommended for this device.

In theory, all of the selected transducers should suffice for the device application. However, laboratory testing is required to confirm this. It is the hope that the testing will confirm the MEMS device as a good alternative to traditional piezoelectric accelerometers. This would result in a savings of approximately $1,000 per device. While bulkier and requiring additional signal processing, the geophones are also analyzed for their potential to save hundreds of dollars per device. A side-by-side of the manufacturer specifications is included in Table 1.

Table 1: Transducer specifications

	MEMS Accelerometer		Piezoelectric Accelerometer		Geophone	
Model Number	ADXL335		PCB353B16		GS-20DM – 14Hz	
Triaxial Material Cost[1]	$20		$960		$165	
Triaxial Mass[1]	1.3 g		6.0 g		129 g	
Sensitivity	330 mV/g		10 mV/g		17.7 V/m/s	
Bandwidth	5 Hz	450 Hz	1 Hz	10,000 Hz	14 Hz	400 Hz
Power Required	1.8 – 3.6 VDC		18 – 30 VDC		0 VDC	

1 – Parameters when using transducer(s) to measure in three orthogonal directions

3.1.4. Transducer Lab Testing

Transducer testing compared the three selected devices, primarily using the piezoelectric accelerometer for comparison. Such piezoelectric accelerometers have become the standard technology for compact geophysical measuring devices, thus, their output is the baseline to which the other transducers are compared. Responses from the transducers were compared, using signal analysis software. Additional testing checked the potential field performance of the instruments. The response signal for the MEMS accelerometer was routed through long field cable and compared against ideal transmission conditions. The long cable is required for downhole receiver use and was investigated due to the possibility of electrical interference with the transmitted signal.

3.1.4.1. Equipment Used

To facilitate testing, a dynamic signal analyzer was used. Such devices enable the user to easily collect and process seismic data. For this testing, the SignalCalc Ace from Data Physics and accompanying software was used. The system is highly portable and easily adaptable, making it a prime candidate for field data collection.

All of the selected transducers have an analog output, which needs to undergo digital conversion prior to analysis. Additionally, both of the accelerometer types require external power to operate. Several pieces of equipment were used in the laboratory testing to accomplish this and facilitate signal interpretation. A signal conditioner was used with the piezoelectric accelerometer, while a signal analyzer was used with all of the tested instruments.

The analyzer hardware provides digital conversion of the transducers' analog outputs and provides power to piezoelectric accelerometers. The power supplied is too high for the MEMS device and would damage the board and components. When testing the MEMS accelerometer, no power was supplied from the analyzer. A battery pack was used as an alternate power source. The battery pack supplies power in the 3.3 – 4.8 V range when used with three AAA alkaline batteries. With the on-board power regulator, the MEMS accelerometer requires voltage in the 3.3 – 5.0 V range. The geophone requires no external power supply. The hardware enables a high sampling rate and is equipped with antialiasing filters, which should ensure accurate measure of the transducers' capabilities (Data Physics, 2013). Due to the capabilities of the analyzer and the robust outputs of the transducers, a signal analyzer was not used.

The analyzer software includes several programmed testing regimes. Each regime processes input data from the transducers to produce several output signals. Signals may be filtered, averaged, added, multiplied, or otherwise transformed into useable data. This testing primarily utilized the Transfer Function test. The signals of interest produced include the input signal time histories and coherence function. The coherence function is a measure of the similarity of two signals. When considering a known input and

measured output, coherence quantifies the output signal energy that is of direct result from the input (Santamarina & Fratta, 1998). In this way the noise in a system can be measured. This testing utilizes the function to compare the output of two different transducers to the same input signal. Using the coherence function, the MEMS accelerometer and geophone outputs may be compared to that of the piezoelectric accelerometer. Coherence is typically expressed as a function across a frequency spectrum. A value of one indicates identical energy responses between the two signals at the given frequency, while a value of zero indicates no response similarity (Santamarina & Fratta, 1998). Plots of the resulting coherence function with values ranging from zero to one across the selected frequency spectrum will be presented.

In addition to these testing regimes, the software also facilitates unit conversion, including automatic differentiation and integration across displacement, velocity, and acceleration domains. This is of particular use when comparing geophones, which output proportionately to voltage, to accelerometers, which measure acceleration. The integration allows all of the selected transducers' signals to be directly compared in terms of acceleration. This was achieved by specifying the sensitivities of the respective transducers. Manufacturer specifications listed in Table 1 were utilized.

The system also includes an anti-aliasing filter. Aliasing occurs when the signal frequency exceeds the sampling rate. This results in reduced, oversimplified recorded signals. Filters establish the maximum frequency recorded by the system. The SignalCalc Ace establishes its sampling rate based on that frequency, ensuring signals below the filter threshold are not aliased (Data Physics, 2013). A filter bandwidth of 1 kHz was used in this testing. The upper limit is sufficiently above the 400Hz maximum required

by this device application so that the true range of the tested transducers may be observed. The system then established a sampling rate of 1 per 0.391 ms. To check the effectiveness of the filter, the Nyquist frequency of the system was checked. The Nyquist frequency is the maximum frequency below which aliasing is unlikely to occur. It can be calculated given the sample rate per the following equation.

$$N_f = \frac{1}{2t} = \frac{1}{2(0.391\ ms)} = 1280\ Hz \tag{3.4}$$

where N_f is the Nyquist frequency and t is the time between samples. Per the calculation, signals below 1,280 Hz should not be aliased. Thus, the filter sufficiently protects against aliasing for the desired range of 0 – 1kHz.

The option to remove the DC offset from the recorded data and prior to integration was selected. The DC offset, or bias, is the voltage measured when the device is on, but at rest. It typically comes from the analog to digital conversion process and results in an offset of the amplitude baseline. The MEMS accelerometer is especially subject to the DC offset, due to its use of electronic systems and processes. The DC offset was observed to be small, but apparent in the MEMS device. Its elimination is vital to capturing accurate accelerations. The SignalCalc Ace does this by removing the mean value of recorded vibrations (Data Physics, 2013).

3.1.4.2. Setup

Several testing setups have been proposed for calibrating and/or comparing MEMS accelerometers to other transducers. Hoffman et al. utilized several techniques to measure different parameters. Sensitivities were compared by affixing the transducers to the end of a steel rod, which was agitated. Another set up involved stacking the

transducers on a metal plate, which was then struck with a hammer to evaluate their frequency responses (Hoffman et al., 2006). Albarbar et al. utilized a shaker to agitate MEMS and piezolelectric accelerometers with periodic, random, and impulsive excitations (2009). Most other literature focused on field studies and comparison in surface monitoring applications.

For this lab testing, a plastic plate set up with impulsive excitation was selected. Using the piezoelectric accelerometer as the baseline for each test, two transducers were placed equidistant from the source location on the plate. The plate was then struck and the signal outputs from the transducers compared using the signal analyzer and software. This constituted the active portion of the testing. Due to the constraints of the laboratory setting, it was easier to consistently excite a significant response in the transducers using P-waves. Additionally, field studies have found P-waves to have a richer frequency content than S-waves, which is important in coherency testing. The impact location for each test was along the plate edge, 12 inches from the transducer. The hammer strike was perpendicular to the axis of interest.

Testing in this manner was repeated for the MEMS and piezoelectric accelerometers and for the geophone and piezoelectric accelerometer. An additional setup compared two MEMS accelerometers. In this case, the signals of one device were passed through a 100 foot foil-shielded PVC field cable. This was done to verify the transducer's field performance. One of the key barriers to MEMS accelerometers' use, as cited throughout literature is the noise level associated with the electronic systems. Electric noise increases over increasing transmission lengths, especially in improperly shielded

cables. Transmission cables are discussed further with the device accessories. Aside from the transmission cable, all other testing parameters were not changed.

Testing was performed in each orthogonal direction of the MEMS accelerometers. All tests were performed in both the active and passive states. Active states consisted of the hammer impact testing, while passive testing was conducted while the transducers were theoretically at rest, with no applied impact. For the accelerometers, passive testing was conducted both with and without the power supply. The focus of passive testing was to establish the legitimacy of active coherence measurements and to check the noise levels of the various transducers. Collected signals included coherence of the two tested transducers, as well as basic time histories of each signal.

3.1.4.3. Results

The coherence plots of active recorded signals for each transducer comparison setup are presented in Figure 23 through Figure 25 below. For cases involving the triaxial MEMS accelerometer, all three orthogonal comparisons are included. Representative plots of the coherence functions of passive recordings are included in Figure 26 and Figure 27. The time histories of passive recordings are presented in Figure 28 through Figure 32. A representative time history of an active recording is presented in Figure 33.

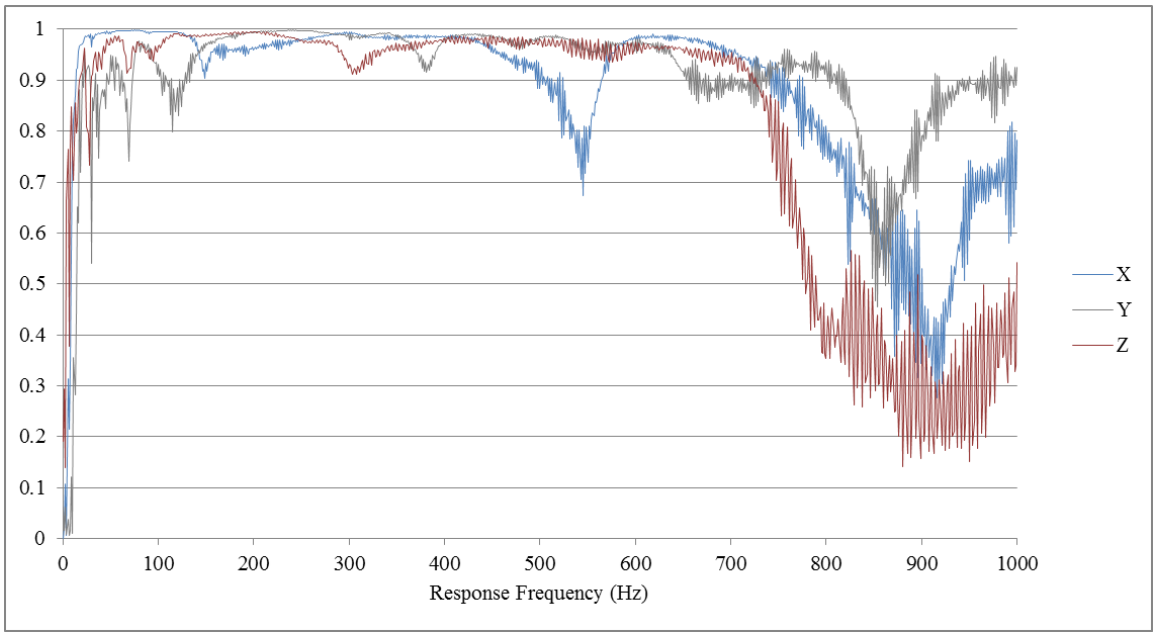

Figure 23: Coherence of active MEMS and piezoelectric accelerometers

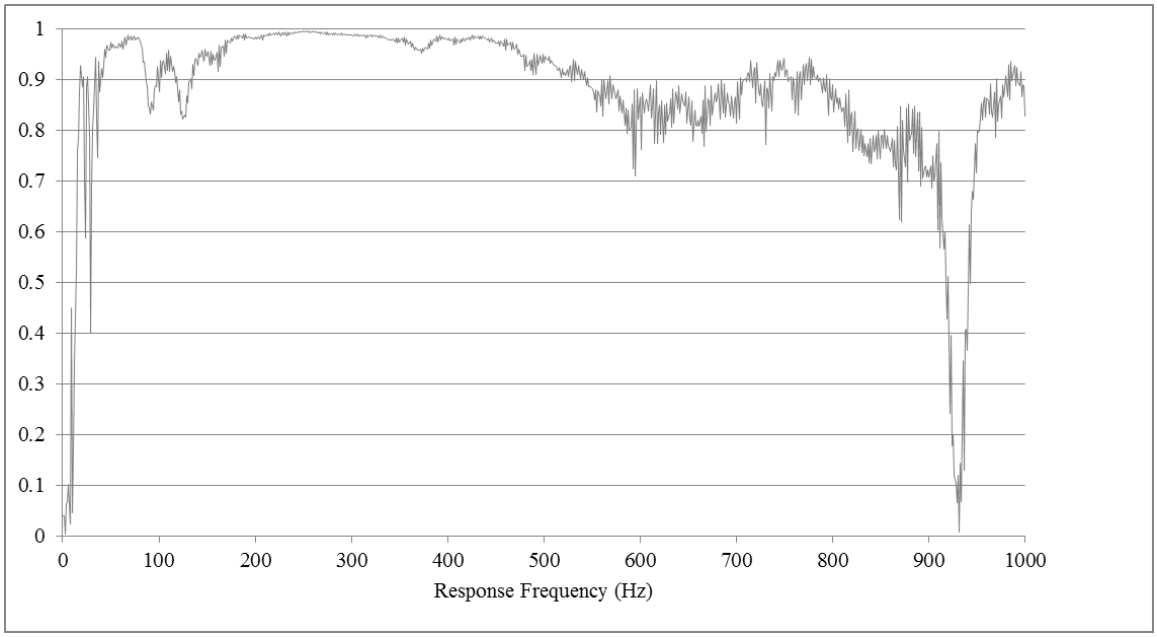

Figure 24: Coherence of active piezoelectric accelerometer and geophone

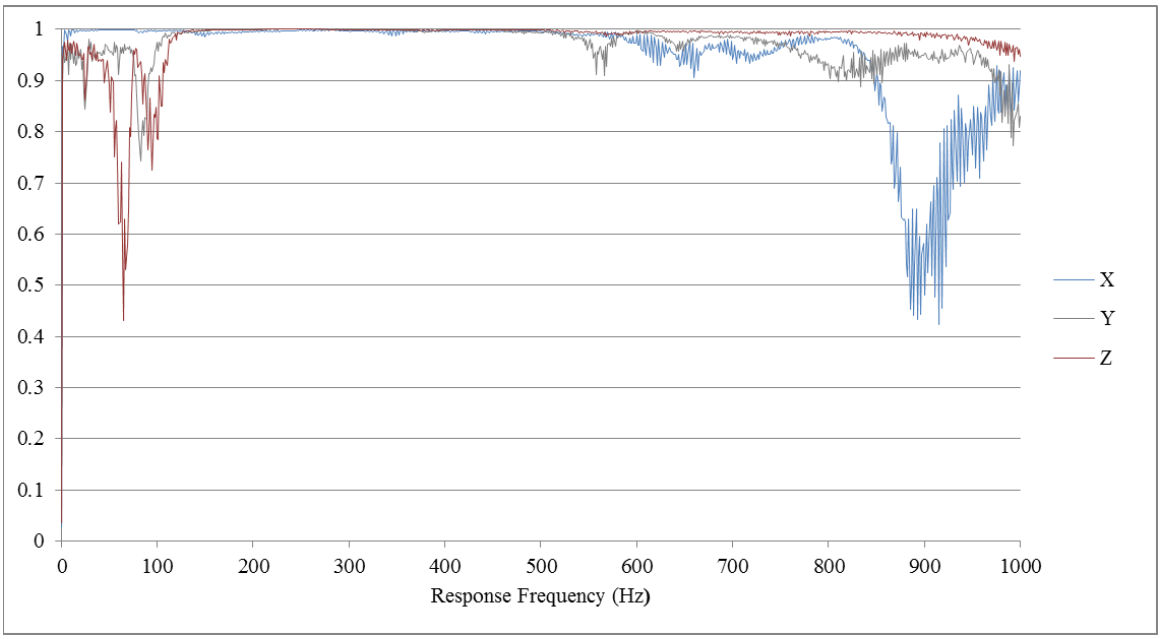

Figure 25: Coherence of active MEMS and cabled MEMS accelerometers

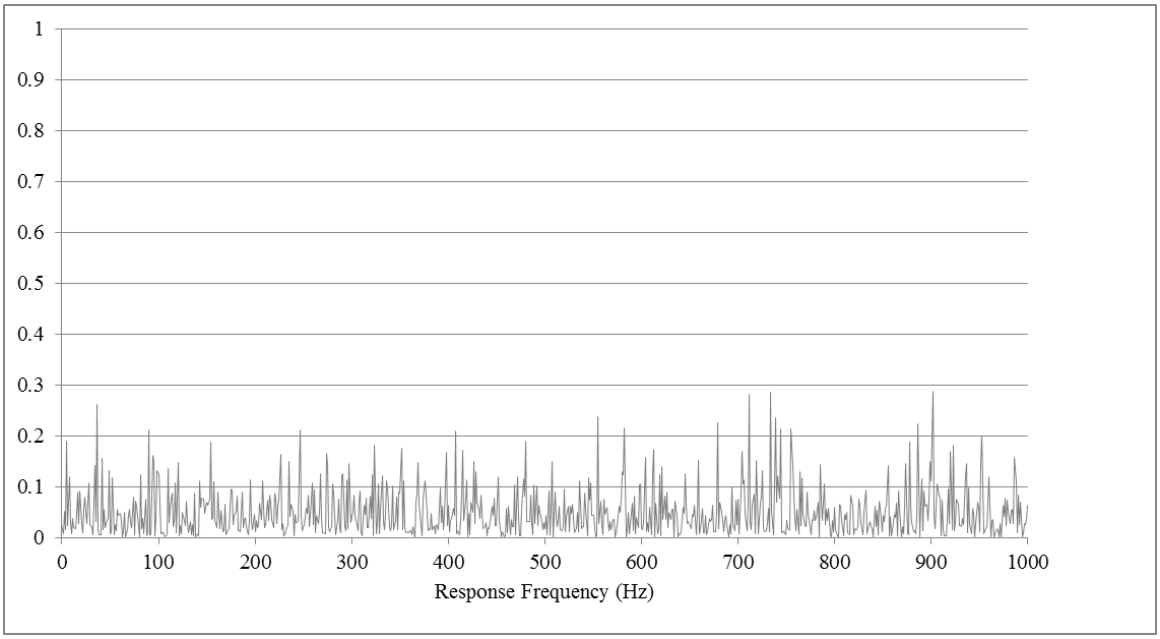

Figure 26: Coherence of passive, powered MEMS and piezoelectric accelerometers

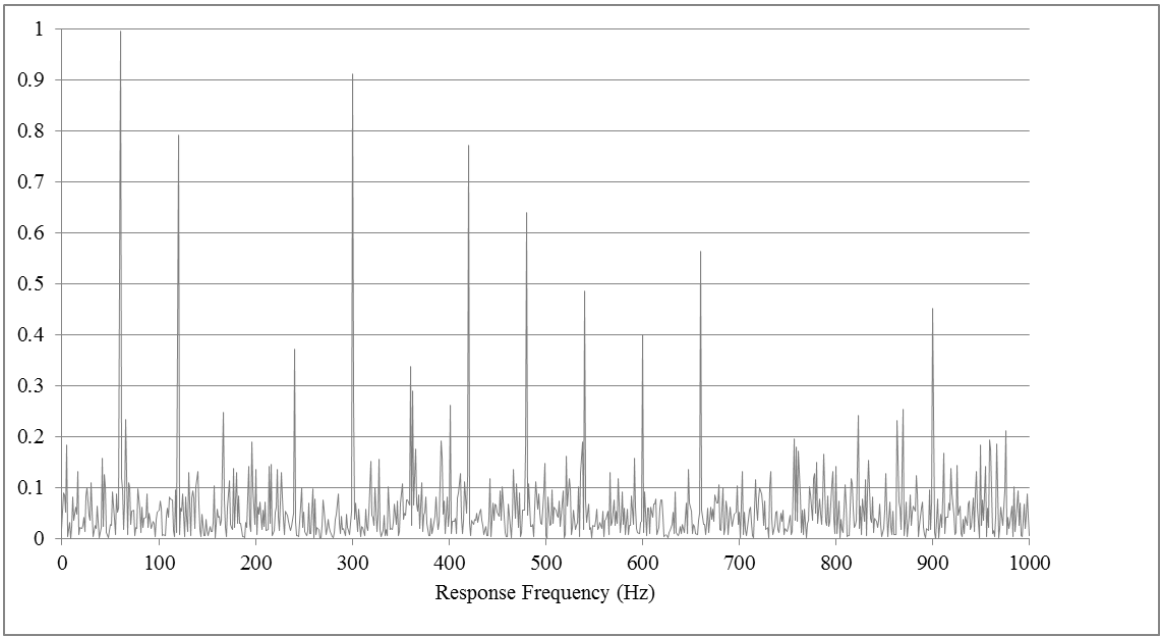

Figure 27: Coherence of passive, unpowered MEMS and piezoelectric accelerometers

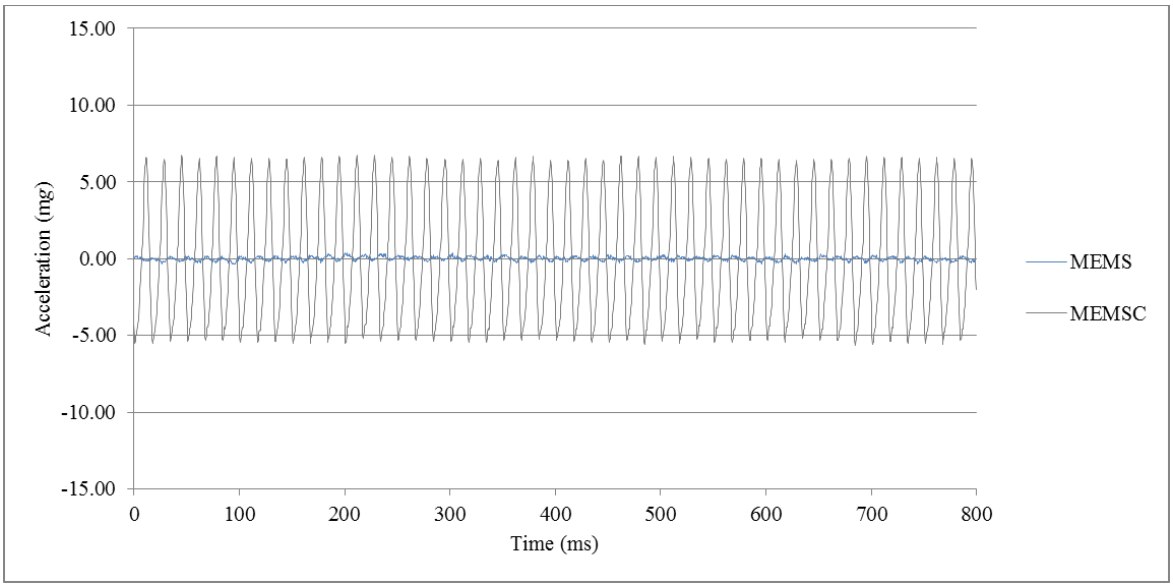

Figure 28: Signals of passive, unpowered MEMS and cabled MEMS accelerometers

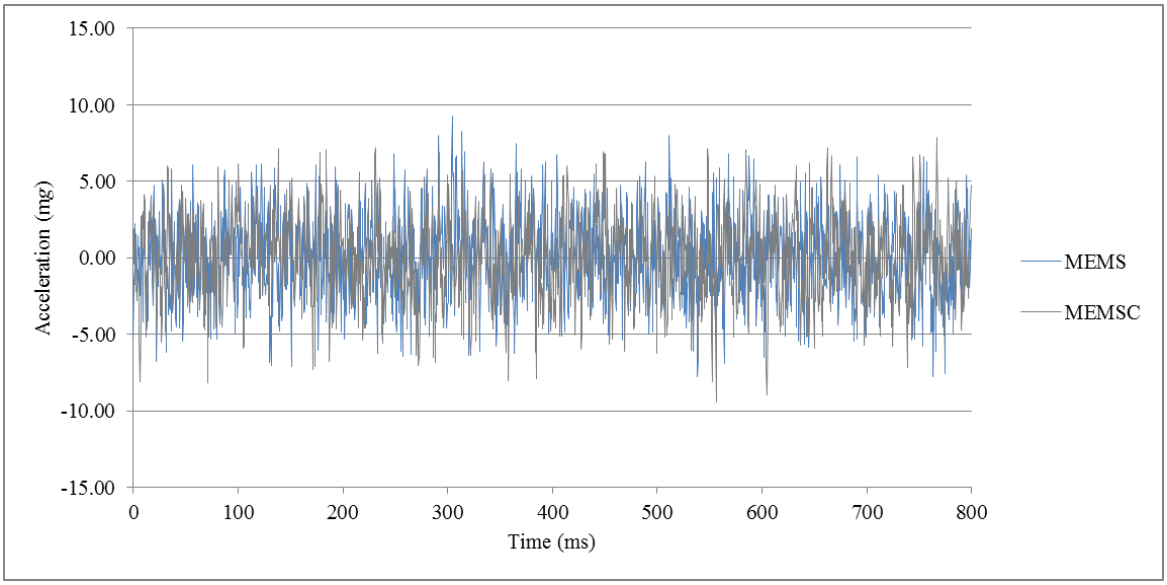

Figure 29: Signals of passive, powered MEMS and cabled MEMS accelerometers

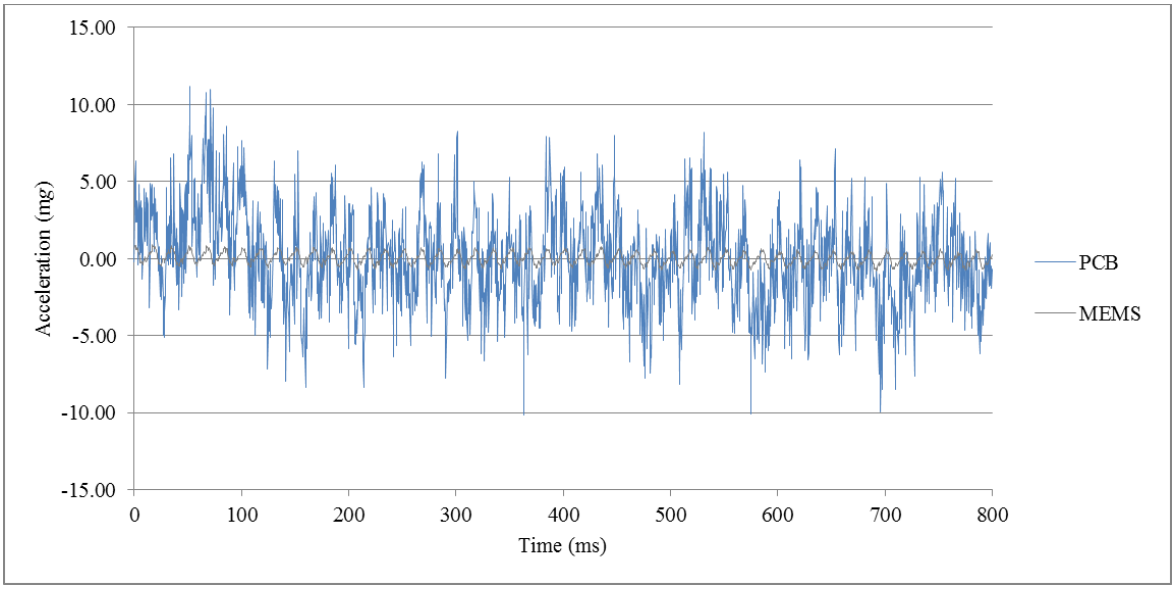

Figure 30: Signals of passive, unpowered MEMS and piezoelectric accelerometers

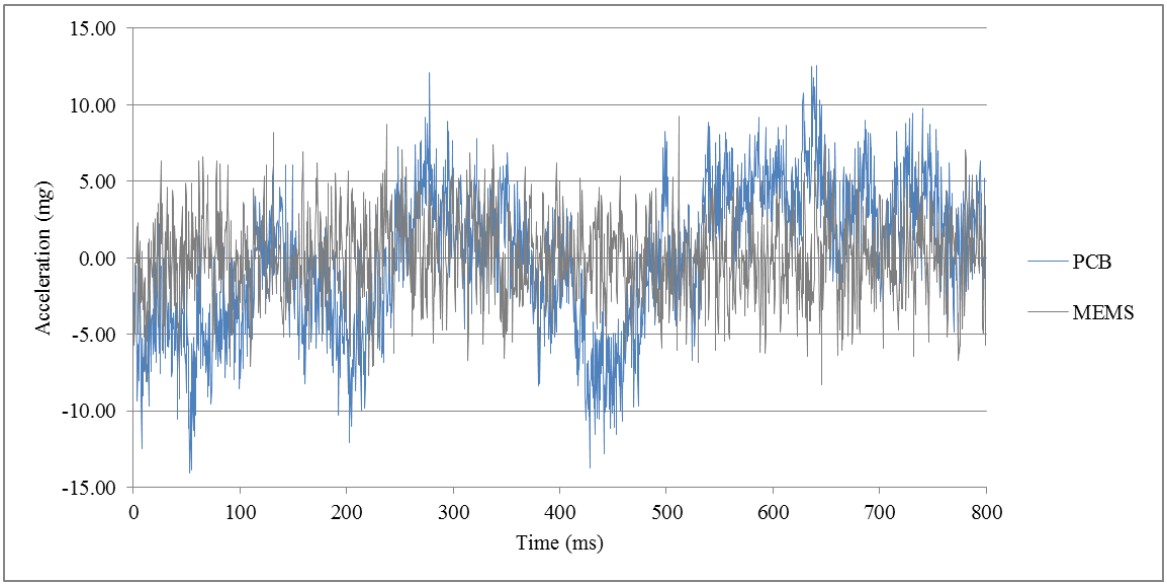

Figure 31: Signals of passive, powered MEMS and piezoelectric accelerometers

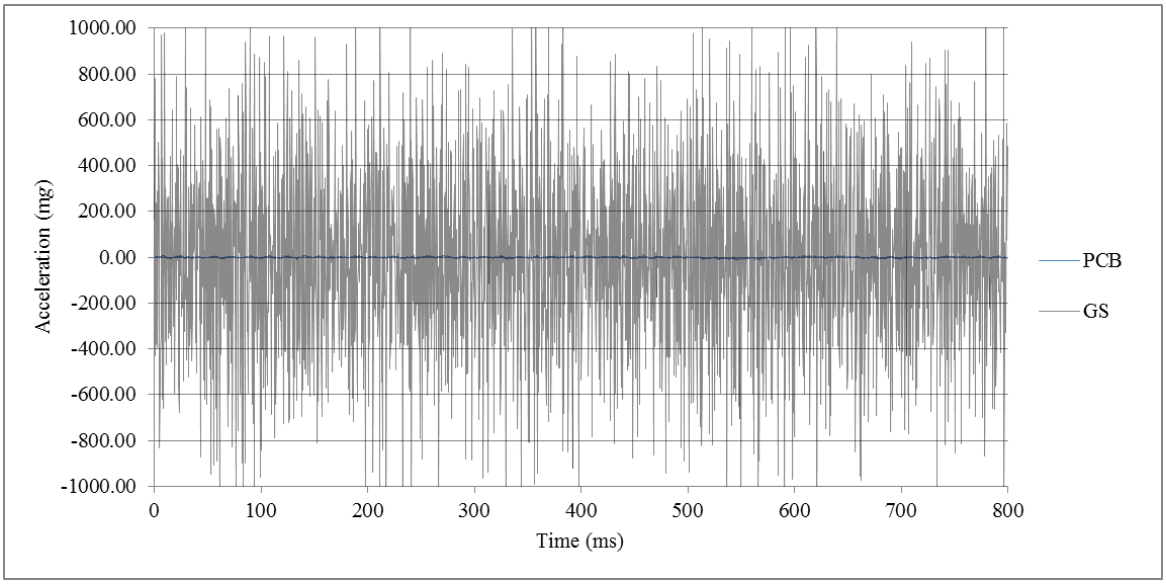

Figure 32: Signals of passive, unpowered piezoelectric accelerometer and geophone

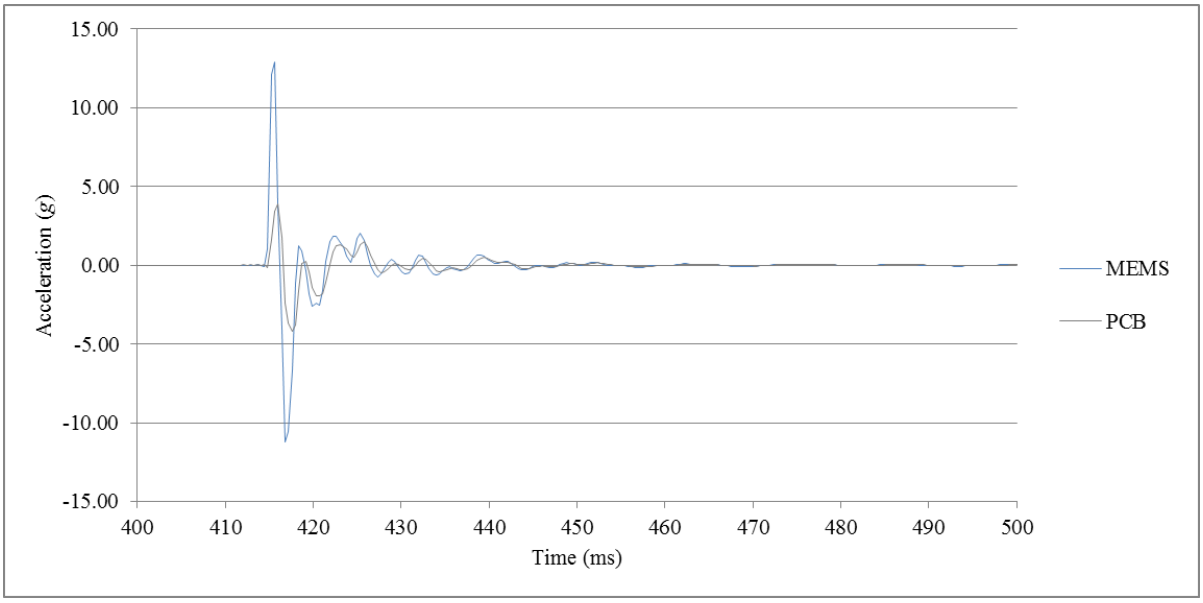

Figure 33: Response of piezoelectric and MEMS accelerometers to impulse source

3.1.4.4. Discussion

Coherence values of one indicated identical signal response from the two transducers for signals at that given frequency. Figure 23 shows relatively good coherence between the piezoelectric and MEMS accelerometers during active testing across all axes of the MEMS device over the frequency range necessary for this application. Figure 24 illustrates comparable coherence between the piezoelectric accelerometer and geophone during active testing. These results indicate the tested ADXL 335 MEMS accelerometer performs well against the piezoelectric accelerometer baseline and is a sufficient transducer for this device. The GS-20DM 14 Hz miniature geophone also performs well, and would be adequate, size considerations aside. Figure 26 and Figure 27 illustrate the coherence of the passive responses of the MEMS and piezoelectric accelerometers. These plots verify the high coherence observed in the active recordings is a direct result of applied signals and not testing conditions. The high

coherence value peaks in Figure 27 may be from ambient noise at those frequencies. Testing was performed in a laboratory setting where other equipment is running. The frequencies of these peaks correspond with that of some discontinuities observed in the active coherence plots.

Noise was further quantified via the passive time histories in Figure 28 through Figure 32. Figure 28 indicates higher noise levels in the cabled MEMS when the devices are unpowered. However, similar noise levels are observed across both instruments once power is introduced in Figure 29. This indicates noise propagation is not of concern with the MEMS device in the field. This is further confirmed in Figure 25, which depicts excellent coherence across all axes of the cabled and uncabled MEMS accelerometers during active testing. MEMS noise levels were observed to be less than or equal to those of the piezoelectric accelerometer and geophone in all passive cases. The geophone exhibited exceptionally high noise levels, up to 1 *g*. However, some of that noise may have been falsely amplified during differentiation from velocity to acceleration terms.

Figure 33 shows the response of the MEMS and piezoelectric accelerometers to an impulsive signal. This time history is representative of the signals received during all of the active testing. While the signals match fairly well, there appears to be a scaling discrepancy in the peak amplitude. This is likely due to error in using the manufacturer's sensitivity rating in the calculations. Sensitivity testing was not feasible in this study, and should be evaluated prior to any additional transducer testing. It should also be noted that none of the devices were calibrated beyond their manufacturer's calibration. Laboratory calibration is recommended to achieve better coherence; however, such resources were not available during this study. Regardless, the presented testing results indicate the

selected MEMS ADXL 335 accelerometer and GS-20DM 14 Hz miniature geophone would be adequate transducers for the borehole receiver device.

3.2. Inflation Mechanism

The coupling device is one of the two major components of borehole receivers. For this instrument, that device is composed of the patented inflatable wrap-around membrane design, and the mechanism used to inflate it. With traditional borehole receivers, the inflation mechanism has often been the limiting factor with regards to instrument mobility. Large, bulky surface air compressors are typically used to inflate the bladders that hold the transducer against the borehole wall. For this device, which has already increased mobility potential by reducing the size, weight, and number of components in the receiver design, improvement in this area was also investigated. Preliminary discussions of potential solutions keyed in on the use of a small pump that could be installed on the instrument. This onboard pump would integrate yet another separate component into a singular, streamlined design. Simplified alternatives are also investigated for their potential use.

3.2.1. Design Considerations

Functionality of the device in water-filled boreholes is of major concern due to the prevalence of shallow groundwater throughout most temperate climate zones. In addition to waterproofing of electronics, which is discussed with the membrane development, the main issues concern the forces associated with the water. The hydrostatic pressure at the bottom of the borehole must be overcome by any inflation mechanism. Additionally, the buoyancy of the device must not interfere with its ease of use and accuracy of readings.

3.2.1.1. Hydrostatic pressure

Hydrostatic pressure increases linearly with depth. To avoid over- or under-estimating its magnitude at the bottom of a borehole, a maximum depth must be selected. This depth will represent the maximum head below which the device's inflation mechanism will operate. The device should be able to fully inflate in a reasonable amount of time and maintain its inflation during all required measurements. When selecting this depth, factors including typical practice and regulations were considered. Typical borehole depths range in the tens to hundreds of feet. When considering the one of the main uses of the device, to develop velocity profiles for site characterization, the International Building Code (IBC) was consulted. Per IBC sections on "Site classification for seismic design," calculations should be performed for the upper 100 feet of the subsurface (International Code Council, 2009). Thus, 100 feet will be assumed for the borehole depth for design purposes. It is not reasonable to assume a water column of the same length. A ground water table depth of 20 feet will be used, which makes the final design head 80 feet. This corresponds to a hydrostatic pressure of 35 psi (241 kPa) at the base of the design borehole per the following equation.

$$u = \gamma H = (62.4\,pcf)(80') = 4992\,psf = 34.67\,psf \qquad (3.5)$$

where u is the hydrostatic pressure at the bottom of the borehole, γ is the unit weight of water, and H is the height of the water column. This pressure represents the force the selected mechanism must overcome to inflate the membrane.

3.2.1.2. Buoyancy

The buoyant force is an upward-acting force equal to the volume of the fluid displaced. If this force significantly exceeds the weight of the device, the unit may, at worst, float to the top of the borehole or, at best, make positioning difficult. To examine the potential effects, the buoyant force was estimated using the initial prototype dimensions in several standard-sized boreholes. A cylinder is assumed for the inflated shape of the membrane. The initial prototype allows for a membrane approximately 6.5 inches long, fastened around two ends with diameters of 2.75 inches. The diameter of the borehole, rather than that of the device fastener, will be used in calculations. The equation for the volume of a cylinder is as follows.

$$V = \pi \frac{d^2}{4} H \tag{3.6}$$

where V is the volume, π is the mathematical constant, d is the diameter, and H is the height. When combined with the weight of water displaced, the buoyant force acting on the inflated instrument can be calculated for a 3-inch borehole using the following equation.

$$F_B = (\gamma_w - \gamma_m) * \pi \frac{d^2}{4} H = (62.4\, pcf - 0\, pcf) * \pi \frac{(3")^2}{4} (6.5) = 1.7\, lb \tag{3.7}$$

where F_B is the buoyant force, γ_w is the unit weight of water, γ_m is the unit weight of the membrane inflation material (air), π is the mathematical constant, d is the diameter, and H is the height. Table 2 shows the buoyant forces for other standard sizes of boreholes.

Table 2: Buoyancy by borehole dimensions

Borehole Diameter (in)	Buoyant Force (lb)
3	1.7
4	2.9
5	4.6
6	6.6

In order to maintain ease of use, the device weight should be greater than or equal to these forces. The initial prototype had a weight around 2 lb. The above calculations assume air as the inflation medium. The force would be reduced if a denser fluid, such as hydraulic oil were used to fill the membrane. These options will be discussed in the following solutions sections.

With the general pressure and force constraints, the following inflation mechanisms were investigated for their potential use. Primary focus was given to the micro air pump, as it would help to streamline and further set apart the design from competitors.

3.2.2. Micro Air Pumps

The appeal of the micro air pump lies in its potential to be integrated into the design, ultimately combining three separate units (the receiver, bladder, and inflation device) into one compact unit. Additionally, if the pump was enabled with the capabilities to filter and use whatever fluid was in the hole for inflation purposes, the need for another surface line would be eliminated, reducing the bulk of the cable by up to

one half. It could also save on energy costs and equipment, as the air compressors typically used are oversized for the application.

Micro air pumps, such as those described for onboard use in the device, have been developed for medical, laboratory, and manufacturing applications. They come in varying shapes, styles, sizes and applications, but most all employ the same positive displacement pumping mechanism. As opposed to centrifugal pumps that depend on increasing fluid pressure and velocity via rotational dynamics, positive displacement pumps utilize the potential of trapped fluid (Matthews, 2014). This simplified design not only allows positive displacement pumps to be very compact, but gives several other advantages over centrifugal pumps. The flow rate of positive displacement pumps is not negatively impacted by decreasing viscosity like that of centrifugal pumps. The efficiency of the pump is slightly reduced by high viscosity fluids, but not nearly as much as those utilizing centrifugal mechanisms. While not of concern with dealing with relatively viscous fluids like air and water, pump performance becomes a major concern when using oils. Of further importance to this application, is the ability of positive displacement pumps to maintain a near constant flow rate and even increasing efficiency with increasing pressure or head, at depths up to and beyond 80 feet (Pump School, 2007).

Many of the examined pumps fall into the category of miniature diaphragm pumps, a subset of positive displacement. They utilize a flexible membrane (diaphragm) to achieve fluid displacement. These pumps are advertised for use in air sampling and laboratory instrumentation. Their compact size and high efficiency made them ideal candidates for this application. One model is depicted in Figure 34. Costs range between

$60 and $300 for varying flow rate and maximum pressures. The cost is reasonable enough, especially when considering the potential transducer savings. However, miniature diaphragm pumps on the market maxed out at pressures of 28 to 30 psi (193 to 206 kPa), significantly below the 35 psi (241 kPa) threshold. Additionally, the higher pressure pumps had drastically reduced flow rates, some requiring upwards of ten minutes to inflate the device membrane in a six-inch hole.

Figure 34: Parker miniature diaphragm pump (Parker Hannifin, 2015)

Another type of positive displacement micro pumps were investigated. Magnetic drive gear pumps are touted as ideal for high head scenarios. They have an internal gear, powered by magnetic propulsion, that forces the fluid through the pump. While not all gear pumps utilize a magnetic drive, it provides the most compact drive to overcome such high pressure differentials. The foremost producer of these pumps, Micropump, was consulted to identify the most applicable pump for this unique application. They recommended an external gear pump and magnetic drive mount, which together could provide 35psi (241 kPa) and fill the largest bladder (for the 6-inch diameter hole) in approximately one minute. These devices are shown in Figure 35. It was noted that gear pumps are highly susceptible to deadheading, the process that occurs when the pump

outlet is blocked (due to the high pressure differential in this application), causing the pump to recycle the fluid and eventually overheat (PSG Dover, 2012). An additional relief valve or return loop was recommended to maintain flow and prevent deadheading (G. Moore, personal communication, July 13, 2015). A centrifugal pump was also quoted, due to its ability to operate despite being deadheaded. However, such pumps do not perform well under high differential pressures, as previously discussed. The cost of the recommended pump-drive combinations were $1,500 without the necessary deadhead-prevention systems. This exceeds the total materials budget for the device. Additionally, when installed on the drive, the pump dimensions exceeded the physical constraints of the instrument.

Figure 35: Micropump GB series external gear pump and magnetic eagle drive

In theory, these pumps are ideal for this application. Miniature diaphragm pumps can be obtained for as little as a couple hundred dollars, roughly the same price as many of the oversized surface air compressors currently used. However, issues arise with the practical aspects of the size and capacity of these pumps. Gear pumps provide the necessary capacity, but are very expensive and require bulky circuitry for operation. The available pumps on the market are not yet suited for this application. There is potential for future developments and custom pump design, but the project status and budget do

not allow for it at this time. In the interest of future work with the on-board pump system, additional general considerations are discussed.

The pump concept has generally been discussed as an air pump; however, most of the devices quoted could also pump water or oil. One of the benefits of the change would be decreased buoyancy from higher density inflation material. Some of the assembly bulk could also be reduced if a pump could use the borehole water to inflate. This would require a rugged pump and sophisticated filter, but would eliminate the need for a surface fluid line. Additional considerations need to be made for the electrical and mechanical operations of a pump. It must be powered in-field, which is easily accomplished with any variety of battery pack. Most examined pumps required power in the 12 – 24 VDC range. Measures should be taken to control the vibrations of the pump, as well. Such powerful systems generate mechanical vibrations, and potentially electrical noise, that could interfere with readings. Vibration mounts will likely reduce much of the excess mechanical motions, but further investigations would need to look at pump placement and any signal propagation through the inflation medium. When micro pump technology becomes more accessible and relevant for this application, these concerns will need to be incorporated into the device design. Until such time, several other inflation mechanism alternatives are proposed.

3.2.3. Alternate Inflators

When exploring alternate inflation mechanisms, underwater recreation and safety applications were examined. Life rafts and flotation devices are often employed with safety inflation mechanisms that automatically inflate when submerged. These large floats are inflated against excessive hydrostatic pressure, like that experienced by the

receiver. All of the floats examined utilized the puncturing of some sort of pressurized tank (typically containing carbon dioxide) to inflate. These tanks cost around $10 – $20 each and are not practical for this application. Pressure regulators used in Scuba diving were also proposed as having potential. While not inflation mechanisms themselves, it was thought that regulators could be used to reduce the pressure differential to allow the membrane to be inflated with a smaller capacity pump. The regulators are used to reduce the pressure of the air contained in tanks to breathable levels. It does not appear that the mechanisms used could be easily re-engineered to reverse the process, to pressurize ambient air for inflation purposes.

After exhausting these underwater inflation mechanisms, more traditional approaches were examined. Portable air compressors are the current practice standard for bladder inflation, but many are oversized. Smaller alternatives were evaluated for their potential to increase the efficiency to bulk ratio of the source. Miniature air compressors designed for bicycle and motorcycle tire inflation are designed to be lightweight, portable, and quickly inflate large volumes to high pressures. One such model weighs 3.5 lbs, has dimensions of 5.5”x4.5”x2.5” (Figure 36), and can be obtained for $30. It includes a guage and can withstand pressures up to 250 psi (1724 kPa).

Figure 36: J&P Cycles mini air compressor

Traditional manual bike pumps may also suffice. In fact, Olson Instruments, a geophysical instrumentation company and partner on this project, uses bike pumps to inflate the bladders in their current borehole receiver system (Figure 37). Bike pumps typically provide between 80 and 150 psi (552 – 1034 kPa), and cost around $20. They weigh 2 -3 lbs, slightly less than the portable air compressor, but they are larger. Any surface pump or compressor should be equipped with a gauge to monitor membrane pressure and prevent damage from over inflation.

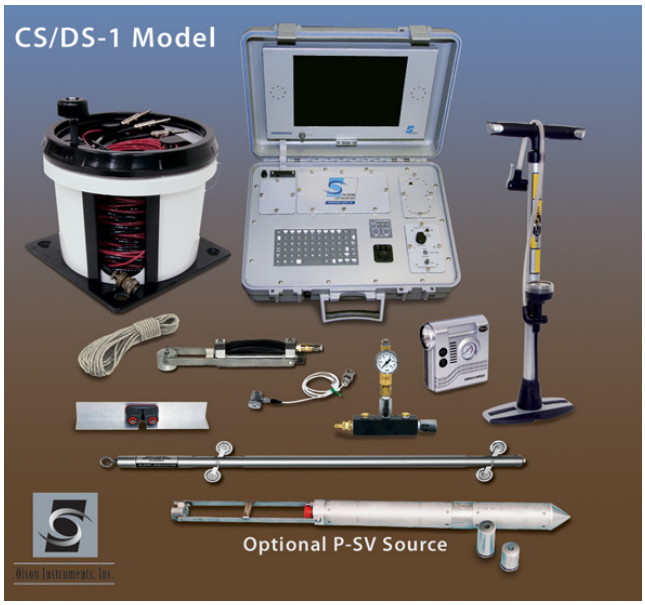

Figure 37: Olson Instruments crosshole/downhole package with bike pump

All of these proposed alternatives utilize air as the inflation medium, so options to counteract buoyancy effect in water-filled boreholes are presented. Per previous discussion, the device weight should exceed the forces presented in

Table 2. Nearly all of the weight is from the device frame, rather than its components. The frame weighs around 2 lb, so buoyancy is of concern in holes larger than 3 inches in diameter. One approach would be to reduce the buoyant forces by using denser inflation

medium. Hydraulic oil and water are both proposed alternatives to air. However, this would require the use of an on-board pump to be practical and efficient. While this is the ideal scenario, pump technology and costs are not at the levels needed for integration with this device. A possible workaround is to partially fill the membrane with water prior to lowering it into the hole. The remainder of the cavity would then be filled with air from surface source per standard procedure. The method would require thorough waterproofing of all internal device components. This is discussed with membrane component.

The other approach is to offset buoyancy with increasing device weight. While this may seem counterintuitive to the goal of creating a lightweight, portable device, it is necessary to allow proper functionality. Additionally, at the maximum required weight (6.6 lbs for a 6-in diameter hole) the device would still be significantly lighter than its competitors, at less than half the weight. The best option for this approach is to utilize some sort of removable counter weights. Simple washers could be bolted to the base of the device and added and removed as needed.

At this time, an onboard inflation mechanism is not feasible for use in this device. Available miniature pumps lack the capacity to overcome the effects of high levels of hydrostatic pressure, and are significantly outside of budget for low-cost instrumentation. Future developments and proper integration of necessary accessories may allow for the eventual addition of an onboard pump. For now, traditional surface inflation techniques may be sufficiently improved for use with the device. Micro air compressors provide lightweight, compact, and powerful inflation. Gauge integration allows for manual monitoring of membrane pressure levels to ensure safe inflation. In addition to cost and

functionality concerns, the micro compressor also scores best for replaceability. If an onboard pump were to malfunction, significant reconfiguring would be needed to operate the device until it could be repaired, which would likely need to be done by an expert. The surface compressor is much more reliable and easily fixed or replaced. Present conditions indicate the micro air compressor is the best inflation mechanism in achieving the device goals of mobility, replaceability, ease of use, and cost-effectiveness.

3.3. Membrane

The patented inflatable bladder component is what makes this device unique and on the cutting edge of seismic measurement. The precision and accuracy of the readings achieved by the increased coupling of the transducer to the borehole wall set the device apart, even without its reduced size and cost. The design focuses on the attachment of the transducer to the membrane, which is then inflated to conform to the shape of the borehole wall. Seismic signals then pass directly through the studied media (soil), through the thin membrane to be read by the transducer. There is no air gap during the transmission. This allows for readings to more accurately reflect the properties of the studied media. This coupling can only be achieved with a properly designed membrane.

3.3.1 Design Considerations

The membrane should meet the same low-cost standards as the other device components, along with a few other considerations. The protection and functionality of the device depends on the membrane. The material used in the membrane and the overall design and integration of the membrane are crucial to device functionality.

The enhanced reading is dependent on the flexibility of the membrane to inflate to a multitude of borehole wall shapes. The bladder should also be able to retain its shape after multiple inflations and deflations. Thus, material elasticity is of concern. While extreme temperatures are not necessarily a major concern, the material properties of the membrane should not be negatively impacted by temperatures encountered during typical field work. The membrane also needs to withstand harsh downhole conditions, including high hydrostatic pressures and potential intrusions from sharp objects in the borehole wall. The nature of the design is such that the membrane encases the entire device, and should protect other components from the elements. If rupture does occur, the membrane material should be such that it could be repaired in the field. Elasticity and durability are the two main considerations when selecting membrane material.

In considering the design of the membrane, replaceability and device protection are the key components. The design of the membrane must be such that it can be easily repaired or replaced in the field. Expensive specialized construction methods should not be used in membrane fabrication for this reason. Some specialization is allowed, and needed, in the manufacturing process, but the product should be cheap enough that, if repairs are improbable, the user could afford to have several replacement membranes on hand. While the overall device design inherently allows membrane protection of the instrument's internal workings, additional care should be given to ensure the design accounts for any future developments. For example, if fluid is used to inflate the membrane, the design should allow for the delicate transducers and any other equipment to be protected from the fluid. Also of importance is the ease of use of the membrane.

The design should allow it to be easily uninstalled and reinstalled without having to dismantle the entire device.

3.3.2 Traditional and Initial Designs

Traditional bladders, as well as the membrane used in the initial prototype of this device, were examined for their ability to meet those needs. Traditional bladders consist of rubber balloon-like forms, inflated adjacent to transducer housing, as depicted in Figure 38. These bladders are very basic, with little design needs or considerations. Because they only need to supply lateral pressure, without any other constraints or limitations, these bladders are typically just elongated round forms with hoses. They are made of cheap, durable rubber. Some commercial devices utilize slightly more sophisticated bladder systems. Olson Instruments' bladder is clamped onto an attachment for its downhole receiver. The bladder consists of a portion of bicycle tire tubing.

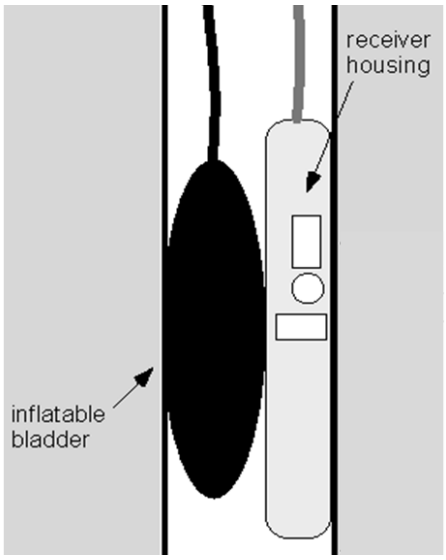

Figure 38: Traditional bladder with separate receiver housing

In the initial prototype, a cylindrical latex membrane like those used in laboratory soil testing applications was used (Figure 39). When affixed to the device with O-rings,

the membrane was able to expand to hold the instrument and transducers against the borehole wall. Latex, or natural rubber, is valued for its elasticity, but degrades and becomes brittle over time. Latex is highly susceptible to chemical, microbial, and UV-light degradation (Rose & Steinbüchel, 2005). It very quickly disintegrates in oil. Additionally, the thin latex is easily punctured when stretched. Thus, the original membrane material is too delicate. The overall membrane design scores well in the areas of replaceability and ease of use. The latex tubes are cheap and obtainable from most laboratory suppliers. The same is true of the O-rings used to hold the membrane in place. The membrane is relatively simple to install, and the O-rings provide ample restraint to maintain pressure when inflated. However, the design lacks sufficient protection for the transducer. If the membrane were to rupture or leak, there is no secondary level of protection for the sensor.

Figure 39: Accelerometer (1) on initial latex membrane (2). (Kalinski, 2012)

3.3.3 Membrane Material Selection

Because the membrane design is likely to depend on the capabilities and restrictions of its composition, membrane material was investigated prior to final design. Several material options were investigated for the new membrane. While latex is valued for its elasticity, polymers like polyurethane are known for their durability. Polyurethanes are rapidly replacing flexible PVC and Hypalon (a synthetic polyethylene rubber) as the

leading material for marine inflatables. Manufacturers tout studies conducted by the U.S. Navy in support of polyurethane's strength, weight, and puncture and abrasion resistance (Wing Inflatables, 2011).

Of the two types of polyurethane, thermoplastic and thermosetting, the former type is considered more applicable for the membrane. Thermosetting polyurethanes tend to be more brittle, and this application does not justify the high-heat resistance. Thermoplastic polyurethane, or TPU, is used across a variety of industries and applications. TPU, like rubber, is an elastomer, meaning they have little to no permanent deformation; they can return to their original shape after stretching more than twice their length (Dupont, 2015). This elasticity can be quantified by Young's modulus, and is compared to other materials in Figure 40 from BASF Polyurethanes below. Rubber (including natural and synthetic), PVC, TPU, and polyethylene (PE) represent materials currently or traditionally used in inflation applications. Rigid TPU (RTPU), polyamide (PA), polycarbonate (PC), and Acrylonitrile butadiene styrene (ABS) are more rigid plastics that are not considered applicable. Aluminum (Al) and antimony (St) are also included on the chart for reference and scale.

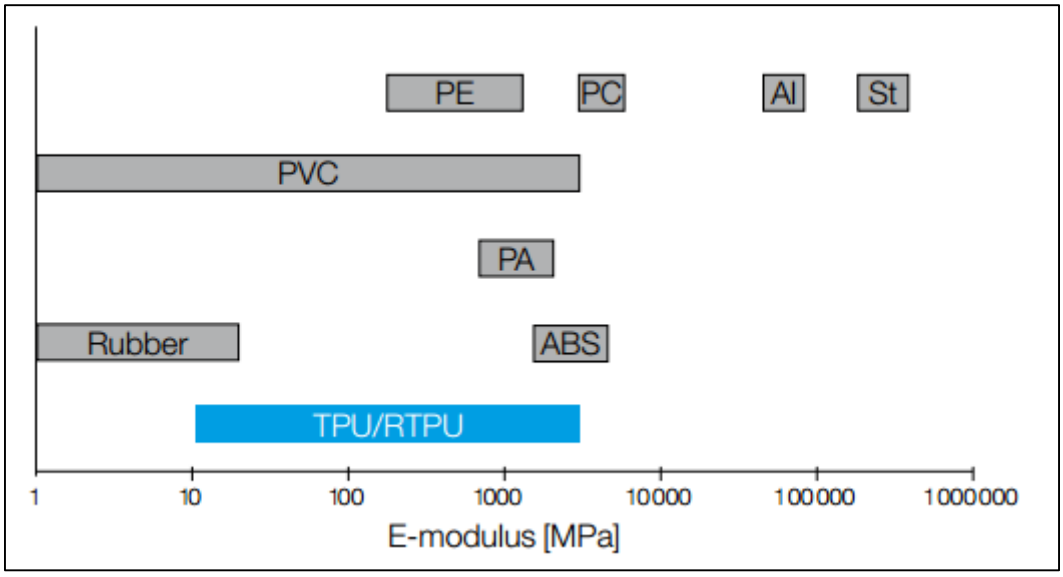

Figure 40: Elasticity of membrane materials (BASF Polyurethanes, 2010).

TPU may be either polyester or polyether based, which further defines its material and behavioral properties. The structure of TPU is essentially a chain of rigid and flexible segments with the flexible portions comprised of ethers or esters, joined with rigid residues by urethane groups (BASF Polyurethanes, 2010). Both types of TPU are flexible, but polyester TPU has reduced low temperature flexibility (Feijen et al., 2001). Polyester TPU also has very poor microbial and hydrolysis resistance (Feijen et al., 2001). The ester groups are susceptible to splitting by enzymes (from microorganisms) and water molecules (Huntsman, 2010). Microbial degradation, common when the material is in repeated contact with soil and water, results in discoloration, thinning, and cracking of the product (BASF Polyurethanes, 2010). Hydrolysis produces similar results during sustained water contact (Huntsman, 2010). However, hydrolysis typically only occurs at high temperatures, greater than those of typical groundwater (BASF Polyurethanes, 2010). The higher microbial and hydrolysis resistance indicate polyethers may be a more suitable choice for the device membrane.

It should be noted, that more flexible TPU grades tend to have higher polyester content, so in selecting a TPU, some elasticity may need to be sacrificed for material stability (BASF Polyurethanes, 2010). Polyester TPU also has significantly better resistance to oil, grease, and solvents (Merquinsa, 2012). Contact with these media will cause damaging swelling and strength reduction in polyether TPU (BASF Polyurethanes, 2010). This would certainly restrict the use of oil as an inflation material for the device. Regardless, polyether TPUs are still the better option of the two.

TPUs may also be divided as aromatic or aliphatic. The classification depends on the diisocyanate used in production. Diisocynates are one of the process reactants and form the long segments of the rigid portions in the TPU chain (BASF Polyurethanes, 2010). Aromatic TPUs are valued for their strength, durability, and flexibility (Huntsman, 2010). However, they are UV-sensitive and prone to resultant oxidation degradation over sustained sun exposure (Merquinsa, 2012). The visible result of the damage is discoloration and increase opacity, but the reduced flexibility and strength are more serious. Aliphatic TPUs are UV-resistant (Huntsman, 2010). However, they also have lower thermal resistance, so their use is typically restricted to applications where transparency is vital (Merquinsa, 2012; Huntsman, 2010). Most commercial TPUs are aromatic (Merquinsa, 2012).

Overall, TPU demonstrates the high tear strength, tensile strength and elongation needed in this application (BASF Polyurethanes, 2010). An aromatic polyether is the best selection among TPUs when considering durability and material availability. This option does have shortcomings with oil and UV reactivity that may hinder device functionality. Additionally, elasticity may be of concern. Most manufacturers reference elasticity in

terms of percent elongation. This value is obtained at the ultimate tensile strength of the material. For most applications, especially this one, the applied pressure would be far below the ultimate. Thus, the concern lies with the percent elongation at very low pressures.

All of the potential materials are considered to be elastomers, thus, Young's modulus (or the modulus of elasticity) and an applied normal force can be used to reasonably predict the elongation of the membrane. In considering applied forces, only the net positive (outward) pressure is used, because that is the pressure providing the force for inflation. The selected micro air compressor provides up to 250 psi (1724 kPa) of pressure. If 35 psi (241 kPa) of this is required to offset the hydrostatic pressure at the bottom of the hole, 215 psi (1482 kPa) remains to pressurize the membrane. This value is the maximum available pressure. It is estimated that only 5 – 10 psi (35 – 70 kPa) of positive (net) pressure is required to hold the receiver against the borehole wall. The minimum required pressure is 10 psi (70kPa). These pressures represent the maximum and minimum normal stresses that would be applied to the membrane material at the bottom of the established test hole. As for the modulus, Figure 40 shows wide ranges of Young's moduli for rubbers, TPUs and other materials. More specific values were obtained for commercial polyether TPU. Brand-name Elastollan was available with a Young's modulus as low as 90 MPa (13 ksi) and as high as 330 MPa (49 ksi) (BASF, 2012). To compare, latex, the material used in the initial prototype membrane, is generally accepted to have a Young's modulus between 10 MPa (1.5 ksi) and 100 MPa (15 ksi) (Engineering ToolBox, 2015). Silicone rubber, another potential candidate has a

Young's modulus ranging from 1 MPa to 50 MPa (0.15 – 7.3 ksi) (AZO Materials, 2001).

To estimate the membrane's elongation during use, these values are used in conjunction with Hooke's Law. As previously stated, Hooke's Law defines Young's modulus as the ratio of a material's stress to strain under normal loading conditions. In these terms, Hooke's Law is defined by the following equation.

$$E = \frac{\sigma}{\varepsilon} \tag{3.8}$$

where E is Young's modulus, σ is the applied normal stress (pressure), ε is the resulting strain. The strain is the change in length over the total length, or the percent elongation. The equation can be rearranged to solve for percent elongation (strain) using the selected pressures and moduli. A sample calculation is shown for the maximum applied pressure and minimum Young's modulus for TPU.

$$\varepsilon = \frac{\sigma}{E} = \frac{215\ psi}{13\ ksi} = 0.016 = 1.6\% \tag{3.9}$$

In other words, by these estimations, the maximum percent elongation of a TPU membrane in this application would be 1.6%, much less than the advertised maximum 550% for the grade (BASF, 2012). This calculation was repeated to estimate the maximum and minimum percent elongations of the device membrane for polyether TPU, latex, and silicone rubber materials. The results are summarized in Table 3.

Table 3: Estimated percent elongations for membrane materials

Material	Minimum Percent Elongation	Maximum Percent Elongation
Polyether TPU	0.4%	1.6%
Latex	1.5%	15%
Silicone Rubber	3.0%	148%

These estimates are very informative regarding the relative elasticity of different membrane options. However, what truly matters is if each material provides enough elasticity for the device to properly function. It is difficult to quantify how much material elongation is needed in the membrane. One percent may be sufficient in smaller diameter holes, where the membrane needs to stretch less than an inch. In larger holes, the membrane may be expected to stretch up to three inches laterally, which could easily require more than 50% elongation. So the question of whether polyether TPU could be the membrane material ultimately depends on the membrane design. If a single membrane is expected to work in multiple holes, it is unlikely that TPU would work. It is possible that a TPU membrane that is significantly oversized for the smaller holes could work across the gamut of diameters, but it would not ensure proper coupling of the transducer to the borehole, negating the device's purpose.

While latex does provide substantially more elongation potential than TPU, it is not a realistic candidate for the membrane. While it is used as the baseline for elasticity since it was successfully used in the initial prototype field work, its durability insufficient for sustained commercial use. Latex, as a natural product, also causes severe allergies and irritations in some people. While not much of an issue for this application, it is a widespread concern in the medical field. As a result, that industry invested considerable

resources in identifying and testing alternative material for uses in everything from bandages and gloves to inflatable medical devices and prostheses. The two most prominent alternatives for medical device balloons are the elastomers TPU and silicone, with silicone rapidly outpacing TPU due to its improved elasticity (Shah, 2001).

Silicone is used throughout industries in other inflation applications as well. Silicone bladders are used throughout manufacturing as gaskets, industrial vacuum bags, and temporary supports. They are also used to form temporary seals and blocks in pipes during construction and repair. All of these applications recognize the toughness and elasticity as silicone as an inflatable membrane material. Like TPU, silicone demonstrates good durability, but elasticity much more in line with that of latex. This unique combination of properties is due to silicone's high bonding energy and, but low intermolecular force (Shin-Etsu, 2005). In other words, the material chains are strong, but the forces between the chains are weak. It allows the chains to aggregate into coils that can stretch and rebound like a spring (Shin-Etsu, 2005). This results in a slightly lower tensile strength than both polyurethane and latex, and a significantly lower modulus of elasticity (AZO Materials, 2001). The low modulus is the main contributor to silicone's higher percent elongation at low pressures. The high bonding energy gives it thermal and UV resistance (Shin-Etsu, 2005). Silicone is not subject to degradation from microbial activity or hydrolysis.

Like TPU, silicone has classifications with varying properties based on composition. The two most common types are methyl vinyl and methyl phenyl, with the names coming from the groups on the polymer chain (AZO Materials, 2001). Methyl vinyl silicone (ASTM class VMQ) is used for most applications. Methyl phenyl silicone

(ASTM class PMQ) is used for applications in extremely low temperatures. In general, silicone has good oil and solvent resistance. However, like TPU, it does have slight swelling when in contact with such solvents (Shin-Etsu, 2005). It does not degrade like latex, or retain permanent damage like TPU. A subset of the general purpose silicone, methyl vinyl fluoro silicone (ASTM class FVMQ), provides additional oil and solvent resistance (AZO Materials, 2001). At this time, oil contact is not predicted for the device. Methyl vinyl (VMQ) is the correct class for this application.

Studies on weatherabilty of VMQ found the material to withstand more than 10 years of full elemental exposure in South America and the U.S. upper Midwest (Shin-Etsu, 2005).This demonstrates the exceptional durability required by this application. As stated, the tensile strength of silicone is significantly lower that of TPU. The polyether TPU formulation with the lowest identified modulus of elasticity had a tensile strength of 60 MPa (8.7 ksi) (BASF, 2011). General purpose silicones have tensile strengths around 10 MPa (1.5 ksi) (Shin-Etsu, 2005). While this seems like a drastic reduction, much of the strength of the TPU was unnecessary for this application; it also contributes to its reduced elongation at low pressures. Latex and natural rubber compounds generally have initial tensile strengths between 15 MPa and 22 MPa (2.2 – 3.2 ksi) (Renner & Pek, 2011). These strengths are rapidly reduced when latex is introduced to chemical, microbial, and UV-light exposure (Rose & Steinbüchel, 2005). Thus, the reported strengths of latex are inflated. The tensile strength of general purpose silicone (VMQ) should suffice for this application. The 10-MPa strength corresponds to a resistance of 1.5 ksi, more than 5 times the capacity of the pump. Rupture is not likely with a VMQ membrane. If the reduced tensile strength is of concern, high-strength silicone

formulations are available that can increase rupture stress to 35 MPa (5.1 ksi) or more (Shin-Etsu, 2005).

Silicone and TPU are both exceptional alternatives to latex for the membrane of this device. Aromatic polyether TPU is widely available and provides exceptional strength and resistance to microbial activity and hydrolysis. However, there are slight concerns with oil degradation and UV sensitivity. These issues, on their own, would not restrict the material's use in the membrane; however, TPU's restricted elongation at the device's low pressures does. It is unlikely that TPU could provide the necessary elasticity for the device to inflate to the multiple sizes needed for us in varying size boreholes. Methyl vinyl silicone possesses outstanding elasticity, with some formulations exceeding that of latex. Like TPU, it has excellent resistance to microbial activity and hydrolysis, but, unlike TPU, it also has improved oil resistivity and little to no UV sensitivity. VMQ does have significantly less tensile strength, but its strength should be more than enough for this application. When considering cost of materials, TPU and silicone have similar manufacturing procedures for both material solution creation, and formation of the final membrane product. Both have relatively high overhead and material handling costs when compared to latex. Costs have been significantly reduced in recent years as demand increases and the materials become more widespread. Both materials can utilize the dip-molding process to manufacture membranes, which can be achieved on the smaller scales needed in this upstart (Shah, 2001). With these considerations, methyl vinyl silicone is the recommended material for the device membrane.

3.3.4 Membrane Design

When identifying potential membrane designs, the key considerations should focus on the overall goals of the device. Any proposed design should contribute to the accuracy, practicality, usability, durability, mobility and cost-effectiveness of the device. For this component, device accuracy is embodied by proper and complete coupling of the transducer to the borehole wall. This is achieved by the elasticity of the membrane material, but also of the design to allow the transducer to be stoutly attached to the bladder wall, which must be sufficiently thin. Practicality applies to methods and means to manufacture and produce the design. Usability considers how easily the membrane can be uninstalled and reinstalled, as well as repaired or replaced. The need for the device to be used in different size boreholes also factors in to useability. The membrane material, itself, primarily contributes to the durability, but the design must not contribute unnecessary strain, and use the material to its full potential. Mobility is not as applicable for this component. All designs are likely to be small and lightweight, but membrane replaceability could impact how far users could travel from a repairer. Cost-effectiveness, while primarily dictated by the material, also comes down to the manufacturing process.

The manufacturing process will likely be the same with any design. Historically, custom bladders and membranes made of synthetic elastomers have been constructed out of flat sheets and epoxy. It is difficult to achieve curved shapes using this method. Additionally, the seams are discontinuities in the structure that may behave differently and weaken over time. Large-scale productions often use injection molding, but this requires a lot of specialized machinery. Extrusion is another common method, but typically can only be used to produce spherical shapes Dip molding, however, can

produce highly elongated round shapes, with wall thicknesses up to one-fifth that of injection molding and extrusion (Vesta, 2015). Similar to concept of candle making, this method is used to produce hollow bladders, inflatables, and from elastomers like silicone and TPU. Dip molding, or dip casting, can be used in smaller operations. It is excellent for prototyping and upstarts due to its low setup and production costs and short lead time (Engineering Fundamentals, 2015).

Shah discusses the method extensively in his article on the state of latex-free medical balloon production (2001). Essentially a mandrel, tooled to the desired shape of the membrane, is heated and then dipped in a solution of the elastomer and a solvent. After dipping, the material stuck to mandrel is allowed to set. The process is repeated to add layers and thicken the bladder. Thicknesses between 1 mm and 6 mm are typical. The mandrel forms the inside of the bladder. Glass and metal are most often used for the mandrel, with glass resulting in a smoother final surface, but metal typically easier to manufacture. The mandrel and material handling concerns make up the majority of the manufacturing costs (Shah, 2001). For larger productions, the mandrel dipping can be automated, but hand-dipping is common and reduces machinery costs. Some concerns with hand-dipping, and the overall process, include difficulty in achieving uniform wall thickness, controlling dip speed and immersion times, and monitoring the temperature of the mandrel and solution (Engineering Fundamentals, 2015). While dip molding could theoretically be performed in a laboratory, partnering with an existing dip molding operation is recommended. Such operations tend to have multiple production lines dedicated prototyping and small orders. These companies either manufacture their own elastomers, or can utilize other commercial products. The molding is performed in a

controlled environment with proper chemical handling and dipping controls. The operations typically also specialize in mandrel formation. The precision achieved will allow the membrane to be sufficiently and uniformly thin, and to the precise specifications of any design.

With the feasibility of production ensured, the focus can shift to the design itself. The initial membrane consisted of a cylindrical latex tube like those used in soil laboratory applications. The elasticity of the material allowed the tube to sufficiently stretch to wedge in the borehole and couple the transducer to the wall. The design is good because of its simplicity and ease of use. The user simply puts the sleeve on the device, then rolls o-rings into notches near the two ends. The ends can be further secured by wrapping the ends in electrical tape. This can be observed in Figure 41. The o-rings hold the membrane in place and the tape stops any small leaks that may occur. It is recommended that this method be used in the design moving forward.

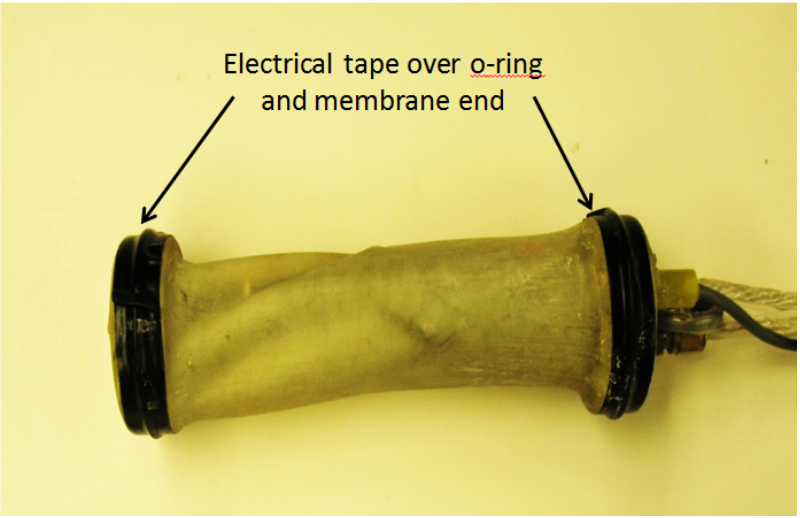

Figure 41: Membrane attachment in initial prototype (Kalinski, 2012)

The simple cylindrical membrane shape may be sufficient, but a rounded design could improve coupling. The membrane would bow out at its center, essentially mimicking a cylinder that had been axially compressed. This would allow the transducer, centrally located at the midpoint of the membrane, to more easily be pushed against the borehole wall. The bowing should be slight, as to not cause any folds when used in small holes.

Additional upgrades to the design should consider transducer protection. An initial suggestion called for the transducer to be sealed in a double-walled membrane. However, issues with wall thickness, wire connectivity, replaceability, and feasibility of manufacturing quickly arose. An alternate solution would attach a small silicone tube to the inside of the membrane where the transducer is. The tube would provide additional protection if the exterior membrane were to leak. The tube can be attached to the membrane using a silicone adhesive or, if applied before the membrane fully cures, a welding technique. The concerns associated with gluing and seaming the membrane do not apply to this attachment, as should not experience the same pressure and exposure. The other end of the tube would be connected to a ribbed nozzle fitting (like those used in laboratory gas lines) in the middle support bar of the device. The initial prototype utilized a solid metal bar. A hollow bar would allow the power and signal cables to pass from outside the top of the device, through the bar, and out the nozzle to the transducer, all in a sealed environment. Such a membrane could still be easily installed. The membrane would be placed on the instrument from the bottom, affixing the bottom with an o-ring first. The transducer would be fed through the tube and attached to the outer wall of the

membrane. The tube would then be attached to the nozzle fitting. The top of the membrane would then be affixed per the initial design with an o-ring.

This membrane design provides sufficient transducer to borehole wall coupling, transducer protection, is easily installed, and can be feasibly manufactured. To fully evaluate its performance in the areas of replaceability and flexibility in different size holes, additional information is needed. Both of these factors depend on the membrane cost. If the cost is low enough, it would be reasonable to provide several membranes to the user for replacing ruptured membranes, or even larger ones for use in different sized holes. The material elasticity is the main factor in using the membrane in different size holes. While silicone is predicted to be sufficiently elastic for the task, only fabrication and testing of membranes of varying formulations and thicknesses can verify that. This will be performed in the next stage of work, which is outside the scope of this thesis. As for membrane repair, silicone can be patched with appropriate adhesives, although it is not recommended due to the likely change in membrane elasticity and behavior near the seam. Replaceability also depends highly on how the transducer is affixed to the membrane. A permanent connection increases the cost and complexity of replacement. It would be ideal if the transducer could be attached in a way that could withstand field use and provide complete coupling, but also be removed from a broken membrane. The transducer attachment is considered in the accessories section of this chapter.

A dip molded silicone membrane is recommended and should satisfy the device goals of accuracy, practicality, usability, durability, mobility and cost-effectiveness. A bowed cylindrical sleeve is recommended for the shape, with a small cylindrical tube, large enough to fit the transducer, attached at the middle of the wall on one side. The

membrane will be affixed to the device frame using o-rings over carved notches. The silicone material provides both elasticity and durability against the elements to ensure transducer coupling and provide transducer protection. Fabrication and testing of sample membranes using different silicone fabrications and thicknesses will be necessary. It is recommended these be fabricated by a commercial dip molding operation. The next section of this chapter will further address the concerns of membrane replaceability with transducer mounting options, as well as consideration of other accessories key to device functionality.

3.4. Accessories

When considering the components essential to device functionality, the most visible and obvious parts garner the most attention. The transducer, the inflation mechanism, and the membrane are what make the device unique, but less flashy accessories, like the power and air lines, are what make the device function. The power and air lines are the literal life lines of the device, and without accelerometer mounting, borehole coupling cannot be achieved. Requirements and options for these device accessories are discussed in this section.

3.4.1. Transducer Protection

Durability and replaceability are the key concerns for the design of the transducer protection and mounting. The harsh borehole environment can cause damage to any transducer, especially to the delicate MEMS accelerometer and board. The selected geophone and transducer can be easily protected with commercial waterproof cases. The MEMS board requires custom design and fabrication of a case. Hoffman et al. (2006) extensively explored the development of a case for their MEMS accelerometer. The study

found the exposed electronics and delicate connections in need of protection. The entire transducer and its soldered connections were encapsulated in a urethane-casting agent. Initial attempts applied thin coats of polyurethane and acrylic, which minimized additional packaging weight, but left connections brittle and mobile. The final product was a clear urethane cylinder that encased the accelerometer with plastic-coated wires coming out of the top. Subsequent testing verified the functionality of the transducer while fully submerged in salt water. The package was celebrated for protecting of the device and connections while allowing the user to clearly see the transducer orientation through the case.

The application of the Hoffman et al. packaging approach to this device raises several concerns. The first is with the practicality of the packaging shape. Hoffman et al. were working with a larger, dual axis accelerometer, sans breakout board. The intended applications for the device included rigid connections where case mass and shape were of lesser concern. A cylindrical case for the MEMS accelerometer configuration used in this device would be unnecessarily large and bulky. The second issue concerns the overall replaceability of the receiver components. If the transducer ever malfunctioned or otherwise needed replacement, the Hoffman et al. design would require either cutting or replacement of the power and signal lines. If the transducer wires were simply cut, significant effort would be needed to waterproof the connection of the new transducer, negating the function of the case to protect the delicate connections. Replacing the signal lines would be very expensive in this application due to their length.

However, overall, the Hoffman et al. approach was very successful, and can likely be used in this application with a few modifications. The encasement material itself was

found to sufficiently protect the accelerometer, with little to no effect on its functionality. The material is a clear urethane casting resin known as Crystal Clear 204 produced by the Smooth-On company. The resins cure within 48 hours at room temperature and can be used in conjunction with silicone molds in any shape. There is minimal shrinkage during the curing process. The hardened resin has high strength and a low refraction index, so the transducer orientation is clearly visible during installation (Smooth-On, 2014a). The Crystal Clear resin or similar material is recommended for the MEMS accelerometer case material. Another group of researchers used an engineering resin known as polytetrafluoroethylene (PTFE); however, the material was sticky even after curing and had to be wrapped in foil, obscuring view of the transducer orientation (Bhattacharya et al., 2012).

As for the design of the case, a flatter prism is recommended. The case should be as close to the size and shape of the breakout board as possible, in order to minimize weight and bulk. The bottom of the board should be attached to the membrane as it would provide the most surface area for the connection, while minimizing distance between the membrane and accelerometer. The breakout board is configured such that all of the wire connections are located along one edge. In order to reduce packaging size and maintain proper orientation on the membrane, the connection leads should exit the top of the board. This can be achieved with the installation of the header included with the board. By soldering the header to the board connections, not only are the leads routed out the top of the device, but connection strength and reliability are also improved. The header is pictured with the board in Figure 42.

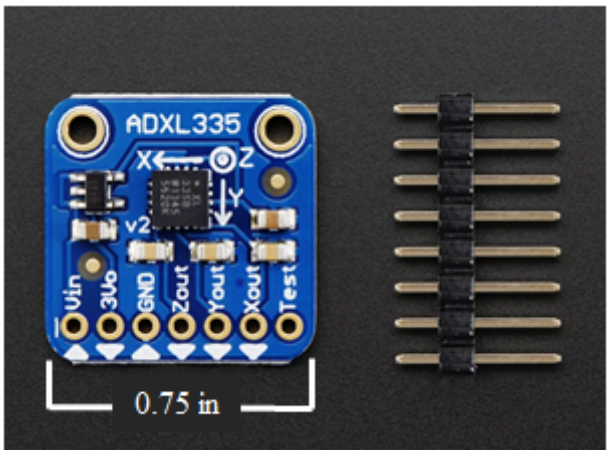

Figure 42: Adafruit breakout board with connection header

Installation of the header would also help with the component replaceability. Connectors, like those shown in Figure 43 provide a secure, stable connection to the board that can be plugged and unplugged countless times.

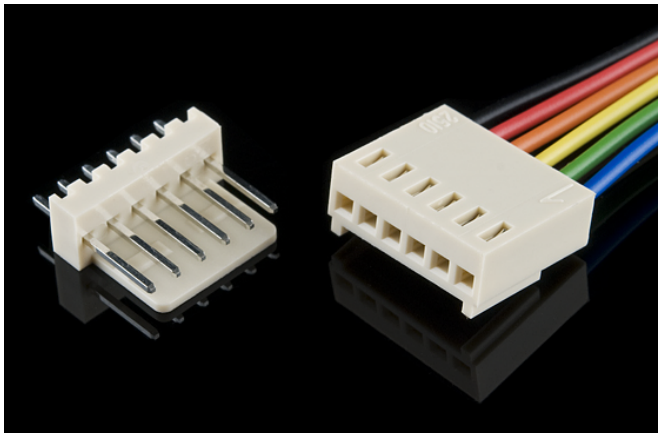

Figure 43: Sparkfun jumper wire cable for header pin connection

In this way, the transducer can be easily detached from the field cable and swapped out or sent in for repairs without reconfiguring or cutting the cable. The header can be soldered to the board, and then encased with it in the urethane resin up to the base of the connection pins. The connections are stabilized, the delicate board components are protected, and the transducer can be easily removed and replaced. Regarding transducer

repair and replacement, the MEMS accelerometers are so inexpensive that repair is unlikely to be economically viable. Replacement is far more likely. However, if transducers do need to be removed for any reason, Hoffman et al. found that the resin case could be purposefully broken open. It is not recommended though due to the delicacy of the accelerometer and board.

3.4.2. Transducer Mounting

The physical attachment of this case to the membrane is vital to device functionality and accurate readings. Coupling between the accelerometer and the media has been studied by independent researchers and instrumentation companies, with little agreement on a singular solution. Waxes have long been praised for their removability, while adhesives are recognized for their permanency. The best coupling material depends on the function it serves. For this application, permanence is valued for contributing to the overall durability of the device. However, that same quality takes away from the replaceability of the components. If the transducer is permanently attached to the membrane, a failure of either component requires the replacement of both, escalating costs. However, if the membrane cannot stay attached to the membrane while undergoing the strains of inflation, the device cannot operate. Ease of use and affordability are at odds with reliability and accuracy. Mounting techniques are investigated that could satisfy the needs of both permanency and flexibility.

The solution to this is a semi-permanent attachment. Such a material would be rigid and industrious throughout the device working conditions, but easily removed when needed. This could be achieved by applying heat or a solvent to remove the transducer without damaging it or the membrane. Semi-permanent adhesive methods include

cyanoacrylate (super glue), some waxes, and hot glue. Cyanoacrylate can be removed with commercial solvents. Rigid waxes with high melt points can also be removed with solvents. Hot glue is typically mechanically removed.

Several accelerometer coupling materials were selected for testing by a group of Colombo et al. (2005). The study focused on the frequency response and other effects on data the coupling materials had. Super glue, soft wax, and hot glue were among the selected materials; however, wax testing was abandoned due to application difficulty. Based on the description, the wax was not likely sufficiently heated prior to application. Hot glue received a poor rating for received signal quality, while superglue performed well across most categories, with an excellent signal quality rating. Another material, a modeling putty known as Plasticine outscored superglue overall, but received a subpar signal quality score. The putty is a temporary adhesive not likely to withstand the horizontal attachment configuration of the receiver. The study concluded superglue provided the best quality data of the materials tested (Colombo et al., 2005).

Superglue is typically not recommended for use with silicone rubber. It does not form the typical bonds and is unlikely to be sufficient for this application. Semi-permanent waxes should be further investigated as an alternative. These waxes are applied to the transducer after heating and then allowed to cool to form the bond (Endevco, 2008). The final product is resistant to water and holds until a solvent is introduced (Stronghold, 2014). The wax "provides excellent transmissibility" of signal (Endevco, 2008). Little information is available regarding the bonding strength and materials of these products. It is well worth testing though, as the waxes are inexpensive and easily removed when needed.

Stronghold 7036 Blanchard wax is the most popular and is removed with acetone (Endevco, 2008). Unfortunately, acetone has an "unsatisfactory" rating for both silicone and polyurethane reactivity per elastomer interaction charts (Mykin Inc., 2015). Other commercial solvents, like ShipShape resin cleaner and methylene chloride have been successfully used to remove the wax (Stronghold, 2014). Methyline chloride also has an "unsatisfactory" rating for both silicone and polyurethane interaction (Mykin Inc., 2015). ShipShape is composed of two main solvents: butyrolactone (GBL) and N-methyl-2-pyrrolidone (NMP) (ISP, 2005). GBL has a "fair" rating for silicone and an "unsatisfactory" rating for polyurethane (Mykin Inc, 2015). The urethane resin recommended for use in the transducer case is thermosetting polyurethane (Eager Plastics Inc., 2000). The polyurethanes evaluated in the interaction charts are thermoplastic. Laboratory investigations should be conducted to determine if the thermosetting polyurethane of the case resin provide ample resistance to the GBL in ShipShape. Less data is available for NMP interaction. It was rated "probably satisfactory" for use with silicone (PSP Inc., 2015). Other research aimed at identifying container materials for NMP identified silicone rubber as one of two elastomers having the best stability (BASF, 1990). It is plausible that Stronghold 7036 Blanchard wax could be used to attach the transducer to the membrane, but physical testing is needed to verify.

If the wax is found to provide insufficient bonding strength, or the removal process found to damage the membrane or transducer, a permanent adhesive will have to be used. Traditional epoxies and bonders used to bond metal-cased accelerometer to metal structural components will likely not adhere to the silicone. An adhesive specially formulated for use with silicone should be used. Several are commercially available. Sil-

Poxy from Smooth-On can bond silicone to itself, as well as urethanes (Smooth-On, 2014b). Any epoxy used should be applied as a thin layer, as to minimize the space and material between the transducer and borehole wall. Temporary adhesive like petro and bee's wax, double-side tape, duct putty should be avoided (PCB Piezotronics, 2004). Only testing can verify if Blanchard wax can provide a semi-permanent adhesive solution or if silicone-formulated epoxies should be used.

3.4.3. Supply Lines

Lines from the surface to the device must supply power to the transducer, air to inflate the membrane, receive signal from the transducer, and support the device as it is raised and lowered through the hole. These functions should be streamlines into as small of a package as possible, reducing the bulk of the device for use and transport. These lines should only enable and not interfere with the device functions. This is of particular concern with the power and signal lines.

The nature of the MEMS accelerometer, an electronic device sending and receiving signal, is such that electronic noise is of utmost concern. As previously discussed, when noise is amplified above signal, the device no longer functions as an accurate receiver. The inherent noise of the accelerometer is small, but it can be amplified and added to during transmission through long cables. Cables must be shielded to protect the signal from outside noise encountered during transmission. A shield consists of a conductive material wrapped, braided, or otherwise secured around the body of the signal lines (Hess& Goldie, 1993). Any outside noise is channeled along the shield, away from the internal signal lines. Any shielding should suffice for this application. Braided shields provide more durability, but less wire coverage, while wrapped foil shield increase

overall cable flexibility and provide complete coverage (AlphaWire, 2009). Combination shielding consisting of multiple layers of both braided and foil shielding are available, but are likely unnecessary for this application. The cable tested in in this study utilized an aluminum foil with polyester tape at 100% coverage (Belden, 2015).

The cable must not only be properly shielded, but have sufficiently low capacitance. Excessive capacitance allows additional noise to amplify in the line, which can override the transmitted signal. Capacitance defines how much charge can be stored in a given object; it is proportional to the surface area between conductors. For cables, the conductors consist of the signal lines and the external shield (Meggitt, 2010). The insulating wires between the conductors actually increase the capacitance by acting as dielectrics (Elert, 2015). The surface area between conductors is directly proportional to length; thus, capacitance increases with each unit length of the cable. Cable capacitance should be in the range of 30 pF/ft to 35 pF/ft to reduce noise amplification (PCB Piezotronics, 2015). The cable tested in in this study has a rating of 33 pF/ft (Belden, 2015).

Another contributor to long cable noise is the triboelectric effect. It is essentially the creation of static electricity by separating the internal cable components, which can occur when the cable is moved or bent (Meggitt, 2010). Low noise barriers are installed in coaxial cables commonly used with accelerometers to reduce this (PCB Piezotronics, 2015). The barriers function by dispersing any generated charges and reducing the separation potential between layers (Meggitt, 2010). This low noise approach may not work for the multicomponent cables required in this application. For multicomponent cables, reducing the likelihood of layer separation also reduces spacing between

conductors, which increases capacitance. The cable tested in in this study does not employ the low noise dispersion layer (Belden, 2015).

Additional cable considerations include flexibility, jacket and insulation coatings, and grounding. The use of foil-shielded cable will increase overall flexibility, as will stranded over solid wires. The jacket and insulation coating should also contribute to flexibility, as well as resist the harsh downhole environments. PVC, the material used in the cable tested in in this study, is the most common and is noted for its good flexibility and durability (Hess& Goldie, 1993). Cable shielding must be grounded to dissipate accumulated noise and prevent "noise-inducing ground loops" (AlphaWire, 2009). The cable tested in in this study uses a tinned-copper shield drain wire, which should suffice (Belden, 2015). Regarding cable size, a five component cable is needed to provide the power source, grounding, and the signal from each of the three axial measurements. Such a cable is available from Belden (Model 9535 060100) for $90 per 100 ft, which is a reasonable cost for this application.

As for the air supply line, the gauge and material used in the initial prototype should suffice. The ¼ inch (outer diameter) size corresponds to the standard bike pump hose. With the proper fittings it should be able to connect directly to the mini air compressor specified in Section 3.2.3 with little effort. The size should provide ample air flow for timely inflation, but not be overly large and cumbersome during device transport. The line material can consist of any standard, industrious plastic, as typically used for laboratory applications. Polyethylene tubing is among the cheapest, most durable, and readily available of these hoses. Rolls of 100 ft of tubing can be obtained for as little as $20. Polyethylene has excellent resistance to most environmental contaminants

that could be encountered and good resistance to oils, which may later be used for inflation (CDF Corporation, 2004). It also maintains good flexibility as a hose, allowing for compacting coiling. Polyethylene tubing with ¼ inch outer diameter is recommended for use as the inflation line.

The initial design called for the air and power line to enter the top of the device at separate locations, with a third line supporting the device. This may be observed in Figure 12 at the beginning of this chapter. The lines were then taped together every few feet or so in an attempt to prevent tangling. The commercial design should streamline the jumbled appearance of these lines and integrate them into a single unit for easier field use and transport. It is proposed that the air and power lines be enclosed in a flexible sleeve that will provide the support for the instrument. The support line in the initial prototype was a basic braided nylon rope knotted onto a metal ring attached to the top of the device. The air and power lines entered the device on either side. In the new design, the lines will enter more closely to the center of the device. This will allow the power line to be funneled through the new hollow bar and out to the membrane, which the air line can then more evenly inflate. It should be noted that the airline should still be installed slightly outside of the middle hollow bar area, otherwise the device will not inflate due to the transducer protection tube attached at the hollow bar's only other outlet. The outer support sleeve encompassing the two lines may either screw on to the instrument around the other two attachments, or be attached to a metal ring like in the current configuration.

The prime material candidate for the support sleeve is woven PET. Short for polyethylene terephthalate, PET is a type of polyester. It demonstrates high tensile strengths and is used for bundling and cable protection applications throughout industry

(Allied Wire & Cable, 2015). The popular water quality instrumentation company YSI utilizes PET sleeving on all of their long field cables. The sleeve allows the heavy devices to be supported by one cable without applying pressure to the delicate electrical connections inside of it. This is achieved by manipulating the PET weave to make a gap through which the end of the cable is threaded. The PET sleeve is then folded and clamped to a small carabiner with heat shrink tubing. The carabiner is clasped onto a rigid support elsewhere on the instrument. Figure 44 shows the PET sleeve around the cable at the bottom right, which then splits off and is attached to the instrument. It should be noted that the cable is significantly longer than the PET sleeve. This slack allows the weight to not shift to the delicate cable connections, but be carried entirely by the PET sleeve. The attachment mechanism could also consist of a fitting around the end of the PET which is then screwed onto the device

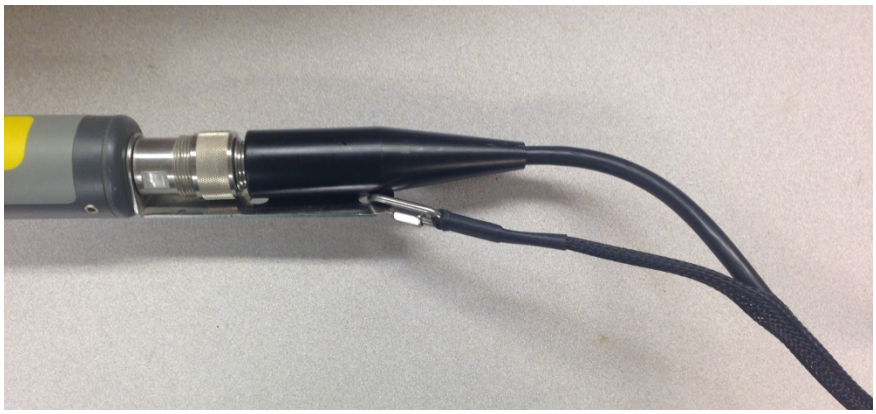

Figure 44: YSI field cable with PET sleeving and sonde attachment

The author has experience with using the described YSI field cables to support a 10 lb device that was submerged in rugged creek conditions over the course of several years. The field cable and sleeve demonstrated no signs of wear or deterioration. The sleeving should provide excellent support in this application. The PET material is very

durable and versatile, and may be used in a variety of ways to streamline the design and support the device. One hundred feet of PET sleeving with ½ inch diameter can be obtained for under $50. The price is approximately three times that of the nylon rope currently being used, but the cable protection and aesthetic improvements are well worth the cost.

4. Final Product

This thesis sought to improve, conceptualize, and develop the design of a recently patented seismic borehole receiver and its components for future commercialization. These are the first steps to bring to market a device that will increase the accessibility to and accuracy of seismic data. By providing a cheaper, lighter, more compact, and more accurate borehole receiver, it is the hope that both the quantity and quality of seismic data vital to the stability of infrastructure can be improved. To achieve this, key device needs were identified and components selected on their merits of efficiency, cost, durability and reliability. All aspects from manufacturing to in-field use of the device were evaluated and considered.

The device design strayed very little from the initial prototype. The patented concept of inflating a flexible membrane around the instrument body to improve transducer coupling needed no improvement. The overall design underwent some changes, but very few. Rather, the primary development goals centered on the components crucial to this functionality. The transducer, as the driver of data accuracy and resolution, was perhaps most crucial to design functionally and affordability. Highly pertinent to the mobility of the device was the inflation mechanism. The membrane was also of utmost importance, due to the innovative nature of the design. The investigation and selection of the materials and parts for each of these components and any necessary accessories was achieved. The process fully incorporated the overall design goals of accuracy, practicality, usability, durability, mobility and cost-effectiveness. Prior to reviewing the intricacies of each of these components, the final, overall design will be

reviewed. The following sections summarize the recommendations for device developers moving forward on the project.

4.1. Overall Design Recommendations

As stated, there are few recommendations for the overall device design. The cylindrical metal frame consisting of two round membrane holders supported by a center bar is good. The solid bar in the initial design should be changed to a hollow bar, to allow transducer power lines to be routed through it. A barbed nozzle fitting should be installed around a small hole in the side of the bar for membrane and transducer attachment. The round metal pieces on either side of the bar should continue to have notches for o-ring placement to secure the membrane. The holes in the top piece for air and power lines should be moved closer to the center. The power line hole should align with the hollow support bar to allow the transducer wires to be routed through and protected. The air line entry should be slightly outside the bar to allow more even inflation. Either a smaller metal ring or a large fitting around the supply line entries should be installed to provide support. This fitting or loop will attach to a woven PET sleeve that is placed around the supply lines. The PET sleeve will replace the rope of the initial design to support the device. It will also replace the electrical tape initially used to hold the power cable, air line, and rope together. On the bottom plate, a bolt may be attached to increase the weight of the device if buoyancy becomes a concern for large diameter water-filled boreholes. The overall size of the frame is sufficient. The 2.75 in diameter is small enough to fit in the smallest feasible boreholes. Its length, at just under 8 in, is sufficiently small for easy transport in the field. The aluminum frame material is lightweight, but also durable.

4.2. Component Overview – final recommendations

4.2.1. Transducer

For the transducer, three classes of instrument were investigated. The initial prototype utilized single-axis piezoelectric accelerometers. These accelerometers were unnecessarily large and heavy. Smaller piezoelectric alternatives were investigated in addition to geophones and MEMS accelerometers. The small piezoelectric accelerometers represent the current state of the field instrumentation, with geophones serving as older, but reliable technology, and MEMS at the forefront of development. Commercially available transducers were selected in each of the categories as having potential for use in the receiver. MEMS accelerometers were identified for their small size, light weight, and low cost. They also could incorporate the three axes of measure needed in the device into one unit, unlike the identified geophones and piezoelectric accelerometers. The geophones were selected for their durability and tested reliability. The also represent a lower cost alternative to the standard piezoelectric accelerometers.

Significant work was done to identify the selected transducers on the bases of their technical capabilities as related to the application, as well as their cost, size, and weight. Transducer sensitivity, frequency response, and signal-to-noise ratio were all considered. Ultimately the selected transducers were the PCB353B16 piezoelectric accelerometer from PCB Piezotronics, the GS-20DM – 14Hz from GeoSpace Technologies, and the ADXL335 from Analog Devices. All identified transducers were tested to verify the accuracy and applicability of the reported parameters. Since piezoelectric transducers are the current standard in the field, testing compare the selected geophones and MEMS device to the PCB accelerometer. The testing confirmed the

suitability of the MEMS accelerometer for use in the device. Coherence functions indicated the PCB and MEMS accelerometers responded similarly to impulses. Passive time histories indicated electronic noise levels are not of concern with the MEMS devices, even when the signal is passed through a long field cable. The GS-20DM – 14Hz miniature geophone was also confirmed to have similar signal responses suitable for this application.

Special care was given to identifying and developing the MEMS accelerometer, since its use is relatively new in commercial receivers. The goal of this review and subsequent testing was to identify the MEMS accelerometer as the primary candidate for the receiver's transducer. It represents the future of the field and a savings of hundreds of dollars as opposed to the traditional alternatives. An extensive literature review was conducted to identify the capabilities of the accelerometer as tested in the field and laboratory for geotechnical applications. The selected ADXL 335 MEMS accelerometer and its predecessors have been used and tested throughout literature. Commercial breakout boards simplify the circuitry needed for its operation. Ultimately, such a system from Adafruit with on-board power regulation and capacitors setting the frequency range was selected. The included capacitors were easily exchanged using a hot air gun to melt the solder. The frequency response range for each axis was raised to 450 Hz with 0.011μF capacitors. This increased the overall device range to 0.5 to 450 Hz, which should be more than ample for the receiver application as verified in the literature review. Power supplied to the board should be at least 3.3 VDC, but no more than 5.0 VDC. A battery pack with three AAA alkaline batteries can be used to supply voltage in this range.

The power should be supplied through a shielded, five-component field cable. A foil shield should provide the necessary protection from outside signal interference while maintaining the overall flexibility of the line. The cable should have low capacitance in the range of 30 pF/ft to 35 pF/ft to reduce noise amplification. The initial prototype should have a cable length of at least 100 feet to be able to properly survey conditions and generate sufficient subsurface velocity profiles. This power line will be encased in a flexible support sleeve with the air line.

The power line will be connected to the transducer through the use of a water-proof multi-component plug. The plug would allow the transducer to be easily replaced as needed. The concept of a board header and plug is presented as a starting point. The header would be soldered to the board to ensure sturdy connections, and then encased in a rigid urethane material. The transparent case would provide protection for the delicate board components and connections, while maintaining visibility of the accelerometer orientation. The case should be as small and similar to the shape of the board as possible to reduce weight and bulk. This case would then be attached to the inflatable membrane.

4.2.2. Inflation Mechanism

The inflation mechanism for this device was one area where the desired technology has not yet developed to the idealized concept. It was desired that an on-board pump be included on the device to eliminate the current practice of lugging around bulky surface air compressors. However, concerns with pump capacity due to high hydrostatic pressures in water-filled boreholes were quickly encountered. Based on International Building Code standards for the development of velocity profiles and regional water table layers, a head value of 80 ft was selected as the benchmark for the pump capacity. This

corresponds to a hydrostatic pressure of 35 psi (241 kPa). At this minimum capacity, available pumps exceeded the dimensions of the device frame and the entire material budget. Underwater inflation applications were investigated for a solution to lower the pressure differential so that a smaller pump could be used. No solutions were identified. Ultimately, a surface air compressor was selected. The recommended compressor is unlike its bulky predecessors. Designed for motorcycle tire inflation, the portable J&P Cycles micro air compressor supplies up to 250 psi (1724 kPa) in a package roughly the size of the receiver housing. The compressor weighs less than 4 lbs and provides a portable alternative until such a time when an on-board inflation mechanism is feasible.

4.2.3. Membrane

The latex material of the initial design was deemed too sensitive for long term use in the field. Flexible polyurethane, or TPU, was initially identified for its durability as a replacement material. However, TPU was deemed to have too little elasticity at the low pressures of this application. Silicone was recognized for its good durability and resistance and high elongations at low stresses. Both TPU and silicone membranes can be manufactured by dip-molding. The process has lower start up and overhead costs than traditional injection molding, making it ideal for the prototyping and custom work required by this application.

The simple cylindrical shape of the initial membrane is sufficient, but coupling may be improved with a slightly rounded design. The shape would mimic an axially compressed cylinder, placing the centrally located transducer closer to the borehole wall. Whatever shape variation is used, its end diameters should be smaller than the top and bottom frame plates, to allow a firm seal. It should also not be wider than the smallest

plausible borehole at its center as to not cause any folds that could interfere with transducer coupling. A small silicone tube attached inside of the membrane would provide housing for the transducer. Its other end will attach around the barb at the inlet of the transducer cable from the center support bar. This will provide additional protection for the transducer from the harsh borehole environment if the membrane were to leak or otherwise malfunction.

Regarding the coupling, the transducer should be affixed to the membrane using semi-permanent, water-resistant wax with a high melting point, or an epoxy specially formulated for silicone. The Blanchard 7036 wax from Stronghold is preferred. However, it is uncertain if removal techniques will damage the membrane or transducer casing. The resin cleaner ShipShape is recommended for removal, as it is the most likely to not cause damage and successfully remove the adhesive. Superglue, which is traditionally used as a semi-permanent adhesive for transducers, is not recommended for use as it does not bond to silicone. Specially formulated silicone epoxies may be used for a permanent hold. If an alternative semi-permanent method is identified that could be removed without damaging the membrane or transducer, that method should be used over the permanent epoxy.

4.2.4. Component Recommendation Summary

The following table and figure briefly summarize the initial prototype components and the recommendations of this report for each of those components in the final design. The identification numbers in Table 4 correspond to the labels in Figure 45.

Table 4: Final design recommendations by prototype component

ID	Component	Initial prototype	Final design
1	Transducer	Wilcoxon accelerometers	MEMS accelerometer
2	Membrane	Cylindrical latex sleeve	Silicone sleeve with transducer tube housing
3	Bottom end cap	Aluminum with o-ring notch	Aluminum with o-ring notch; Potential buoyancy control weights
4	Top end cap	Aluminum with o-ring notch	Aluminum with o-ring notch
5	Support bar	Solid aluminum	Hollow with transducer lead exit and membrane attachment
6	Transducer lead	Loose in inflated membrane	Contained within support bar and membrane tube
7	Air line	¼ in Polyethylene tube	¼ in Polyethylene tube; entry moved closer to center of cap
8	Suspension rope	Rope knotted onto device, taped around supply lines	Woven PET sleeve encasing supply lines
9	Rope attachment	Large metal ring	Small metal ring and carabiner or screw-on fitting
10	Power line	4-component shielded PVC cable	5-component shielded PVC cable; entry moved to center of cap

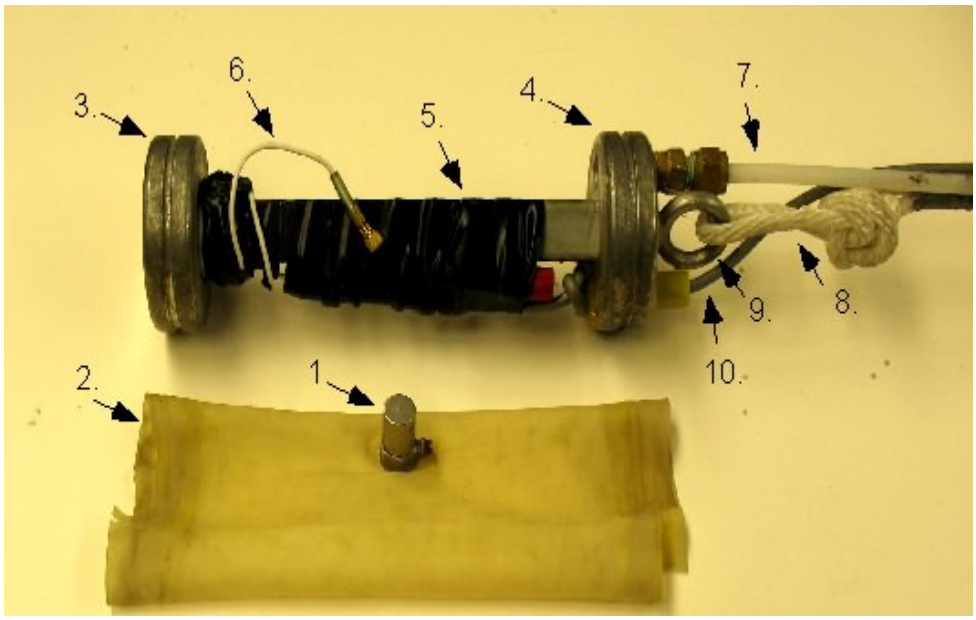

Figure 45: Initial prototype and components (Kalinski, 2012)

4.3. Estimated Costs

The initial device budget included the categories of materials, miniature accelerometers or geophones, air pump, compass, orientation motor, and labor. At the beginning of this phase of the project, the compass and orientation motor were identified as additional features nonessential to basic device functionality. They will be developed at a later date and are discussed in the upcoming section on future work.

The materials category included aluminum for the frame, polyurethane for the membrane, and wire for the transducer. This budget totaled $200. The budget for miniature accelerometers or geophones was established at $500. The air pump, compass, and orientation motor were budgeted at $100, $200, and $100, respectively. An amount of $500 was also established for labor. Excluding the compass and orientation motors, this totaled an ideal budget of $1300 for the device.

Additional considerations for the transducer coupling adhesive, transducer case, and transducer connections were added to the materials category throughout the course of this project. The initial materials also excluded an air line and suspension line. The budget has been reconfigured and recalculated with these additions using the production cost research performed. The device budget is presented in Table 5 below.

Table 5: Estimated device costs

Frame materials	**$50**
Hollow aluminum support bar	$30
Aluminum end plates	$20
Supply lines (100 ft)	**$170**
5-component shielded cable	$90
1/4-in polyethylene air tube	$20
Woven PET support line	$50
PET line connection	$10
Transducer	**$20**
MEMS accelerometer board	$20
3 piezoelectric accelerometers	*$960*
3 miniature geophones	*$165*
Transducer accessories	**$20**
Connections & wires	$10
Urethane resin casing	$5
Adhesive	$5
Miniature air compressor	**$30**
Silicone Membrane	**$50**
Labor	**$500**
Total unit cost	**$840**

The drastically lower cost of the MEMS accelerometer as compared to the other transducers greatly reduced device cost. Despite adding additional materials, the overall costs are lower than what was initially predicted. This frees up more capital for the

development of some of the other device features like the compass and internal motor. Alternatively, it allows for an even more affordable receiver. Either way, the cost estimation indicates this device can be sold for a fraction of the cost of other commercially available seismic borehole receivers. This greatly increases access to seismic data for researchers and infrastructure developers all over the world. More data means safer infrastructure for citizens throughout disaster-prone regions. The design recommendations present a device that can also improve the quality of seismic data. This, too, contributes to seismic stability. This is one of the first steps in achieving this vision, but with the work presented in this thesis and the future work outlined in the following chapter this is certainly an achievable goal.

5. Future Work

The achievement of this objective depends on the continual development of the device. New prototypes need to be created and tested. The details of the manufacturing processes for each of the components, specifically the membrane, need to be developed. A group of engineers and researchers specializing in geophysical instrumentation development, production, and use has been assembled and will carry the project forward.

5.1. Next steps

Over the course of the next few months research will continue and device prototypes will be generated through work at this university and with Olson Instruments. Specializing in geophysical field instrumentation, Olson Instruments will provide industry and manufacturing experience as the device is commercialized and brought to market. With the provided background and research on the basic device components, the team at Olson Instruments will work with the device inventor Dr. Kalinski to incorporate the designed components into several prototypes. These prototypes will then be distributed among researchers at this and other universities, as well as a separate geophysical services company. Olson Instruments will also continue to test their prototype. This step is crucial in the device development as the prototype recipients represent the researchers and field investigators that are the target consumer of the product. Their ongoing feedback of the device prototype will enable the development of a better commercial device. In this way, potential problems hindering device functionality will be eliminated prior to market.

Olson Instruments will be receiving the final product license at the end of the project. Thus, some of the prototype work will likely include configuring the device to

work with some of the company's pre-existing seismic data collection systems. The instrumentation company will also play a large role in the considerations and development of a large scale manufacturing plan. Their experience with membrane manufacturers, complex electrical systems, and general product development will ensure the receiver comes to market in an efficient and affordable fashion.

5.2. Device add-ons

Other future work with Olson Instruments may include the development of several additional device features. These include the orientation mechanism, device inclinometer, and depth tracker previously discussed as potential improvements. Available on other commercial borehole receivers, these features help to position the transducers relative to the source to simplify data processing and improve data quality. Regardless of the source or survey method used, known alignment of the sensor relative to the source helps the user dissect and properly evaluate the data collected by the transducers.

This device utilizes three orthogonal transducers, which will help with the analysis of the complicated wave propagation common in downhole and crosshole surveys. That propagation and resultant signal is dependent on its source and the medium it passes through. The source parameters are typically known, and referenced in relation to the receiver. At the basic level, these proposed devices would report the orientations and alignments to the operator, who could use the information to evaluate the signal and propagation medium. A more sophisticated system would include a means to manipulate the transducer positions. This is vital in shear wave surveys where the receiver could be aligned in such a way that the signals from only two of the transducers would need to be

evaluated, saving valuable processing time. It also enables the user to employ field techniques to eliminate noise and amplify signal (Crice, 2002). These techniques include reversing the polarities of the source signal and the receiver. It becomes more complicated and difficult to achieve good results with this approach when the signal and noise are split across several transducers. This is common when the transducers are not aligned with the source.

The orientation mechanism would rotate the device about the vertical axis to align one of the horizontal transducers with the source, or in any other alignment desirable to the user. For example, alignment with magnetic fields may prove pertinent to a user looking at regional trends in subsurface geology. The Geostuff BHG model utilizes this approach and has a servo mechanism to rotate to a user-selected magnetic azimuth measured from the on-board fluxgate compass. Other measurement methods include a tracking mechanism to rotate the receiver in a hole with grooved casing (Crice, 2002). This approach is not practical in the majority of surveys. A MEMS compass is proposed for development with this device. It uses the same affordable technology employed by the accelerometers to magnetically track orientation. A servomotor would rotate itself to the user-specified orientation. A cheaper, more traditional rotary motor could be rotated by the user to their desired alignment, with the MEMS compass tracking its orientation. Otherwise, the receiver would be manually rotated in the hole via the support cable to best align the transducers with the borehole wall adjacent to the source. The compass would be used to measure how far off the alignment is. It has been suggested that vector sum software be developed to process the readings using the orientation. This approach would reduce the costs of the device hardware, but would add to the processing costs and

effort. A MEMS compass and user-controlled rotary motor are proposed for further development.

The vertical alignment of the receiver is also important. Precise drilling of boreholes is difficult given the equipment scale and subsurface uncertainties. Therefore, it is rare that boreholes are exactly vertical. Depending on the geography of the region, the surveys may also be performed in boreholes that are intentionally angled. This is done in cases where features could not be accessed by a vertical hole, or surface drilling was restricted. For the most accurate surveys, the receiver should not be assumed to be vertical or normal to the ground surface; rather, its inclination should be measured. A MEMS device can also perform this function. A MEMS inclinometer can be integrated to measure the device's deviation from the zenith. The inclinometer will help the user determine distances between the source and receiver in crosshole testing, where the lateral distance between two slightly skewed holes can rapidly change with depth. Knowing the inclination of the hole, and thus, that of the receiver and transducers, will also help with the phase correction of data during processing.

Another important add-on is a depth-monitoring device. Also related to understanding the wave propagation space between source and receiver, depth monitoring is of utmost importance. For ground characterization, identifying the presence and thicknesses of multiple subsurface layers is essential. This requires testing at various known depths during a survey. Depth monitoring is also required for the basic time and distance relationships used to determine wave speed through the medium. Various concepts have been proposed to accomplish this. The initial prototype simply attached a long, flexible measuring tape to the support line, bundling it with the air and power

supplies. Applying depth increments directly to the device cable, via paint or adhesive, has been suggested, but could prove difficult with the woven PET line encasement. The most promising solution is a depth wheel. Utilized for cable measurement throughout industry, including the oilfield, depth wheel count their rotations as the cable either passes around them, or is rolled off of them. The rotations are then converted to distance using the known diameter of the wheel. A depth counter where the cable simply passes over it after being rolled off another spool is recommended. In this way a more accurate length is obtained because there is no variation in the wheel's diameter.

The development of these additional mechanisms will enable the device user to more accurately and precisely record and analyze data by properly aligning, measuring, and orienting the receiver. Of these proposed features, the priorities should be the orientation and depth measurement. The rotation mechanism and inclinometer are nice and would expand the use and marketability of the device, but are not as essential to its functionality. These additional components will be developed by the electrical and mechanical engineers at Olson with continued consultation from the inventor and input from the prototype testers.

5.3. Additional Developments

The incorporation of additional features will improve the device, but focus should also be given to the continual improvement of the other components. It is highly recommended that the device maintain the most current technology in order to remain relevant in the field. As MEMS technology continues to develop, newer, more precise accelerometers should be included. The inclusion of an on-board pump should also be considered as technology allows it. The background research on micro pumps provided in

this work should aid in that process. During all of these additional developments, the creators should keep in mind the overall goals of this device. The receiver is to provide a small, affordable, lightweight alternative to the borehole receivers currently on the market. The device should be easy to use and maintain the patented coupling technique that provides more accurate seismic readings. Developers should not become engrossed with adding so many additional features that the merits of this design are lost. The introduction of this device to the market could signal a change in the accessibility of seismic data. The importance of this to the developing world and the state of infrastructure in our own nation cannot be overstated.

Appendix A

MEMS accelerometer guide

This appendix is meant to serve as a guide for the incorporation of MEMS accelerometers in the continued development and testing of the new seismic borehole receiver device. Details and methodology concerning the MEMS accelerometer configuration and development are presented.

A triaxial MEMS accelerometer should be used to minimize device bulk. It is recommended that the MEMS accelerometer be soldered to a breakout board to maintain the integrity of the connections and streamline transducer incorporation. MEMS accelerometers pre-installed on the breakout boards are readily available and may be purchased for $15. The transducer system tested and recommended in this work is the ADXL 335 MEMS accelerometer on the AdaFruit breakout board with 3.3 V LP298XS power regulator and 0.1 µF filter capacitors. The board is pictured in Figure A.1 with its components labeled.

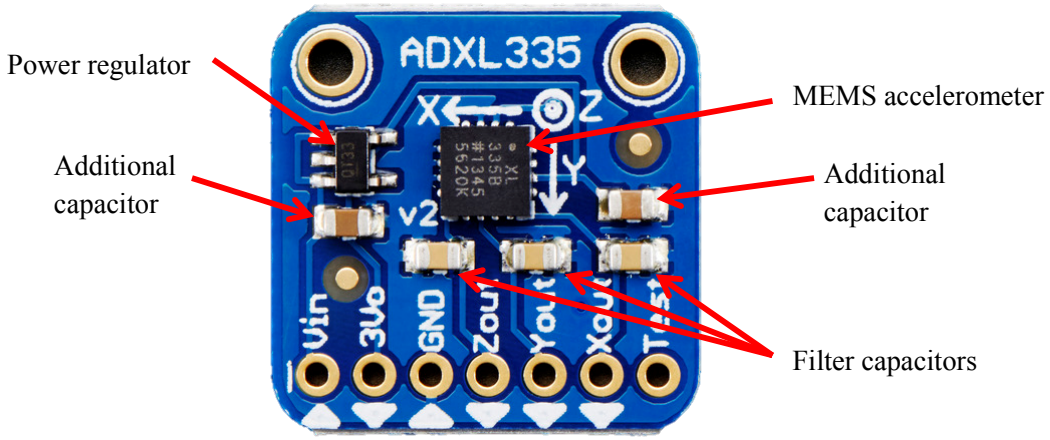

Figure A.1: Adafruit ADXL 335 breakout board

A power regulator is highly recommended due to the delicacy and low power requirements of the accelerometer. Three filter capacitors are required to set the frequency bandwidth of the accelerometer axes. Utilizing a board that is already set up in

this configuration will streamline production. The three bandwidth-regulating capacitors on the board were exchanged for higher capacitance devices in order to raise the bandwidth across the axes. For the ADXL 335 MEMS accelerometer, the resultant bandwidth from a given capacitance can be calculated using the following equation, where *F* is the bandwidth produced by capacitance, *C*.

$$F_{-3dB} = \frac{1}{2\pi(32k\Omega)C_{(X,Y,Z)}} \quad \text{(A.1)}$$

This basic relationship is supplied by the manufacturer and can be used to size the capacitors based on the desired frequency range. In this study, 0.011μF capacitors were used to set the bandwidth of each axis to approximately 450 Hz. A hot air gun was used to melt the solder of the existing capacitors on the board. The new surface mount capacitors were then soldered in place. When selecting replacement capacitors, consideration must be given to physical size of the capacitor, in addition to its capacitance. The spacing of the capacitor connections must fit the existing connections on the breakout board. Capacitors 0.95 mm long were found to fit the existing connections on the breakout board. The locations of the filter capacitors are shown in Figure A.2.

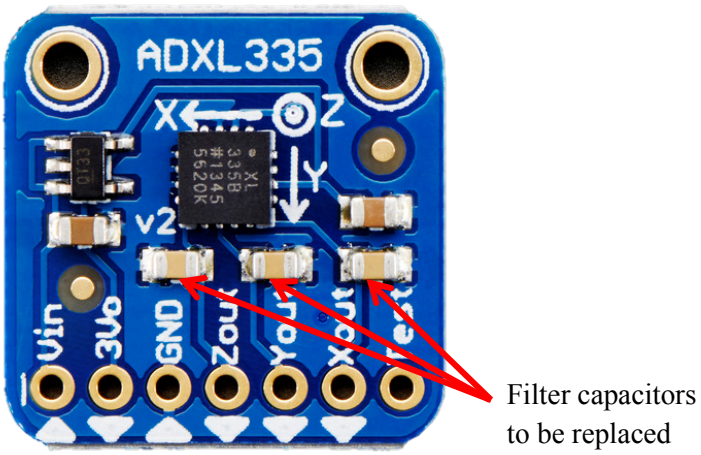

Figure A.2: Filter capacitors on breakout board

The breakout board also simplifies wiring of the device. All inputs and outputs are clearly marked, but are further identified in Figure A.3. Power is supplied through the voltage input pin. Input voltage must be between 3.3V and 5.0 V. The onboard power regulator reduces the input voltage to 3.3 V to protect the MEMS accelerometer, which cannot receive input greater than 3.6 V, and maintains the proportionality of its output signal. The system is grounded through the ground output. Signal from the MEMS accelerometer and filter capacitors is received through three output locations.

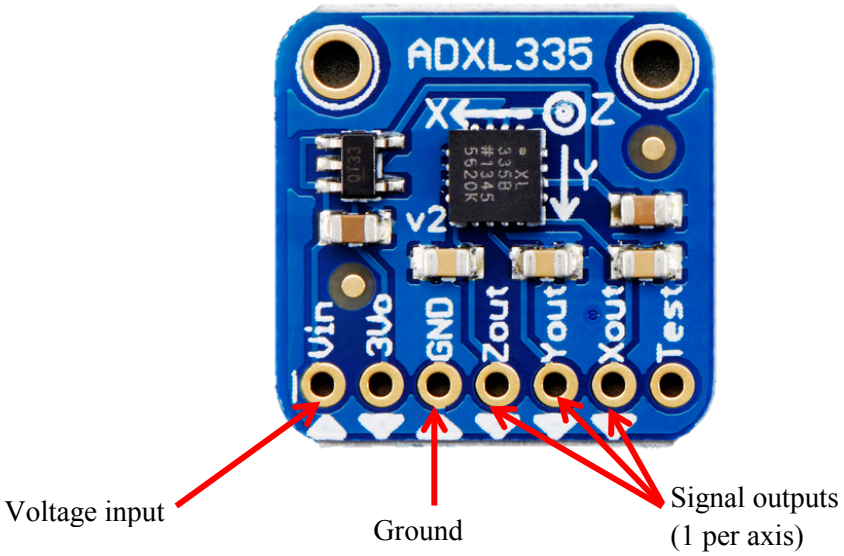

Figure A.3: Breakout board inputs and outputs

To ensure more secure connections at the input and output locations, a header pin should be connected to the board. All pins should be soldered in place. A jumper wire outlet fitted to the header plug will provide sturdy, yet easily removable connection. The jumper wires will be connected to the power supply and signal processors to provide and receive the necessary inputs and outputs, respectively. The header pin and jumper wire outlet from Sparkfun are shown in Figure A.**4**.

Figure A.4: Sparkfun header pin connectors

The device power should be provided by an alternative source. Traditional ICP signal inputs provide too much voltage and should not be used with the MEMS accelerometer. If signal analyzers are used, their output should be set to an unpowered setting, like what is used for geophones. A basic battery pack with lead wires and an on/off switch can easily be configured to provide power in the necessary 3.3 V to 5.0 V range. Three AAA alkaline batteries output between 3.3 V to 4.8 V over their lifetime use. Other battery types may provide more than the 5.0 V maximum and should not be used without careful consideration and calculation. The recommended wiring diagram with battery pack is shown in Figure A.5.

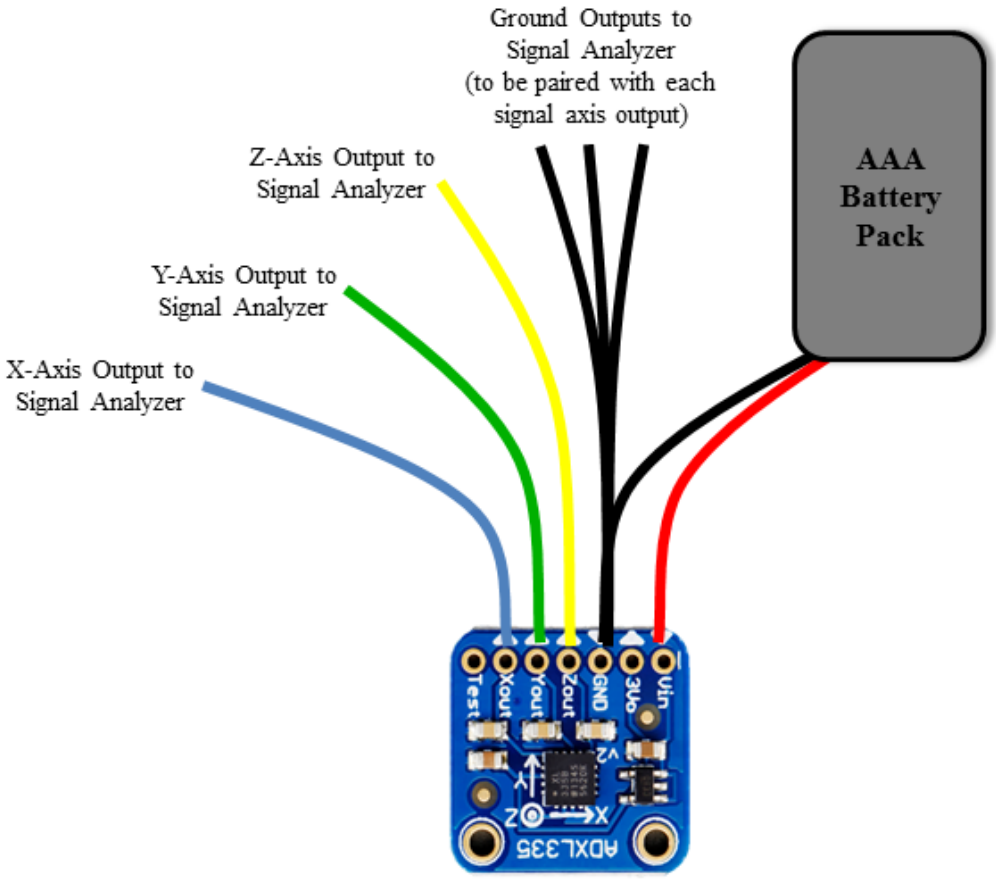

Figure A.5: Proposed MEMS wiring diagram

REFERENCES

Acar, C. and Shkel, A. M. (2003). *Experimental evaluation and comparative analysis of commercial variable-capacitance MEMS accelerometers.* Journal of Micromechanics and Microengineering, Vol. 13, No. 5, pp. 634.

Albarbar, A., Badri, A., Sinha, J. K., Starr, A. (2009). *Performance evaluation of MEMS accelerometers.* Measurement, Vol. 42, No. 5, pp. 790-795.

Allied Wire & Cable. (2015). *FIT Expandable Polyester Braided Sleeving.* http://www.awcwire.com/mfg/alpha/product/fit-expandable-polyester-braided-sleeving.

AlphaWire. (2009). *Understanding shielded cable. Elizabeth, NJ.* http://www.newark.com/pdfs/techarticles/alphaWire/Understanding_Shielded_Cable.pdf.

Analog Devices. (2009). *Small, low power, 3-Axis ±3g accelerometer - ADXL335.* http://www.analog.com/en/products/mems/mems-accelerometers/adxl335.html.

Andrejasic, M. (2008). *MEMS Accelerometers*. Seminar work, University of Ljubljanan, Department of Physics. http://mafija.fmf.uni-lj.si/seminar/files/2007_2008/MEMS_accelerometers-koncna.pdf.

ASTM International. (2014). *ASTM D4428/D4428M-14, Standard Test Methods for Crosshole Seismic Testing*, West Conshohocken, PA: ASTM. http://www.astm.org/Standards/D4428.htm

ASTM International. (2014). *ASTM D7400-14, Standard Test Methods for Downhole Seismic Testing*, West Conshohocken, PA: ASTM. http://www.astm.org/Standards/D7400.htm.

AZO Materials. (2001). *Silicone Rubber.* Granta Designs Limited. http://www.azom.com/properties.aspx?ArticleID=920.

BASF. (1990). *N-methylpyrrolidone handling and storage.* Technical Information. Parsippany, NJ. http://infohouse.p2ric.org/ref/30/29008.pdf.

BASF Polyurethanes. (2010). *Thermoplastic Polyurethane Elastomers (TPU) Elastollan Material Properties.* Technical Information. BASF: Lemforde, Germany. http://www.polyurethanes.basf.de/pu/solutions/us/function/conversions:/publish/content/group/Arbeitsgebiete_und_Produkte/Thermoplastische_Spezialelastomere/Infomaterial/elastollan_material_uk.pdf.

BASF Polyurethanes. (2012). *Thermoplastic Polyurethane Elastomers (TPU) Elastollan Product Range.* Technical Information. BASF: Lemforde, Germany. http://www.polyurethanes.basf.de/pu/solutions/en/function/conversions:/publish/content/group/Arbeitsgebiete_und_Produkte/Thermoplastische_Spezialelastomere/sortiment/tpu_sort_en.pdf.

Baziw, E. and Verbeek, G. (2010) *Geophones or Accelerometers?* BCE Technical Note 10. Baziw Consulting Engineers. Vancouver, BC: http://www.bcengineers.com/images/BCE_Technical_Note_10.pdf.

Belden. (2015). *9535 multi-conductor - computer cable for EIA RS-232 applications.* Detailed Specifications & Technical Data. http://www.belden.com/techdatas/metric/9535.pdf.

Bhattacharya, S., Krishna, A. M., Lombardi, D., Crewe, A., Alexander, N. (2012). *Economic MEMS based 3-axis water proof accelerometer for dynamic geo-engineering applications.* Soil Dynamics and Earthquake Engineering, Vol. 36, pp. 111-118.

CDF Corporation. (2004). *Polyethylene chemical resistance chart.* CDF Technical Memo.http://www.cdf1.com/technical%20bulletins/Polyethylene_Chemical_Resistance_Chart.pdf.

Central Intelligence Agency. (2014). *Country comparison: GDP-per capita*. The World Factbook: CIA. https://www.cia.gov/library/publications/the-world-factbook/rankorder/2004rank.html.

Colombo, S., Giannopoulos, A., Forde, M. C., Hasson, R., and Mulholland, J. (2005). *Frequency response of different couplant materials for mounting transducers*. NDT & E International, Vol. 38, No. 3, pp. 187-193.

Crice, D. (2002) *Borehole shear-wave surveys for engineering site investigations.* Sartoga, CA: Geostuff. http://www.geomatrix.co.uk/tools/application-notes/Shearwaves.pdf.

Das, B. M., & Ramana, G. V. (2011). *Principles of soil dynamics* (2nd ed.). Stamford, CT: Cengage Learning.

Data Physics. (2013). *SignalCalc dynamic signal analyzer user manual.* San Jose, CA.

DuPont. (2015). *A guide to elastomer properties.* http://www.dupont.com/products-and-services/plastics-polymers-resins/elastomers/articles/guide-to-elastomer-properties.html.

Eager Plastics, Inc. *(2000). Crystal Clear 200, 202, 204 and 206 Part A material safety data sheet.* Chicago, IL. http://www.eagerplastics.com/cca.htm.

Economic Research Service. (2015). *Real per capita GDP historical*. The ERS International Macroeconomic Data Set: USDA. http://www.ers.usda.gov/data-products/international-macroeconomic-data-set.aspx.

Elert, G. (2015). *Dielectrics. The Physics Hypertextbook.* http://physics.info/dielectrics/.

Endevco. (2008). *Guide to adhesively mounting accelerometers.* Meggitt: TP 312. https://www.endevco.com/download/TP312.pdf.

Endevco. (2009). *Practical understanding of key accelerometer specifications.* Meggitt: TP 328. https://www.endevco.com/news/archivednews/2009/2009_09/TP328.pdf.

Engineering Fundamentals. (2015). *Introduction to dip molding and coating.* eFunda. http://www.efunda.com/processes/plastic_molding/molding_dip.cfm.

Engineering ToolBox. (2015*). Young's Modulus.* Fabrication Extrusion Company. http://www.engineeringtoolbox.com/young-modulus-d_417.html.

Esu, O.O, Flint, J.A. and Watson, S.J. (2013). *Integration of low-cost accelerometers for condition monitoring of wind turbine blades* in European Wind Energy Conference, Vienna, pp. 1–4.

Feijen, D. H.W., Müller, J.L., Julià, J., Salvatella ,D., and Riba, M. J. (2001). *Technological advantages of polyether copolymer based TPUs.* Proceedings of the PU Latin America Conference. http://www.merquinsa.com/literature/PULatinAmerica_English.pdf.

Geospace. (2012). *GS-20DM – The small digital grade geophone.* http://www.geospace.com/geophones-gs-20dm/.

Goldberg, H., Gannon, J., Marsh, J, Reichert, B., Zavaleta, M. (2000) *An Extremely Low-Noise MST Accelerometer Using Custom ASIC Circuitry.* Proceeding of Sensor Expo Fall 2000. pp. 479-482.

Hess, D. & Goldie, J. (1993). *A practical guide to cable selection.* National Semiconductor Corporation: Application Note 916. http://www.ti.com/lit/an/snla164/snla164.pdf.

Hoffman, K., Varuso, R., and Fratta, D. (2006). *The use of low-cost MEMS accelerometers for the near-surface monitoring of geotechnical engineering systems.* Proceedings from GEOCongress 2006: Geotechnical engineering in the information technology age. Atlanta, GA: ASCE.

Homeijer, B., Lazaroff, D., Milligan, D., Alley, R., Wu, J., Szepesi, M., Bicknell, B., Zhang, Z., Walmsley, R.G., Hartwell, P.G. (2011). *Hewlett Packard's seismic grade MEMS accelerometer.* Proceedings of the IEEE International Conference on Micro Electro Mechanical Systems (MEMS). 2011. pp. 585-588.

Homeijer, B. D., Milligan, D. J., Hutt, C. R. (2014). *A brief test of the Hewlett-Packard MEMS seismic accelerometer.* United States Geologic Survey, Geologic Hazards Science Center. Series No. 2014-1047. http://pubs.er.usgs.gov/publication/ofr20141047.

Hons, M. S., Stewart, R. R., Lawton, D.C., and Bertram, M.B. (2008). *Field data comparisons of MEMS accelerometers and analog geophones.* The Leading Edge, Vol. 27, No. 7, pp. 896-903.

Hunter, J.A., Pullan, S. E., Burns, R. A., Good, R. L., Harris, J. B., Pugin, A., Skvortsov, A., and Goriainov, N. N. (1998). *Downhole seismic logging for high-resolution reflection surveying in unconsolidated overburden.* Geophysics63, Special Section: Shallow Seismic Reflection Papers, pp. 1371-1384.

Huntsman. (2010). *A guide to thermoplastic polyurethanes (TPU)* http://www.huntsman.com/portal/page/portal/polyurethanes/Media%20Library/global/files/guide_tpu.pdf.

Incorporated Research Institutions for Seismology. (2014). *Computing distance.* https://www.iris.edu/hq/Wiki/Computing_Distance

International Code Council. (2009). *2009 International building code.* Country Club Hills, Ill: ICC. http://publicecodes.cyberregs.com/icod/ibc/2009/index.htm.

ISP. (2005). *ShipShape resin cleaner material safety data sheet.* Mississauga, ON. http://www.cleanersolutions.org/downloads/msds/309/Ship%20Shape%20Resin%20Cleaner%20MSDS.pdf.

Johnson, W. J. and Clark, J. C. (1992). *Improving subsurface resolution with the seismic reflection method: use S-waves.* 6th Nationa1 Outdoor Action Conference, Nationa1 Ground Water Association, Proceedings, pp. 655- 663.

Kalinski, M.E. (2012). *A small, lightweight borehole receiver for crosshole and downhole seismic testing.* Geotechnical Testing Journal, Vol. 35, No. 2, pp. 363-366.

Kalinski, M. E., Jean-Louis, M. and Lissade, H. (2014). *Transferring technology for surface wave testing and seismic site response analysis in Haiti.* The Leading Edge, Vol. 33, No. 12, pp. 936-940.

Kalinski, M.E. (2011). *Lightweight Inflatable Borehole Receiver Unit for Seismic Testing.* United States Patent No. 7,954,595.

Knapp, R. W. and Steeples, D. W. (1986). *High-resolution common-depth-point reflection profiling: Field acquisition parameter design*. Geophysics Vol. 52, No. 2, pp. 283-294.

Lainé, J. & Mougenot, D. (2014). *A high-sensitivity MEMS-based accelerometer.* The Leading Edge, Vol. 33, No. 11, pp. 1234-1242.

Margrave, G. F., Mewhort, L., Phillips, T., Hall, M., Bertram, M. B., Lawton, D. C., Innanen, K, Hall, K. W., and Bertram, K. (2012). *The Hussar low-frequency experiment.* CSEG Recorder, Vol. 37, No. 7, pp. 25-39.

Matthews, C. K. (2014). *The differences between centrifugal pumps vs. positive displacement pumps.* Empowering Pumps. Tuscaloosa, AL: http://empoweringpumps.com/differences-centrifugal-pumps-vs-positive-displacement-pumps/.

Mougenot, D. (2004). *How digital sensors compare to geophones?* SEG Technical Program Expanded Abstracts 2004, pp. 5-8.

Meggitt. (2010*). Ask the expert: low noise cables.* Measurement News. https://www.endevco.com/news/archivednews/2010/2010_06/f1.html.

Meggitt. (2012). *Wilcoxon Research models 736/736T Compact, high sensitivity, high frequency accelerometer.* http://www.wilcoxon.com/vi_index.cfm?PD_ID=17

Merquinsa. (2012). *Polyurethane Types.* http://www.merquinsa.com/whats/FPPUtypes1.pdf.

Mougenot, D. & Thorburn, N. (2004). *MEMS-based 3C accelerometers for land seismic acquisition: is it time?* The Leading Edge, Vol. 23, No. 3, pp. 246-250.

Mykin Inc. (2015). *Rubber chemical resistance chart*. Technical Resources. South Lyon, MI. http://mykin.com/rubber-chemical-resistance-chart.

National Academy of Engineering. (2008). *21 Century's grand challenges unveiled*. http://www8.nationalacademies.org/onpinews/newsitem.aspx?RecordID=02152008.

Parker Hannifin Corporation. (2015). *Miniature Pumps*. Precision Fluidics Division. Hollis, NH: http://www.parker.com/literature/Literature%20Files/Precision%20Fluidics%20Division/UpdatedFiles/PPF_Pumps_Catalog.pdf.

Patil, R. P., Chaudhari, V. D., and Rane, K. P. (2015)*ARM based 3-axis seismic data acquisition system using accelerometer sensor and graphical user interface*. International Journal of Engineering Research and General Science, Vol. 3, No. 2.

PCB Piezotronics. (2002). *Model 53B16 Installation and Operating Manual*. http://www.pcb.com/contentstore/docs/PCB_Corporate/Vibration/Products/Manuals/353B16.pdf.

PCB Piezotronics. (2004). *Introduction to Piezoelectric Accelerometers*. https://www.pcb.com/techsupport/tech_accel.aspx.

PCB Piezotronics. (2015). *Low Noise Coaxial Cables for Sensors.* http://www.pcb.com/TestMeasurement/Cables/LowNoise.

PSG Dover. (2012). *Flow Rates and Deadheading.* Dangerous Chemicals Resource Center. http://www.psgdover.com/en/pump-technologies/compare-pump-technologies/flow-rates-a-deadheading.

PSP Inc. (2015). *O-ring fluid compatibility guide.* Centennial, CO. http://www.pspglobal.com/fluid-compatibility/chemicals-n.html.

Pump School. (2007). *When to use a positive displacement pump.* Viking Pump, Inc. http://www.pumpschool.com/intro/pd%20vs%20centrif.pdf.

Renner, T. & Pek, L. (2011). *Comparing strength properties of natural and synthetic rubber mixtures.* Sustainable Construction and Design. Vol. 2, No. 1, pp. 134.

Rose, K., & Steinbüchel, A. (2005). *Biodegradation of natural rubber and related compounds: recent insights into a hardly understood catabolic capability of microorganisms*. Applied and Environmental Microbiology, Vol 71, No. 6, pp. 2803–2812.

Salehian, A. (2013). *Predicting the dynamic behavior of coal mine tailings using state-of-practice geotechnical field methods.* University of Kentucky Theses and Dissertations.

Santamarina, J.C., and Fratta, D. (1998). *Introduction to Discrete Signals and Inverse Problems in Civil Engineering*. Reston, VA: ASCE Press.

Shah, T.K. (2001). *Dip molding of polyurethane and silicone for latex-free, nonallergenic products.* Medical Device and Diagnostic Industry. http://www.mddionline.com/article/dip-molding-polyurethane-and-silicone-latex-free-nonallergenic-products.

Shin-Etsu. (2005). *Characteristic properties of silicone rubber compounds.* Shin-Etsu Silicone: Japan. http://www.shinetsusilicone-global.com/catalog/pdf/rubber_e.pdf.

Smooth-On. (2014a). *Crystal Clear Series*. http://www.smooth-on.com/tb/files/CRYSTAL_CLEAR_200_TB.pdf.

Smooth-On. (2014b). *Sil-Poxy Silicone Rubber Adhesive*. http://www.smooth-on.com/tb/files/Sil_Poxy_Silicone_Adhesive.pdf.

Stauffer, J.M. (2006). *Current capabilities of MEMS capacitive accelerometers in a harsh environment.* Aerospace and Electronic Systems Magazine, IEEE, Vol. 21. pp. 29-32.

Stewart, R. R. (2009). *A brief history and extended future of full-wave seismic exploration.* CREWES Research Report, Vol. 21, Ch. 68.

Stokoe II, K. H., Wright, S.G., Bay, J.A., and Roesset, J.M. (1994). *Characterization of geotechnical sites by SASW method* in Woods, R. D., Ed., Geophysical Characterization of Sites, volume prepared by ISSMFE Technical Committee #10 for XIII ICSMFE Meeting, New Delhi, International Science Publisher: New York, pp. 15-24.

Stotter, C. & Angerer, E. (2011). *Evaluation of 3C microelectromechanical system data on a 2D line: direct comparison with conventional vertical-component geophone arrays.* Geophysics, Vol. 76, No. 3, pp. B79-B87.

Stronghold. (2014). *Stronghold 7036 blanchard wax.* J.H. Young Company. Charlotte, NC. http://www.strongholdwax.com/7036.htm.

United States Geologic Survey. (2014). *Largest and deadliest earthquakes by year: 1990-2014*. Earthquake Hazards Program: USGS. http://earthquake.usgs.gov/earthquakes/eqarchives/year/byyear.php.

Vesta. (2015) *Choosing the right manufacturing process for your silicone medical balloon.* Lubrizol. http://www.vestainc.com/resources/articles/best-balloons.aspx.

Werner, M. H., Radtke, R. P., Stokes, R. H., and Glowka, D. A. (2013*). A low frequency downhole sparker for borehole seismic applications.* CSEG Recorder, Vol. 38, No. 8, pp. 50-56.

Wightman, W. E., Jalinoos, F., Sirles, P., and Hanna, K. (2003). *Application of geophysical methods to highway related problems. Lakewood, CO: Federal Highway Administration,* Central Federal Lands Highway Division, Lakewood, CO, Publication No. FHWA-IF-04-021. http://www.cflhd.gov/resources/agm/.

Wing Inflatables. (2011). *Polyurethane: the most advanced material for sponsons and inflatable boats.* http://www.wing.com/polyurethane.php.

VITA

Rachel Adams was born and raised in Central Kentucky. She is a graduate of Woodford County High School where she was Valedictorian of her class. She graduated Summa Cum Laude with a Bachelor of Science in Civil Engineering at the University of Kentucky in May 2014. She obtained Engineer-in-Training (EIT) certification upon graduation. She is a member of the Kentucky Society of Professional Engineers, the Society of Women Engineers, and the American Society of Civil Engineers. She is currently serving as Secretary of the American Society of Civil Engineers Bluegrass Branch. While at UK, Rachel was also active in the Tau Beta Pi Engineering Honorary, the Chi Epsilon Civil Engineering Honorary, and the Phi Sigma Rho National Engineering Sorority. In addition to being a Patterson Scholar, she is the recipient of several awards, including the 2012 KSPE Past President's Award, the 2012 and 2013 UK College of Engineering Ralph D. and Janice Young Scholarships, the 2013 TFISE Research Showcase Undergraduate Award, a 2013 UK Undergraduate Summer Research and Creativity Fellowship, the 2013 Southeast Chapter of the International Erosion Control Association Scholarship, the 2014 Most Outstanding University Scholar in Civil Engineering, the 2015 Most Outstanding Graduate Student in Civil Engineering, and the Raymond Fellowship.